Anna Maria Knaus, BSc

Synthesis of red/far-red emissive rylene dyes for the application in optical sensors

MASTER'S THESIS

to achieve the university degree of

Diplom-Ingenieur (Dipl.-Ing.)

Master's degree programme: Technical Chemistry

submitted to

Graz University of Technology

Supervisor

Assoc.Prof. kand. Sergey Borisov

Institute of Analytical Chemistry and Food Chemistry

Graz, May, 2020

Abstract

This work focuses on the synthesis of novel rylene fluorescence indicator dyes for the potential application in optical pH sensors. The structure of the rylene dye class is based on a framework of naphthalene units, which comprises various homologues such as terrylenes and perylenes.
The presented synthesis describes the extension of the π-conjugated system of a perylene tetracarboxylic dianhydride to obtain a bathochromically shifted terrylene diimide structure which can undergo further modifications. These modifications include functionalization at the bay-region and the terminal imide position to gain enhanced solubility, pH sensitivity and further bathochromically shifted absorption and emission bands. Two novel asymmetric terrylene diimide dyes bearing four phenyl groups or 4-benzoyl-morpholino groups were successfully synthesized and characterized. These dyes exhibit extraordinary photostability, high molar absorption coefficients, far-red fluorescence emission and suppressed aggregation behavior. Attempts to gain pH sensitivity were not successful due to synthetic limitations.
The second part of this work focused on the modification of perylene diimide dyes at the bay-position to enhance the solubility in polar media. Different synthetic strategies did not lead to the desired result due to challenging purification. Furthermore, a novel way to introduce a pH-sensitive group at the terminal imide position was attempted but calls for further, more detailed investigation in future.

Kurzfassung

Im Rahmen dieser Arbeit wird die Synthese von neuartigen Rylen-basierten, fluoreszierenden pH-Indikatoren für die Anwendung im Bereich der optischen Sensorik behandelt.
Die Struktur der Rylen-Farbstoffklasse basiert auf einem Naphthalen-Grundgerüst und beinhaltet verschiedene Homologe, wie das Perylen oder das um eine Naphthalen-Einheit vergrößerte Terrylen.
Im ersten Teil dieser Arbeit wird der Syntheseweg vom Perylentetracarboxydianhydrid zum Terrylendiimid beschrieben, welches im Vergleich zum Perylen bathochrom verschobene Absorption und Emission aufweist. Diese Verbindung wurde als Ausgangspunkt für weitere Modifikationen an der terminalen Diimidposition und der Bay-Region genutzt. Diese Modifikationen sollten zu einer Verbesserung der Löslichkeit, Erlangen von pH-Sensitivität, sowie weiter bathochrom verschobenen Absorptions- und Emissionsspektren führen. Es wurden zwei neuartig modifizierte Terrylendiimide synthetisiert und charakterisiert, wovon eines mit vier Phenyl Gruppen und das Zweite mit vier 4-benzoyl-morpholino Gruppen in der Bay-Region substituiert wurde. Diese Farbstoffe zeigen außergewöhnlich gute Photostabilität, hohe molare Absorptionskoeffizienten und Fluoreszenzemission im tiefroten Bereich des Spektrums. Aufgrund synthetischer Hürden konnte keine pH-Sensitivität erreicht werden.
Der zweite Teil dieser Arbeit behandelt die Modifizierung eines Perylendiimids im Bereich der Bay-Region. Als Folge dieser Modifikation sollte die Löslichkeit der Verbindung in polaren Medien steigen. Hierfür wurden verschieden Synthesestrategien angewendet, jedoch ohne Erfolg. Des Weiteren wurde versucht, eine pH-sensitive PET Gruppe am terminalen Imid einzubringen.

Eidesstattliche Erklärung

Ich erkläre an Eides statt, dass ich die vorliegende Arbeit selbstständig verfasst, andere als die angegebenen Quellen/Hilfsmittel nicht benutzt, und die den benutzten Quellen wörtlich und inhaltlich entnommenen Stellen als solche kenntlich gemacht habe.

Statutory declaration

I declare that I have authored this thesis independently, that I have not used other than the declared sources / resources, and that I have explicitly marked all material which has been quoted either literally or by content from the used sources.

……. ……...

Datum/date Unterschrift/signature

Danksagung

An erster Stelle möchte ich mich bei Sergey dafür bedanken, die Möglichkeit bekommen zu haben, meine Masterarbeit im Bereich der optischen Sensorik zu absolvieren. Deine Begeisterung für diesen Forschungsbereich hat mich immer wieder aufs Neue beeindruckt und mir gezeigt, dass man gut ist indem was man tut, wenn man es gerne tut.
David – nicht nur Büro-Sitznachbar, sondern auch Betreuer. Danke, dass du stets ein offenes Ohr für meine Fragen und Anliegen hattest, du mich auch mal angetrieben hast, wenn ich zu langsam war, der Spaß an der Sache aber nie zu kurz gekommen ist.
Auch beim restlichen Büro möchte ich mich bedanken: Iris - Danke, dass du das Büro immer wieder mit dem Duft von Chai Tee erfüllt hast! Tobi – Danke für jegliche statistische Auswertung meiner Anwesenheit nach feierfreudigen Abenden! Tanja – Danke für die stetige Versorgung mit Schokolade und Tee!
Auch möchte ich mich bei der gesamten Arbeitsgruppe bedanken. Neben etwas seltsamen Fragerunden, Baustellen-DJ Sets oder Bananaphone Anrufen wurde es niemals langweilig. Auch weiß ich sehr zu schätzen, dass ihr mir immer geholfen habt, wenn ich Fragen hatte.
Danke Silvia dafür, dass ich für dich arbeiten durfte und dadurch den Weg in die ACFC fand.
Ein ganz besonderes Dankeschön gilt meinen Studienkollegen: Vici (immer an meiner Seite), Fabi (wird mich seit Tag eins nicht mehr los), Feri (immer da um mal eine Kaffeepause zu machen), Resi (zusammen durch die letzten Prüfungen). Jakob (Bachelor-Buddies), Valen (im Herzen immer Chemikerin), Flo (lädt mich irgendwann sicher mal auf seine eigene Insel ein) und allen anderen mit denen ich viel Zeit verbracht habe. Ohne euch wäre ich nicht so weit gekommen. Alex, danke für deine Freundschaft und die mentale Unterstützung über die Jahre.
Bernhard, bei Dir möchte ich mich für sehr vieles bedanken. Du bereicherst mein Leben in jeglicher Hinsicht und ich bin sehr froh dich an meiner Seite zu wissen.
Elisabeth, Sophie und Lea ihr seid die besten Schwestern die man sich vorstellen kann. Danke fürs Zuhören, wenn ich mal wieder übers Studieren gejammert habe und für die schöne Zeit die ich mit euch habe.
Mama und Papa, vielen Dank, dass ihr immer an mich geglaubt und mich in meinen Entscheidungen unterstütz habt. Egal worum es geht, ich weiß immer, dass ihr da seid und das ist unbezahlbar.

Contents

1. Introduction

The aim of this work was the synthesis of new rylene based indicator dyes for application in optical chemical sensors.
The structure of the rylene dye class is based on a framework of naphthalene units, which comprises various homologues. These are distinguished in the size of their π-conjugated system such as perylenes, terrylenes and quaterrylenes. This work focuses on the synthesis and characterization of new terrylene diimides and perylene diimides for potential application as pH indicator dyes in optical sensors.

The synthesis of far-red emitting and pH-sensitive terrylene diimides includes preparation of the ground structure, structural modifications in bay region and introduction of a pH-sensitive PET-receptor. Structural modification of the bay region was performed via bromination followed by Suzuki-cross coupling. The introduction of a pH-sensitive receptor was attempted via various synthetic methods including Suzuki-coupling, chlorosulfonation and saponification reactions.
The presented synthesis turned out to be challenging, due to the low solubility of some intermediate products, low yields in many synthetic steps and time-consuming purification procedures.
The synthesis of two novel bay-modified terrylene diimide dyes bearing four phenyl groups or 4-benzoyl-morpholino groups in the bay region was successfully performed. The novel dyes exhibit extraordinary photostability, enhanced solubility, supressed aggregation and fluorescence emission in the far-red region of the electromagnetic spectrum. However, introduction of a pH-sensitive PET-receptor was not possible by the presented synthesis pathways. Importantly, the new terrylene diimide dyes show good brightness only in apolar solvents, whereas in polar solvents fluorescence quantum yields were found to be low.

The perylene derivate synthesis focused on enhancement of the solubility in polar media such as polyurethane hydrogels and the introduction of a pH-sensitive receptor. The structural modifications to enhance solubility were conducted in the bay region whereas introduction of the receptor was attempted at the terminal imide position. The functionalization with four tetraethylene glycol-groups in the bay region and the pH sensitive groups was attempted using various pathways but was not successful.

2. Theoretical Background

2.1. Fundamentals of Luminescence

This chapter is based on the books “Molecular Fluorescence” by Valeur and “Principles of Fluorescence Spectroscopy” by Lakowicz.[1,2] Assertions which are based on other references are mentioned independently.

Luminescence describes the emission of photons from an electronically excited species, accompanied by relaxation of the system. The excited species can emit in different ranges of the electromagnetic spectrum (UV, VIS, IR), dependent on structural properties of the molecule. A wide range of molecules exhibit luminescence, such as organometallic complexes, organic compounds (mostly aromatic) and inorganic compounds (crystals, glasses, ions). Excitation of an electron from its ground state (S_0) to an electronically higher state (excited state (S_n)) occurs due to an external energy impact. When the excited electron falls back to its ground state, energy is released in form of radiation or heat.

Luminescence is classified according to the type of excitation (photoluminescence, chemiluminescence, electroluminescence, thermoluminescence, etc.) and the nature of the excited state from which emission occurs. In the case of photoluminescence, excitation happens due to absorption of photons. The emission is either defined as fluorescence or phosphorescence, if relaxation of the electron is spin-allowed or spin-forbidden, respectively. Molecules pursuant to this phenomenon, are called luminophores or dyes.

2.1.1. Absorption

In photoluminescence, a photon with certain energy is absorbed by a molecule and an electron is promoted from its ground state to an electronically higher energy level. The energy difference between the ground state and the excited state equals the energy of the absorbed photon. Possible transitions of an electron between orbitals upon the absorption of light, are shown exemplary in **Figure 1**.

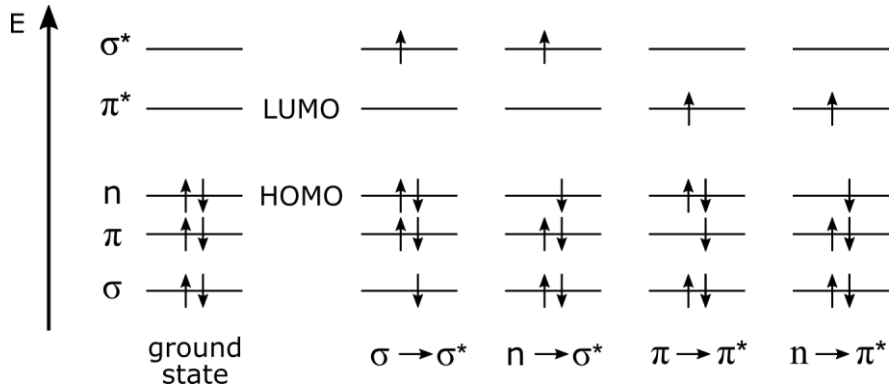

Figure 1: Exemplary presentation of possible electronic transitions upon absorption of light

The energy required for different transitions is dependent on the energy difference of the involved orbitals. The transition from HOMO (highest occupied molecular orbital) to LUMO (lowest unoccupied molecular orbital) requires the lowest amount of energy. Therefore, it is the most common transition possibility. The energies required for different transitions vary in the following order:

$$n \rightarrow \pi^* < \pi \rightarrow \pi^* < n \rightarrow \sigma^* < \sigma \rightarrow \pi^* < \sigma \rightarrow \sigma^*$$

In the case of luminescence, mostly $\pi \rightarrow \pi^*$or $n \rightarrow \pi^*$ transitions are observed, which require light energy in the UV-VIS range. The energy for $\pi \rightarrow \pi^*$ transitions can be decreased by extension of the conjugated system of the fluorescent dye.

The absorbance A(λ) is defined as the absorbance efficiency of a medium (luminophore) at a certain wavelength and is expressed by Lambert-Beer law. The molar absorption coefficient Ɛ describes the ability of a medium to absorb light and is specific for different compounds.

$$A(\lambda) = \log(\frac{I_0}{I}) = \varepsilon(\lambda) \cdot c \cdot d \qquad \textbf{Equation 1}$$

A… absorption

I_0… intensity of incident beam

I…. intensity of beam leaving the medium

d… length of cuvette (1 cm)

c… concentration of absorbing species $[\text{mol} \cdot \text{L}^{-1}]$

Ɛ… molar absorption coefficient $[\text{mol} \cdot \text{L}^{-1} \cdot \text{cm}^{-1}]$

2.1.2. Franck-Condon Principle

According to the Born-Oppenheimer approximation, the motions of electrons are much faster compared to the motions of the nuclei (10^{-15} s for electron transitions compared to 10^{-10}-10^{-12} s for molecular vibrations). The more rapid motion of electrons is possible due to the low mass of electrons compared to the mass of a nucleus. This indicates that the positions of the nuclei do not change while an electronic transition takes place. This means, that the distance of the atoms to each other are equal in the ground state as well as in the excited state (**Figure 2**)

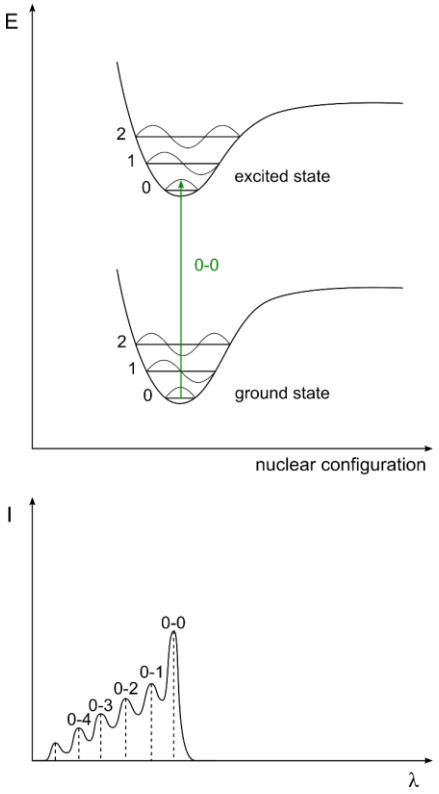

Figure 2: Franck-Condon principle; TOP: Potential energy diagram and vertical transition represented by green arrow; BOTTOM: shape of absorption bands

The promotion of an electron to an energetically higher vibrational state is immediately followed by vibrational relaxation (non-radiative) to the energetically lowest level of the excited state.

The absorption spectrum of a molecule gives information about the vibrational levels of the excited state and the emission spectrum gives information about the vibrational levels of the ground state.

2.1.3. Perrin-Jablonski Diagram

The Perrin-Jablonski diagram (**Figure 3**) illustrates the different energy states of an electron, which can be reached via light energy impact. Radiative transitions such as fluorescence and phosphorescence are depicted as well as non-radiative transitions such as internal conversion, intersystem crossing and vibrational relaxation. Within the Perrin-Jablonski diagram, energy is vertically and spin multiplicity is horizontally arranged.

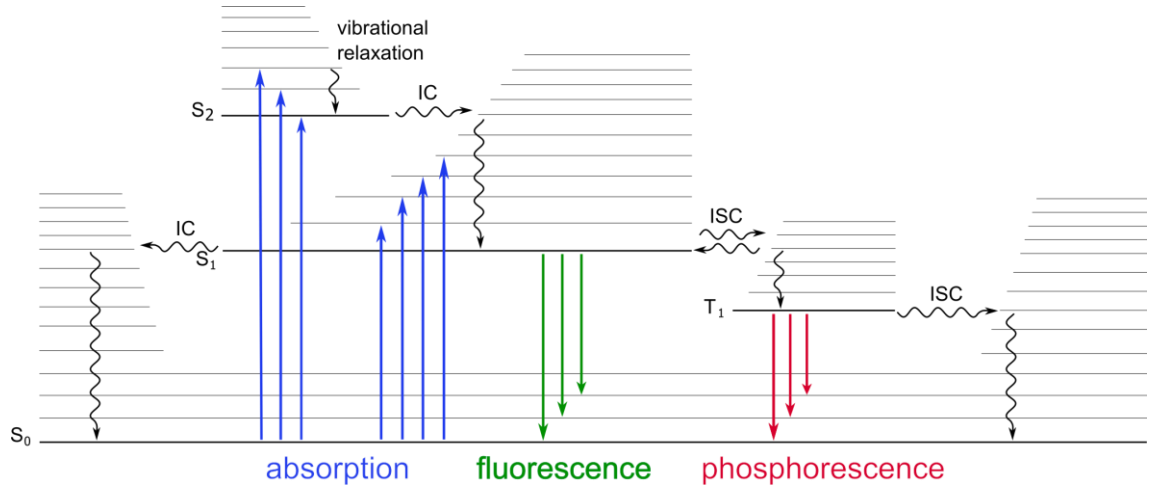

Figure 3: Perrin-Jablonski diagram

Via light absorption, an electron can be promoted from its ground state S_0 to one of the vibrational levels of the excited singlet states S_1 or S_2. Once, in an excited state, relaxation to the ground state is possible in multiple ways. Perrin-Jablonski diagram displays the possible de-excitation processes, which are described in the following sections.

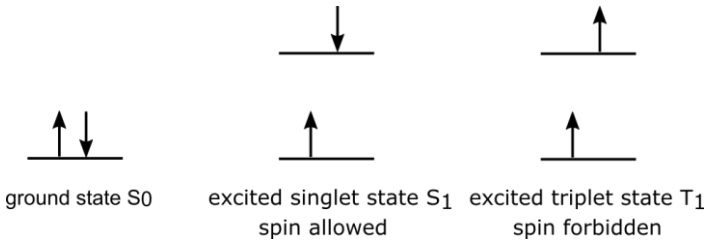

Figure 4:Spin pairing in S_0, S_1 and T_1 state

In **Figure 4** spin pairing of the ground state S_0 and the spin allowed excited singlet state S_1 as well as the spin forbidden exited triplet state T_1 is illustrated.[3]

Internal conversion

Internal conversion (IC) is a non-radiative transition of an electron from an energetically higher to an energetically lower state within the same multiplicity. The efficiency of IC is dependent on the energy gap between the involved states and decreases with increasing energy gap. Due to this, a conversion from S_2 to S_1 is more efficient than a conversion from S_1 to S_0. Therefore, IC from S_1 to S_0 competes with other transition possibilities such as fluorescence and intersystem crossing (ISC) to the triplet state T_1.

Fluorescence

Fluorescence is the emission of photons, released during relaxation of an electron from the excited singlet state S_1 to different vibrational levels of the ground state S_0. The lifetime of fluorescence is in the nanosecond range (**Table 1**). The emitted light has lower energy than the absorbed light and leads to bathochromically shifted fluorescence spectra in respect to the corresponding absorption spectrum. This can be explained by prior vibrational relaxation of the electrons to the lowest vibrational level of the S_1 state before emission takes place. The shift between absorption maximum and emission maximum is called “Stokes shift”. In general, the emission and absorption spectra are mirror images. This phenomenon occurs due to similar spacing of the vibrational energy levels in ground state and excited state.

Intersystem crossing

Intersystem crossing (ISC) is another possible de-excitation process originating from S_1 state towards the triplet state T_1 between isoenergetic vibrational levels. This transition includes a change in multiplicity, which is quantum-mechanically forbidden. This transition occurs if spin-orbit coupling is strong enough.

Phosphorescence

Phosphorescence is the emission of photons, released during relaxation of electrons from the triplet state T_1 towards the ground state S_0. This transition is quantum-mechanically forbidden due to different multiplicities of T_1 and S_0. Phosphorescence always follows intersystem crossing, which is also quantum-mechanically forbidden. Hence, the time rate of

phosphorescence is very slow and can be up to seconds (**Table 1**). Non-radiative relaxations (reversed ISC, vibrational relaxation) are favoured at higher temperatures. In contrast, rigid media or low temperatures enhance the lifetime of the triplet state and phosphorescence can be enhanced. Emission spectrum of phosphorescence has even lower energies than fluorescence and thus its further bathochromically shifted.

Delayed fluorescence

Delayed fluorescence is the emission of photons, released during relaxation from S_1 towards S_0 after ISC to T_1 and following reversed intersystem crossing back to S_1 took place. Reversed ISC can happen if the energy difference between excited singlet state S_1 and triplet state T_1 is small enough and the lifetime of T_1 long enough. The emission spectra of fluorescence and delayed fluorescence are identical. However, the lifetime of delayed fluorescence is much longer (10^6 longer) due to the intermediate triplet state of the electrons. Delayed fluorescence is thermally activated and is favoured at higher temperatures. This process is called thermally activated delayed fluorescence (TADF). Delayed fluorescence can also occur via triplet-triplet annihilation (TTA). In this case, energy is transferred from one excited molecule in the triplet state to a second molecule in the triplet state. As a result, one molecule returns to the ground state and the other molecule is promoted to an energetically higher state.

Table 1: Characteristic duration of absorption and possible de-excitation processes

Process	characteristic duration
Absorption	10^{-15} sec
Vibrational relaxation	10^{-12}-10^{-10} sec
Fluorescence	10^{-10}-10^{-7} sec
IC	10^{-10}-10^{-8} sec
ISC	10^{-11}-10^{-9} sec
Phosphorescence	10^{-6}-1 sec

2.1.4. Quantum Yield

Excited molecules which are able to fluoresce or phosphoresce do not release their entire energy via radiative de-excitation processes. The quantum yield is a value which describes the probability of de-excitation through fluorescence or phosphorescence, rather than by a non-radiative mechanism and is defined as the ratio between the number of absorbed and emitted photons. The quantum yield Φ can be calculated via **Equation 2**.

$$\Phi = \frac{emitted\ photons}{absorbed\ photons} = \frac{\tau_s}{\tau_r} = k_r \cdot \tau_s \qquad \textbf{Equation 2}$$

τ_s ... lifetime of excited state
τ_r … radiative lifetime
k_r … radiative rate constant

Experimental determination of the quantum yield can be performed in two different ways. The "relative quantum" yield is obtained by comparison of the emission spectra of the examined sample and a reference with known quantum yield. Calculation can be done using **Equation 3**. Within this work, quantum yields were determined through this comparative method.

$$\Phi = \Phi_{ref} \cdot \frac{A_{em}}{A_{em,Ref}} \cdot \frac{1 - 10^{-abs_{ref}}}{1 - 10^{-abs}} \cdot \frac{\eta^2}{\eta_{ref}^2} \qquad \textbf{Equation 3}$$

Φ ..... quantum yield of the sample
Φ_{ref} ..... quantum yield of reference
A_{em} ..... integrated emission spectrum of sample
$A_{em,\ ref}$ ...integrated emission spectrum of reference
abs_{ref} ... absorption of sample at excitation wavelength
abs_{ref} ... absorption of reference at excitation wavelength
η ..... refraction index of solvent

The second possible method is the "absolute measurement" of the quantum yield using an integrating sphere. An integrating sphere is a device which collects all the emission originating from the sample and thus enables an absolute measurement of the quantum yield.[4]

2.1.5. Luminescence Lifetime

After promotion of a molecule to its excited state, several processes of de-excitation can occur such as fluorescence emission or non-radiative transitions (IC or ISC). These de-excitation processes do not occur immediately, which means the molecule remains in the lowest vibrational level of the excited state for a certain time period. The average time before luminescence occurs is defined as luminescence lifetime $\boldsymbol{\tau}$. For determination of the lifetime it is important to know that the mentioned de-excitation processes follow first order kinetics.

$$-\frac{d\,[A^*]}{dt} = k \cdot [A^*] \qquad \textbf{Equation 4}$$

[A^*] …concentration of species A in the excited state

k……..sum of all de-excitation rates (radiative and non-radiative)

Integration of **Equation 4** yields in **Equation 5**, where $\boldsymbol{\tau}$ is the lifetime of the excited state.

$$[A^*]_t = [A^*]_0 \cdot e^{\frac{-t}{\tau}} \qquad \textbf{Equation 5}$$

$[A^*]_t$ …time evolution of the excited state

[A^*] …concentration of excited molecules at time 0

2.1.6. Quenching

Quenching decreases the intensity of an emission and thus is a de-excitation process. In contrast to all prior mentioned de-excitation processes, quenching is no intrinsic phenomenon. It describes a photophysical interaction between an excited molecule M^* and a quencher molecule Q, which leads to de-excitation of the excited molecule M^*. Intrinsic de-excitation processes compete with these intermolecular quenching processes and thus luminescence characteristics such as quantum yield and lifetime are strongly affected. Intermolecular quenching is a bimolecular process and can occur by different mechanisms, classified as either dynamic or static quenching. Both quenching mechanisms require contact between the fluorophore and the quencher molecule.

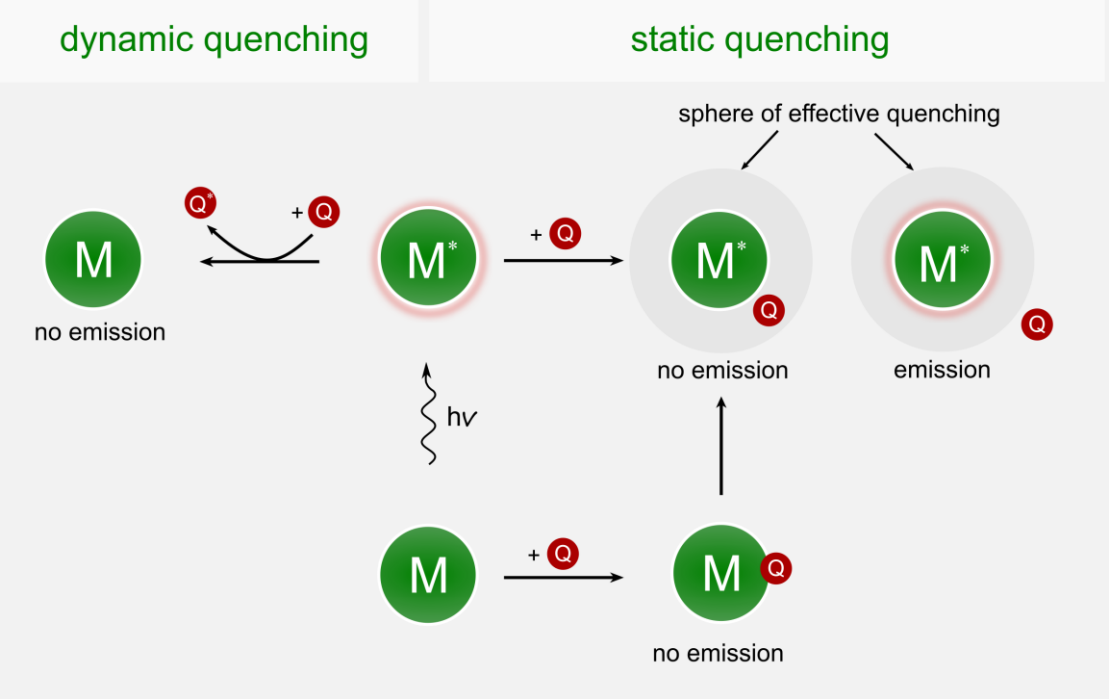

Figure 5: Mechanisms of dynamic and static quenching

Dynamic Quenching

Dynamic quenching describes a de-excitation process which occurs by collision of an excited molecule (M^*) with a quencher molecule (Q). Collisions of M^* and Q result in a non-radiative energy transfer and thus in de-excitation of the molecule to its ground state. The probability of dynamic quenching is higher, if the excited state of the molecule (M^*) exhibits long lifetime. It is a diffusion-controlled process, which means the rate constant of dynamic quenching is time dependent. Dynamic quenching leads to a decrease of fluorescence intensity and the lifetime. This quenching process can be described by the Stern-Volmer equation (**Equation 6**)

$$\frac{I_0}{I} = \frac{\tau_0}{\tau} = 1 + k_q \cdot \tau_0 \cdot [Q] = 1 + K_{SV} \cdot [Q] \qquad \textbf{Equation 6}$$

I_0….fluorescence intensity in absence of Q

I…..fluorescence intensity in presence of Q

τ_0…lifetime in absence of Q

τ….lifetime in presence of Q

[Q]..concentration of quencher

K_{SV}..Stern-Volmer constant = $k_q \cdot \tau_0$

Static Quenching

Static quenching describes a de-excitation process which occurs via formation of a non-fluorescent complex out of the fluorescent molecule M and the quencher molecule Q. The formation of complex MQ is possible in the ground state (M) or in the excited state (M^*). The area within Q can be located to gain quenching is called sphere of effective quenching. If the distance is larger, no quenching occurs. Static quenching causes a decrement of fluorescence intensity. However, it does not influence the lifetime of the un-complexed fluorophore M.

2.1. Chemical Sensors

This chapter is based on the books “Chemical sensors” by Gründler and “Molecular fluorescence” by Valeur.[1,3] All other references are cited independently.

A chemical sensor is an analytical instrument that combines a sensitive layer, which goes through chemical changes during contact with a specific analyte, and a transducer which converts this chemical change into a signal suitable for measurement. Chemical sensors can be based on different transduction methods and are classified as either electrochemical or optical sensors.[5,6]

Ideally, a sensor should work reversibly and continuously. This means, the response of the sensor to changes of the analyte concentration needs to be dynamic to enable real-time information on the presence and concentration of an analyte in a certain sample.[7] Furthermore, chemical sensors should:

- be able to transform chemical quantities into an electrical signal,
- have short response time,
- show constant long-time activity,
- be small and cheap,
- and should be selective to one specific analyte.

2.1.1. Optical Chemosensors (Optodes)

The working principle of optical chemosensors is based on systems where information is collected by measurement of photons. This means, the principle is based on the measurement of reflectance, absorbance and luminescence which occurs in the UV, VIS and NIR range as well as infrared and Raman radiation or the refractive index. Optical sensors have found many applications in medicine, biotechnology and the chemical industry. An optical sensor consists of a receptor, an optical transducer and a photodetector. The receptor is a specific recognition element and can be of synthetic or biological origin (chemo- or biosensor) and is connected to the transducer. The transducer is the part of the molecule which changes its optical properties dependent on the presence or absence of an analyte. The photodetector records the signal differences and supplies the output signal in the form of an electrical signal. Optical sensors are suitable for the sensing of a broad range of analytes such as O_2, CO_2, pH, NH_3 or ionic species

(e.g. Na^+, K^+). Furthermore, temperature determination is possible. Fluorescence sensors are probably the most common due to the variety of parameters which can be measured (intensity, decay time, quenching efficiency, etc.), their high sensitivity and selectivity.[8,9]

2.1.2. Optical pH sensors

pH, a value of huge importance in many aspects of life. The pH value strongly influences many biological processes and thus is of great interest in a wide range of fields such as medicine, environmental and marine science as well as in biotechnology. Furthermore, pH is often a crucial parameter for chemical reactions that take place in an aqueous environment which makes pH an important parameter in chemical process control too. Due to that, there is a huge interest in the development of new pH sensors.

The pH value is defined as the negative decadic logarithm of the proton activity:

$$pH = -\log a\,(H^+) \approx -\log c\,(H^+) \qquad \textbf{Equation 7}$$

Following equilibrium reactions occur in aqueous solutions:

$HA + H_2O \rightleftharpoons A^- + H_3O^+$… for acids characterized by the equilibrium constant $\mathbf{K_a}$

$B + H_2O \rightleftharpoons BH^+ + OH^-$… for bases characterized by the equilibrium constant $\mathbf{K_b}$

$$K_a = \frac{[A^-] \cdot [H_3O^+]}{[HA]} \qquad \textbf{Equation 8}$$

$$K_b = \frac{[BH^+] \cdot [OH^-]}{[B]} \qquad \textbf{Equation 9}$$

The decadic logarithm of the equilibrium constant (K_a, K_b) gives either the pK_a or pK_b, which are commonly used to classify the strength of an acid or base, respectively.
By derivation the so-named Henderson-Hasselbalch equation (**Equation 10)** can be obtained. The Henderson-Hasselbalch equation can be used to calculate the pH of a buffer solution, which consists of an acid and the salt of their conjugated base. A buffer has the ability to compensate the addition of certain amounts of acid or base and thus prevent changes of the pH value.

$$pH = pK_a + log\frac{[B]}{[A]}$$ **Equation 10**

This relation can be adapted for photometric signals of fluorophores to **Equation 11**, where A describes the form of the fluorophore in acidic and B in basic environment.

$$pH = pK_a + log\frac{I - I_A}{I - I_B}$$ **Equation 11**

The most common chemical sensor used for pH measurement is the glass electrode. Its working principle is based on electrochemical transduction. As alternative to the glass electrode, optical sensors can be utilized. The advantage of optical sensors compared to the pH electrode is the easy miniaturization, insensitivity against electrical interferences, possibility of contactless measurements and cost-effective production. In addition, optical sensors do not require a reference electrode and thus eliminating commonly known drift phenomena caused by the reference electrode of pH electrodes. On the contrary, optical sensors only have a limited dynamic range, have low stability at high temperatures and different origins of drift.

Optical pH sensors typically utilize a pH-sensitive indicator dye which is immobilized in a polymer matrix to obtain a sensor layer. The indicator dye can be protonated/deprotonated and changes its optical properties based on the protonation degree.
Additionally, the indicator dye needs to fulfil many requirements in order to be successfully used in optical pH sensing. The indicator dye needs to have a suitable pK_a, good photostability, high molar absorption coefficients and absorption bands in the VIS region as well as thermal and chemical stability.
In order to obtain a solid-state sensor layer, the indicator dye needs to be incorporated in a polymer matrix. This matrix needs to be hydrophilic to enable proton diffusion. Typically, sol-gel materials or hydrogels are utilized for this purpose.[10] However, the low mechanical and thermal stability can lead to problems during steam-sterilization and be a potential cause of drift. Additionally, low compatibility of the sensor matrix with the indicator dye can lead to leaching of the dye out of the matrix and therefore cause drift. This can be overcome by covalent attachment of the dye to the sensor matrix.

An optical pH sensor does not directly measure the concentration of hydronium ions in the solution but measures the concentration of the pH indicator dye in its (de-)protonated form. High sensitivity is limited within a range of ±1.5 pH units around the pK_a of the used receptor, which can be explained by the Henderson-Hasselbalch equation (**Equation 10**). At the pKa value of the indicator, the ratio of protonated and deprotonated form is 1:1 and the highest sensitivity is obtained. However, at e.g. two pH units above or below the pKa, the ratio is already 99:1 leading to hardly any sensitivity.

The detection range can be extended if a mixture of dyes, exhibiting different pK_a values, is used.[11] However, in most cases the sensitivity in a distinct pH range is sufficient. For example, in marine science the highest sensitivity is required at around pH 8.0 while in biotechnology high sensitivity is important at around pH 6.0. In biological applications, emission of the indicator dye in the far-red or NIR region is desired due to the low fluorescence background of biological molecules in this wavelength region.[10]

PET effect based pH indicators

The photoinduced electron transfer (PET) is one of the most common sensing mechanisms applied in optical pH sensing.

PET indicator dyes need to carry a pH-sensitive group (receptor), which can exist either in protonated or deprotonated form. Such functional groups usually are phenols or amines. The receptor and the fluorophore are linked via a spacer. The purpose of the spacer is to electronically separate the conjugated π-system of the fluorophore and the receptor. In **Figure 6** a schematic illustration of the PET effect (**A**), and an inhibited PET effect (**B**) is shown.

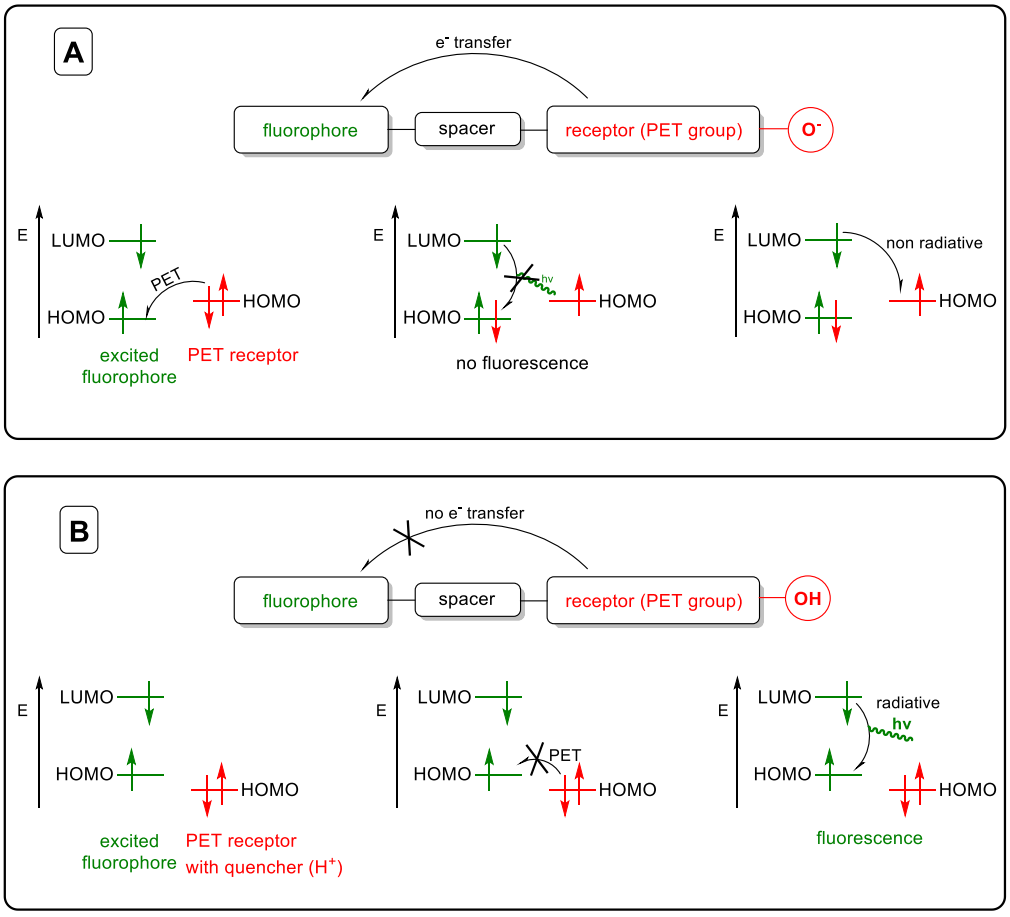

Figure 6: A) schematic illustration of a PET process, B) inhibition of a PET process which leads to fluorescence emission

In case of a reductive PET effect, the indicator dye is in the so-called "off-state" if the pH-sensitive PET group is deprotonated (**Figure 6**, **A)**. In the "off-state" an intramolecular electron transfer from the HOMO of the PET group to the HOMO of the excited fluorophore can occur. The transferred electron inhibits radiative de-excitation of the excited electron, which means fluorescence is quenched.

If the pH-sensitive PET group gets protonated, the involved energy levels are shifted to a lower values due to a change in the redox potential **(Figure 6, B)**. In this case, the PET effect is inhibited and radiative de-excitation is possible. Now, the indicator dye is in the "on-state."
In case of an oxidative PET the effect is reversed. This means, protonation of the pH-sensitive group leads to the "off-state" and deprotonation to the "on-state" of the dye.
The absorption spectrum of a PET indicator dye is not affected by changes in pH, whereas the intensity of the emission spectrum is drastically affected. Importantly, the shape of absorption and emission spectrum is not dependent on pH.

ICT effect based pH indicators

In contrast to the PET effect, indicator dyes based on the ICT (intramolecular charge transfer) mechanism undergo changes in spectral properties upon interaction with an analyte. Mostly, a spectral shift occurs due to a change in the internal charge distribution of the molecule. This influences the HOMO-LUMO levels of the dye. Therefore, the pH-sensitive group need to be in direct contact with the π-conjugated system of the fluorophore to generate a "push-pull" electron system.[12]

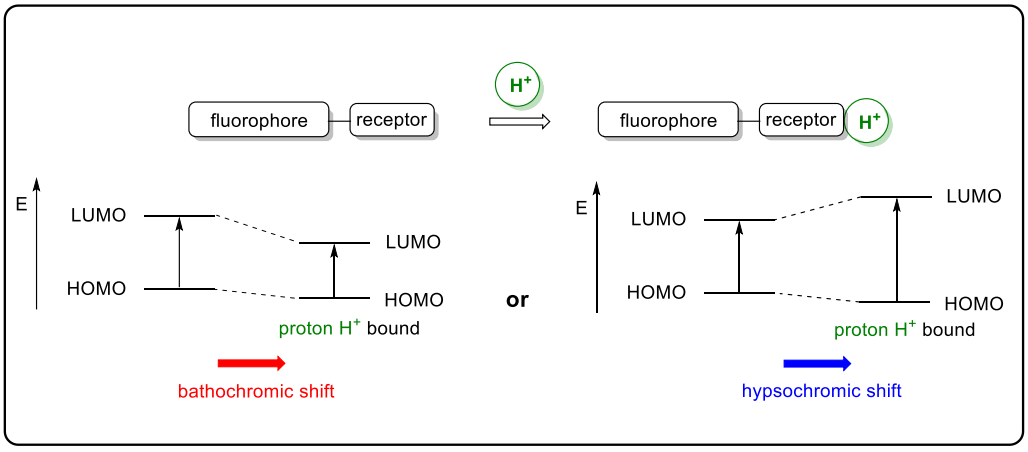

Figure 7: Schematic illustration of ICT effect; influence on HOMO and LUMO levels upon interaction with the proton H^+

2.2. Rylene dyes

The rylene structure is based on naphthalene units. Perylenes are the most popular and lowest homologues within this dye class, exhibiting the smallest conjugated π-system with an absorption around 420 nm Its structure is based on two naphthalene units, linked in peri-position. Further extension of the perylene core by additional naphthalene units in peri-position leads to the formation of higher rylene homologues such as terrylenes and quaterrylenes. Different rylene homologues are illustrated in **Figure 8**. The prefix peri is used when a 2-fold substitution at the 1,8-position of the naphthalene occurs. Rylene derivates are well known for their extraordinary photophysical and photochemical stability and their high fluorescence brightness (product of fluorescence quantum yield and molar absorption coefficient).[13,14]

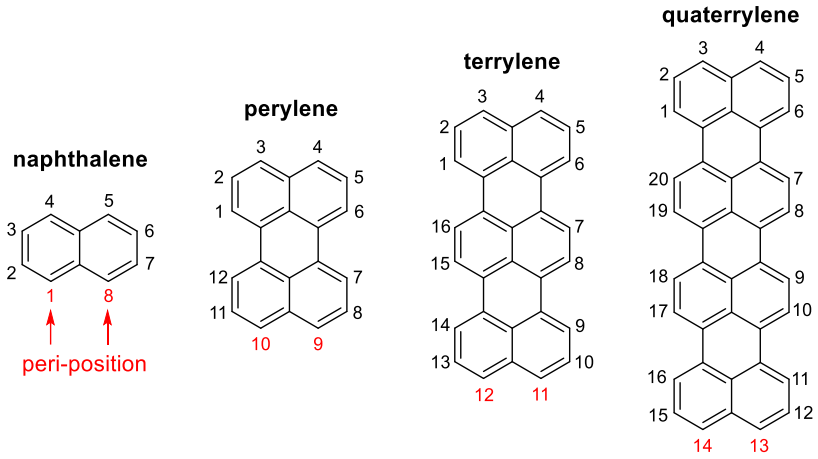

Figure 8: Ground structure of rylene homologues, red marked = peri-position

The solubility as well as the absorption and emission of rylene dyes can be influenced by modification with hydrophobic/ hydrophilic or electron-withdrawing/electron-donating groups. The introduction of such groups can be conducted at the bay region and the terminal regions of the rylene dye. Enlargement of the π-conjugated system and other modifications enables covering the visible (400-760 nm) and NIR region (760-1200 nm) of the electromagnetic spectrum with this rylene series (**Figure 8)**.[15] For example, the addition of one naphthalene unit (**PDI** to **TDI**) results in a bathochromic shift of the absorption maxima of about 100nm.

2.2.1. Rylene diimides

This work focuses on rylene diimides. Rylene diimides possess an imide group, bearing a bulky alkyl or aryl substituent, at each terminal position of the hydrophobic rylene core and thus exhibit enhanced solubility in organic solvents (**Figure 9**). Rylene diimides have gained importance as industrial colorants and vat dyes and are suitable for applications in photovoltaic devices, light-emitting diodes, dye lasers, fluorescence light collectors and optical sensors in the last decades. Within the family of rylene diimides, perylene diimides (**PDI**) are the most known and investigated ones and were first commercialized in 1913. [16–19]

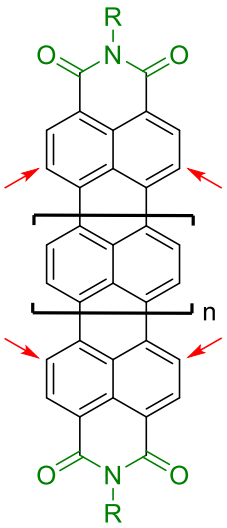

Figure 9: Exemplary structure of a rylene diimide (green marked = terminal imide position, red marked = bay region, perylene n=0, terrylene n=1, quaterrylene n=2)

Perylene diimides

Perylene derivates have gained much attention in research over the last decades. Perylene diimides are the most established modifications of perylenes and exhibit optical properties desirable for the application in optical sensing. They exhibit high molar extinction coefficients of 30 000 – 90 000 mol L^{-1} cm^{-1} and quantum yields close to 1 as well as high thermal, chemical and photochemical stability.[20,21] By extension of the π-conjugated system of a perylene diimide the higher homologues terrylene diimide and quaterrylene diimide can be obtained. The extension of the conjugated π-system causes a bathochromic shift of the absorption and emission spectrum. The solubility of a perylene diimide is strongly influenced by substituents at the terminal imide position. Introduction of sterically demanding groups inhibits plan parallel

stacking of the molecules and thus strongly increase the solubility of the compound.[22] Modification at the bay region can lead to enhanced solubility and a bathochromic shift of absorption and emission spectra. The usage of perylene diimides as indicators for optical pH sensing was already successfully examined several times but showed hysteresis and migration effects of the dye.[18,23,24] Due to this, further optimizations for the usage as pH indicators were attempted within this work.

Terrylene diimides

The first red-emitting terrylene diimide was synthesized in 1997 to close the emission gap between perylene diimides and quaterrylene diimides emitting in the yellow to red range and in the NIR range, respectively.[25] In general, unsubstituted terrylene diimides absorb at about 650 nm. The blue colored fluorophore features very good photophysical properties over many other deep-red emitting fluorophores such as high photostability and high quantum yields.[16] Solubility improvement of the hydrophobic terrylene core can be reached by modification of the terminal imide position and the bay region. Optical and electronic properties are not significantly affected by functionalization of the terminal imide position. However, modification of the bay region has a strong influence on these properties and can be deployed to tune absorption and emission bands of the chromophore to the desired range.[26] In contrast to perylene diimides, terrylene diimides have not been used so far as pH indicators in optical sensors. Within this work, the synthesis of a pH-sensitive terrylene diimide emitting in the far-red range was attempted.

2.3. Palladium catalyzed organic reactions

2.3.1. Suzuki-Miyaura cross-coupling

The Suzuki-Miyaura cross-coupling (or Suzuki cross-coupling) is a palladium catalyzed C-C cross coupling reaction between an organoboronic acid and a halide in a basic environment. Since the discovery of the carbon-carbon bond forming reactions in the 1917's, they attained strong interest and became one of the most important processes in the field of organic synthesis.[27] As reagent not only boronic acids but organoboranes, organoboronic esters and potassium trifluoroborates can be used. Besides the mild conditions required, this versatility of the boron species is the main advantage of the Suzuki reaction over other C-C bond formations. Furthermore, this reaction is compatible with aqueous conditions and shows excellent functional group tolerance.[28–30] The catalytic cycle of Suzuki cross-coupling is illustrated in **Figure 10**. The mechanism begins with an oxidative addition of the halide to the Pd^0 catalyst. In this step, the Pd(0) is oxidized to Pd(II). In the next step, the halide is replaced by the used hydroxide or alkoxide base. Simultaneously, the base adds to the organoborane and a borate is formed. As a result, the R_2 residue attached to the organoborane gets more nucleophilic. This reaction is followed by transmetalation reaction. In this step, the nucleophilic R_2 residue attacks the Pd(II) and replaces the hydroxyl residue. By reductive elimination, the final C-C coupled product is released and the palladium catalyst is regenerated. The catalytic cycle can start again.[28]

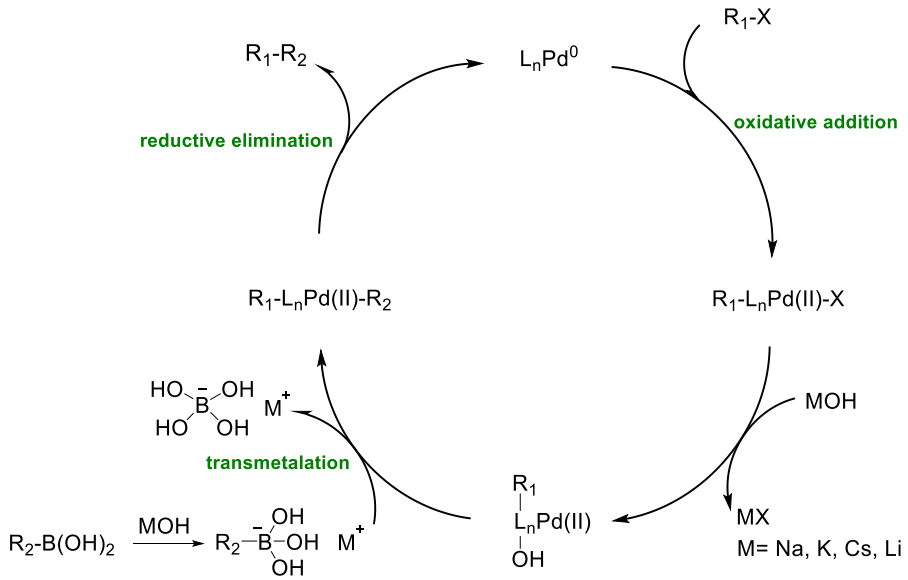

Figure 10: Catalytic cycle of palladium catalyzed Suzuki cross-coupling reaction

2.3.2. Miyaura-borylation

As mentioned in the previous section, the Suzuki cross-coupling is one of the most important methods for C-C bond formation. For this reaction certain reagents such as organoboronic acids, organoboranes or organoboronic esters are necessary. The Miyaura-borylation reaction enables the synthesis of a variety of organoboron compounds and thus provides the access to a wide range of different educts for the use in Suzuki cross-coupling without lithium or magnesium intermediates.[31] The Miyaura-borylation is a palladium catalyzed reaction between an organohalide and a borylation reagent and shows high tolerance for functional groups. The most common borylation reagent is bis(pinacolato)diboron (**Figure 11**).[32]

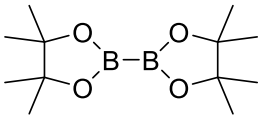

Figure 11: Bis(pinacolato)diboron; common borylation reagent for Miyaura-borylation

2.3.3. Palladium catalyzed C-O cross coupling of primary alcohols

Another palladium catalyzed reaction is the C-O cross-coupling of primary alcohols and aryl halides. The reaction occurs in the presence of a base, a primary alcohol and an aryl halide. The general catalytic cycle is illustrated in **Figure 12**.

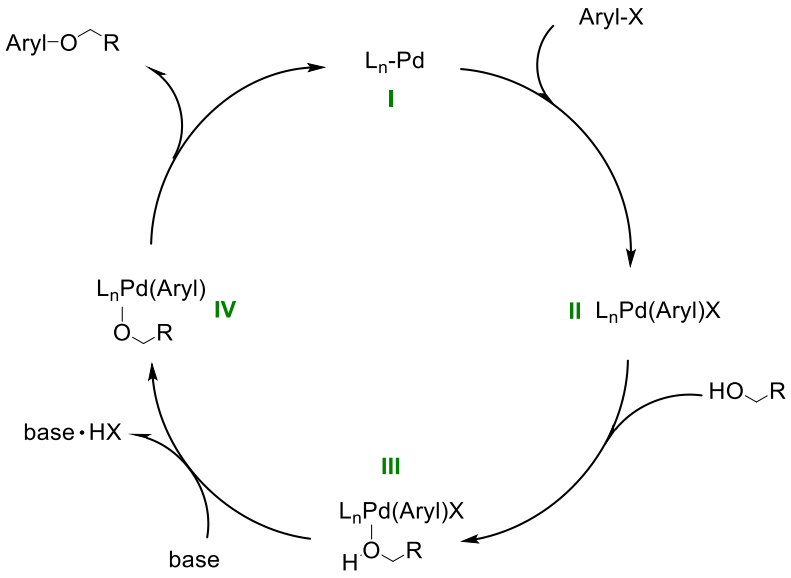

Figure 12: Catalytic cycle of palladium catalyzed C-O cross coupling

3. Materials and Methods

3.1. Materials

The solvents cyclohexane (Cy), ethanol (EtOH), methanol (MeOH), tetrahydrofuran (THF), ethylacetate (EE), toluene, NaCl and HCl conc. were obtained from VWR chemicals (www.vwr.com). Dichloromethane (DCM) was purchased from Fisher Scientific (www.fishersci.com). Methyl 3-formyl-4-hydroxybenzoate was obtained from Fluorochem (www.fluorochem.co.uk). Lumogen Red was purchased from Kremer Pigmente (www.kremer-pigmente.de). The deuterated solvents Chloroform-*d* and Methylene Chloride-d_2 for NMR were purchased from Eurisotop (www.eurisotop.com). Silica-gel 60 (0.063-0.200 mm) for column chromatography was obtained from Merck (www.merck.at). All other chemicals were purchased from Sigma Aldrich (www.sigmaaldrich.com) or TCI Europe (www.tcichemicals.com). The purchased chemicals were used as received without further purification.

3.2. Methods

Mass spectroscopy was executed on Micromass TofSpec 2E Time-of-Flight Mass Spectrometer (HR-MS) at TU Graz, at the ICTM and on Advion expression CMS (MS). ^{1}H and COSY spectra were recorded on a 300 MHz Bruker Instrument (www.bruker.com) in $CDCl_3$ or CD_2Cl_2 as solvent using TMS as standard. Absorption spectra were recorded via a Cary 50 UV-Vis photometer from Varian (www.agilent.com) utilizing optical glass cuvettes from Hellma Analytics (www.hellma-analytics.com). Excitation and emission spectra were recorded with a FluoroLog 3 spectrofluorometer from Horiba Scientific Jobin Yvon (www.horiba.com), equipped with R2658 photomultiplier from Hamamatsu. Relative fluorescence quantum yields Φ were determined with the same spectrofluorometer using dibutoxy-azaBODIPY (Φ = 0.36 in toluene)[33] and diethylthiadicarbocyanine iodide (Φ = 0.35 in EtOH)[34] as reference dyes.
Fluorescence decay times were determined using time correlated single photon counting (TCSPC). This was performed on a FluoroLog 3 spectrofluorometer with a DeltaHub module and NanoLEDs (λ = 435 nm and 635 nm, Horiba) as light source. Data analysis was done with DAS6 software (www.horiba.com) with a mono-exponential fit.

Photostability of the dyes was determined by illumination with a Metal-Halogen-lamp (ConstantColor™ CMH Precise™, GE Lightening) with 14.000 nominal lumens. An UV blocking filter (UV-B, QIOPTIQ)and a heat protection filter (CALFLEX X; QIOPTIQ) were used to narrow the lamp spectrum of 400 to 700 nm. The dye solution in THF was stirred in a screw-capped quartz cuvette during irradiation. The photon flux, transmitted through the quartz cuvette, was measured via a light-meter (LI-250A). To avoid saturation of the light sensor, a neutral-density filter (25%; QIOPTIQ, www.qioptiq.de) was placed in front of it. The absorption spectra were recorded after irradiation periods of 30 min for TDI-4Br, TDI-4Mo, TDI-4Ph and 10 min for dibutoxy-azaBODIPY.

4. Experimental

4.1. Terrylene

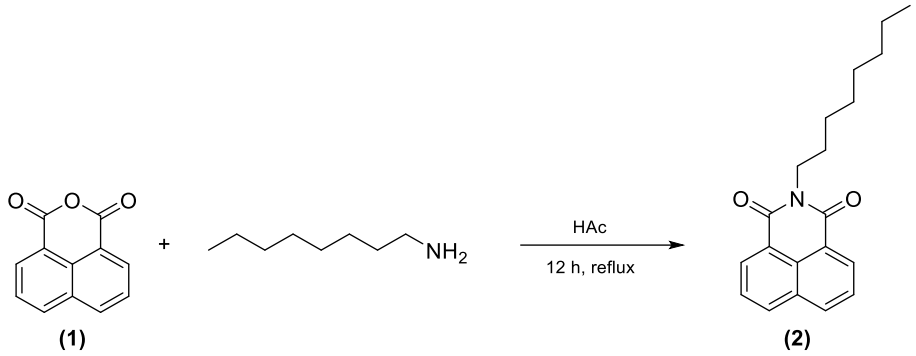

2-octyl-1H-benzo[de]isoquinoline-1,3(2H)-dione (2): The following reaction was carried out under argon atmosphere according to literature.[35] 1,8-naphtalic anhydride **(1)** (4.00 g, 1.00 eq) and 125 mL acetic acid were placed in a dry Schlenk tube. The mixture was heated to 130°C and stirred until the solid was dissolved. Subsequently, n-octylamine (11.4 mL, 3.39 eq.) was added. The reaction mixture was heated to reflux for 14 h. After the reaction was cooled to room temperature, acetic acid was removed under reduced pressure. The crude product was purified by column chromatography (silica gel, cyclohexane (Cy)/ dichloromethane (DCM); from 10:1 to 3:2) to obtain the product as a yellowish oil. To remove other impurities, the product was washed with heptane After the washing process the oil crystallized at ambient conditions yielding a white solid. (3.32 g, 53 %).

^{1}H NMR (300 MHz, Chloroform-*d*) δ 8.53 (d, *J* = 7.2 Hz, 2H), 8.14 (d, *J* = 8.1 Hz, 2H), 7.69 (t, *J* = 7.7 Hz, 2H), 4.23 – 4.04 (m, 2H), 1.71 (dq, *J* = 15.2, 7.7, 6.9 Hz, 2H), 1.43 – 1.18 (m, 10H), 0.84 (t, *J* = 6.3 Hz, 3H).

MS of **(2)** m/z: [MH^+] calc. for $C_{20}H_{23}NO_2$: 309.4; found: 310.2

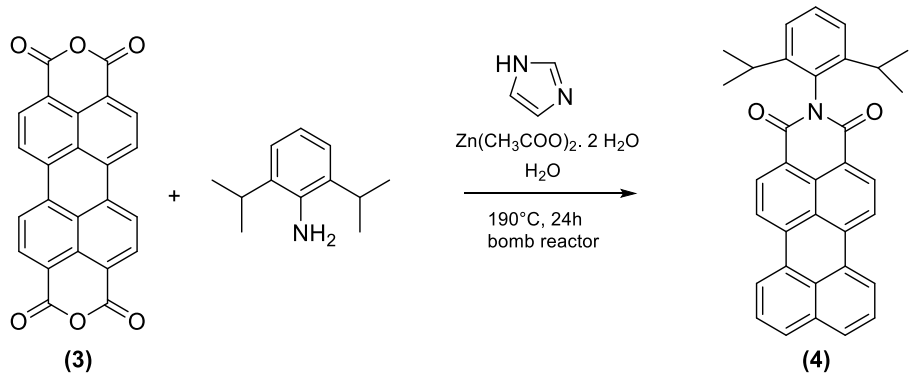

(3) (4)

2-(2,6-diisopropylphenyl)-1H-benzo[10,5]anthra[2,1,9-def]isoquinoline-1,3(2H)-dione (4): The reaction was carried out according to literature[36], in a bomb reactor with a volume of 23 mL. Diisopropylaniline (0.254 g, 1.00 eq.), perylene-3,4,9,10-tetracarboxylic dianhydride **(3)** (1.18 g, 2.00 eq.), imidazole (5.68 g, 55,6 eq.), zinc acetate dihydrate (0.346 g, 1.36 eq.) and 2.5 mL deionized water, were mixed in the bomb reactor. The bomb reactor was screwed tightly and heated to 190 °C for 24 h. Before the bomb reactor was opened, it was allowed to cool down to room temperature and 1.8 mL HCl conc. were added to the mixture. The mixture was filtered, washed with water and dried in the vacuum drying oven at 60 °C. The reaction was conducted three times. To isolate the crude product out of the filter cake, Soxhlet extraction was performed using chloroform as solvent. The dry filter cakes received from the three reactions were combined and dispersed in 200 mL $CHCl_3$. Prior to the extraction, the mixture was put into an ultrasonic bath to ensure homogeneous particle sizes. Soxhlet extraction was carried out for 17 h. The crude product was purified by column chromatography (silica gel, Cy/DCM, 7+3, 6+4) yielding a red solid (1.93 g, 93 %).

^{1}H NMR (300 MHz, Chloroform-*d*) δ 8.66 (s, 2H), 8.49 (s, 4H), 7.92 (s, 2H), 7.67 (s, 2H), 7.48 (s, 1H), 7.35 (s, 2H), 2.77 (s, 2H), 1.18 (d, *J* = 6.8 Hz, 12H).

MS of **(4)** m/z: [MH^+] calc. for $C_{34}H_{27}NO_2$: 481.6; found: 482.0.

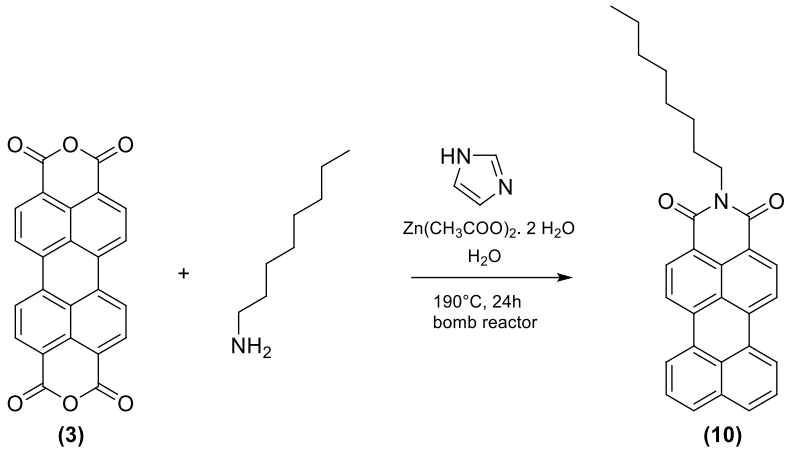

2-octyl-1H-benzo[10,5]anthra[2,1,9-def]isoquinoline-1,3(2H)-dione (10): The reaction was carried out analogously to the synthesis of **(4).** Purification of the crude product was conducted via column chromatography (Cy/EE; 7+3) yielding a red solid (404 mg, 73 %).

^{1}H NMR (300 MHz, Methylene Chloride-d_2) δ 8.00 (d, J = 61.0 Hz, 6H), 7.68 (s, 2H), 7.40 (s, 2H), 4.06 (s, 2H), 1.72 (s, 2H), 1.32 (s, 15H).

MS of **(10)** m/z: [M^+] calc. for $C_{30}H_{27}NO_2$: 433.6; found: 434.1

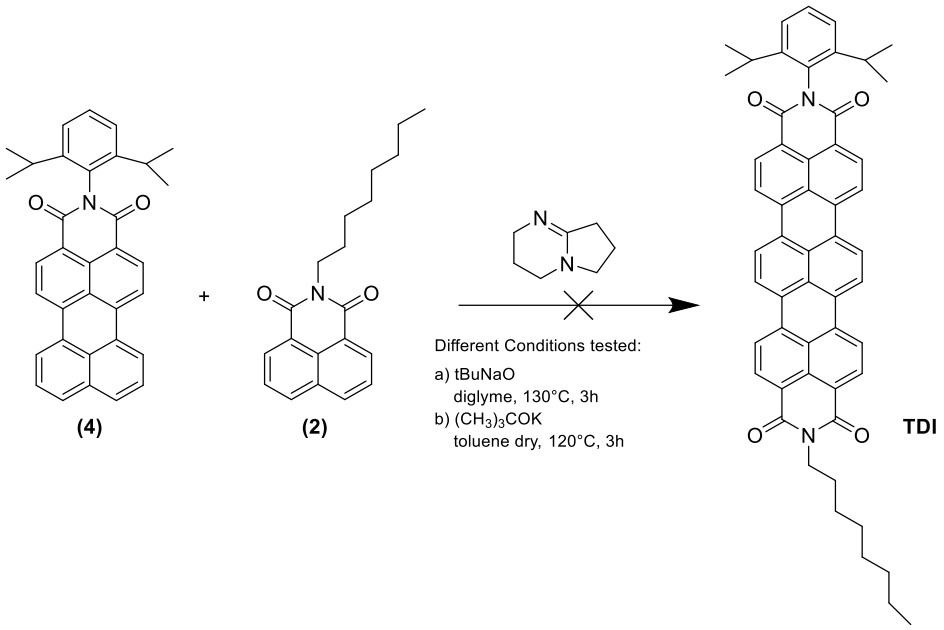

N',N-(2,6-Diisoproplyphenyl)-N'-(5-octyl)terrylene-3,4:11,12-tetracarboxydiimide (TDI): The following reaction was carried out under argon atmosphere according to literature.[17]

Trial a1) one pot synthesis

Compound **(2)** (260 mg, 4.03 eq.), compound **(4)** (100 mg, 1.00 eq.) and sodium tert-butoxide were added into a dry and inert Schlenk tube. 5.3 mL diglyme and 6.7 mL 1,5-diazabicyclo[4.3.0]non-5-ene were added, using a septum. The reaction mixture was heated to 130 °C and stirred for 3 h. During heating, it turned from a red coloured to a dark green coloured mixture. The mixture was allowed to cool down to room temperature and water was added to yield a precipitate. Immediately, the reaction mixture turned red again. During washing with $CHCl_3$ and MeOH, the red precipitate dissolved. No formation of the product was observed by reaction control via TLC and MS method.

Trial a2)

Synthesis of TDI was performed again, using dry toluene as solvent instead of diglyme under argon atmosphere.[35] Therefore, compound **(4)** (50.5 mg, 1.00 eq.) and, compound **(2)** (58.0 mg, 1.74 eq.) were combined in an inert 10 mL Schlenk tube and 2 mL of dry toluene were added.

A second Schlenk tube was charged with potassium tert-butoxide (54.1 mg, 4.59 eq.), diazabicyclo[4.3.0]non-5-ene (77.4 mg, 5.92 eq.) and 2 mL of dry toluene. Both suspensions were heated to 100 °C until the solids were completely dissolved. The solution containing **(2)** and **(4)** was transferred to the second Schlenk tube, containing the bases. The mixture was heated to 120 °C and stirred for 3 h. Afterwards, the mixture was allowed to cool down to room

temperature and was then quenched with 1 M HCl. The green coloured reaction mixture turned red under ambient conditions, immediately. An absorption spectrum was recorded, showing no formation of product.

The reaction was carried out again, using conditions **b)** and again showed no formation of the product.

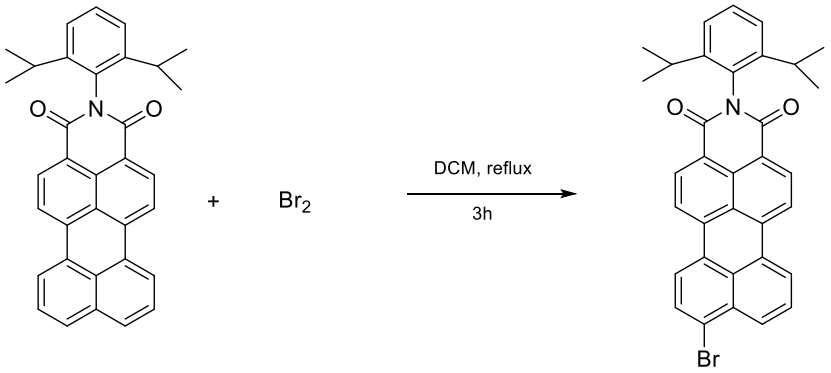

(4) **(9)**

8-Bromo-2-(2,6-diisopropylphenyl)-1H-benzo[5,10]anthra[2,1,9-def]isoquinoline-1,2(2H)dione (9): The reaction was carried out under argon atmosphere according to literature.[35] Compound **(4)** (498.1 mg, 1.00 eq.) and 65 mL DCM were added in a dry 250 mL 2-neck-flask which was adjusted with a reflux condenser and a bubbler. After the solid was dissolved, bromine (0.07 mL, 1.00 eq.) was added in one portion. The reaction mixture was heated to 40 °C (reflux) for 3 h and then cooled to room temperature. The solvent was removed under reduced pressure. The resulting residue was purified by column chromatography (silica gel, Cy/DCM, 7:3, 6:1) to obtain the product as a red solid with a yield of 441 mg (76 %). Due to low solubility of the product, only mass spectrometry was used for identification of the compound.

MS of (**9)** m/z: [MH^+] calc. for $C_{34}H_{26}BrNO_2$: 560.5; found: 560.0.

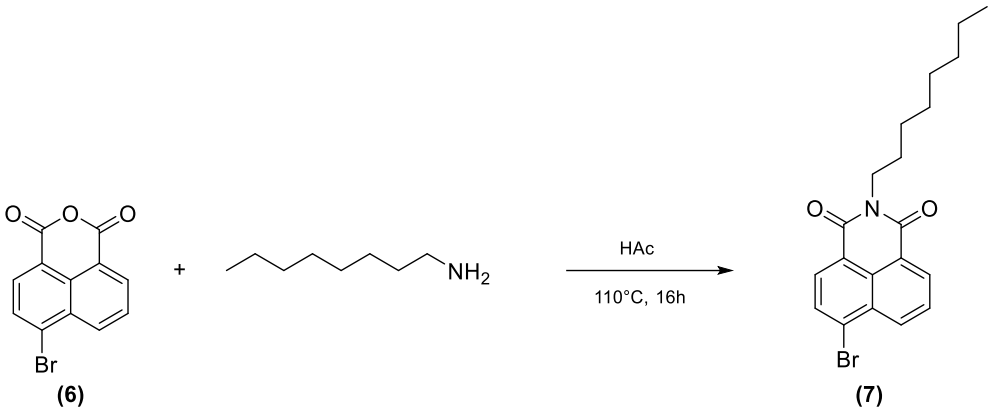

6-Bromo-2-octyl-1H-benzo[de]isoquinoline-1,3(2H)-dione (7): The reaction was carried out analogously to synthesis of **(2)**. A Schlenk flask was charged with 4-bromo-naphthalic anhydride (2.03 g, 1.00 eq.) and 50 mL acetic acid. After the anhydride derivate was dissolved, n-octylamine (3.8 mL, 3.20 eq.) was added. The mixture was heated to reflux for 16 h. After completion it was allowed to cool down to room temperature and acetic acid was removed under reduced pressure. The crude product was purified via column chromatography (silica gel, Cy/DCM) resulting in a white solid (2.63 g, 92 %).

^{1}H NMR (300 MHz, Chloroform-*d*) δ 8.65 (s, 1H), 8.41 (s, 1H), 8.06 (s, 1H), 7.85 (s, 1H), 4.16 (s, 2H), 1.73 (s, 2H), 1.27 (s, 10H), 0.87 (s, 3H).

MS of (**7**) m/z: [MH^+] calc. for $C_{20}H_{22}BrNO_2$: 388; found: 388.0.

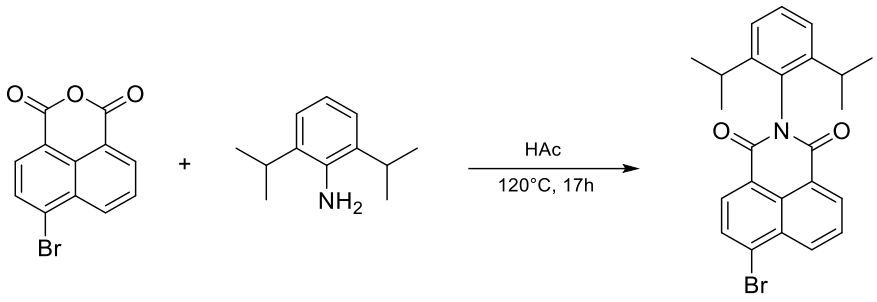

(11) **(12)**

6-Bromo-2-(2,6-diisopropylphenyl)-1H-benzo[de]isoquinoline-1,3(2H)-dione (12): The synthesis of **(12)** was carried out analogously to the synthesis of **(7).** After all reactants were combined, the reaction mixture was heated to 120 °C for 17h. The work up was performed as described in synthesis of **(7)**. The crude product was purified via column chromatography (Cy/DCM; 1/1) resulting in 202 mg of a colourless solid (78%).

^{1}H NMR (300 MHz, Methylene Chloride-d_2) δ 8.70 (s, 2H), 8.45 (s, 1H), 8.12 (s, 1H), 7.93 (s, 1H), 7.50 (s, 1H), 7.35 (s, 2H), 2.71 (s, 2H), 1.12 (d, J = 6.8 Hz, 12H).

MS of (**12)** m/z: [MH^+] calc. for $C_{24}H_{22}BrNO_2$: 436.1; found: 436.2.

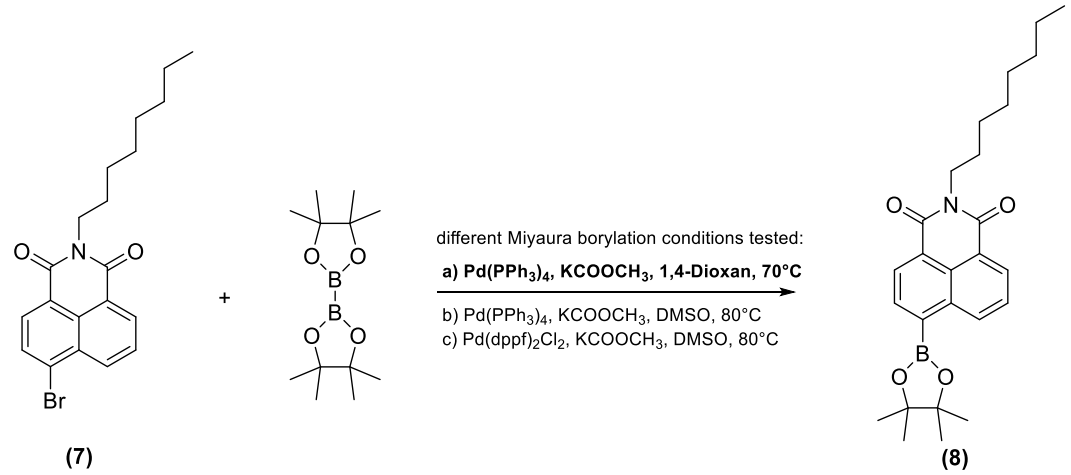

2-octyl-6-(4,4,5,5-tetramethyl-1,3,2-dioxaborolane-2-yl)-1H-benzo[de]isoquinoline-1,3(2H)-dione (8): The reaction was carried out under argon atmosphere and dry conditions according to literature.[35] Bis(pinacolato)diboron (72.0 mg, 1.10 eq.), **(7)** (103 mg, 1.00 eq.) and potassium acetate (78.9 mg, 3.10 eq.) were combined in a dry 10 mL Schlenk flask and 2 mL of 1,4-dioxane were added. The reaction mixture was bubbled with argon for 15 minutes. As catalyst, $Pd(PPh_3)_4$ was added and then the mixture was heated to 70 °C. After stirring for 22 h, TLC showed the formation of product but also presence of unreacted educts. Therefore, 64.6 mg of bis(pinacolato)diboron were added additionally. The mixture was stirred for another 72 h at a temperature of 70 °C. Then the reaction mixture was cooled to room temperature and then washed with water. Afterwards, extraction was done with DCM and the mixture was dried over Na_2SO_4. The solvent was evaporated under reduced pressure and a yellow oil was obtained. The crude product was purified by column chromatography (silica gel, Cy/DCM; 6:4 to 2:8) yielding 40.1 mg (35 %) of a yellowish oil. The oil crystallized after several days at ambient conditions.

The reaction was repeated twice under different conditions. The described procedure with conditions **a)** showed highest yields. The reaction carried out under conditions **b)** showed very low yields. Conditions **c)** showed primarily the formation of the naphthalene dimer **(23)**.

^{1}H NMR (300 MHz, Chloroform-*d*) δ 8.76 (s, 1H), 8.66 (s, 1H), 7.79 (s, 1H), 7.67 (s, 2H), 4.23 (s, 2H), 2.04 (s, 1H), 1.78 (s, 2H), 1.27 (d, *J* = 9.2 Hz, 20H), 0.88 (s, 5H).

MS of **(8)** m/z: [MH^+] calc. for $C_{26}H_{34}BNO_4$: 435.4; found: 436.3

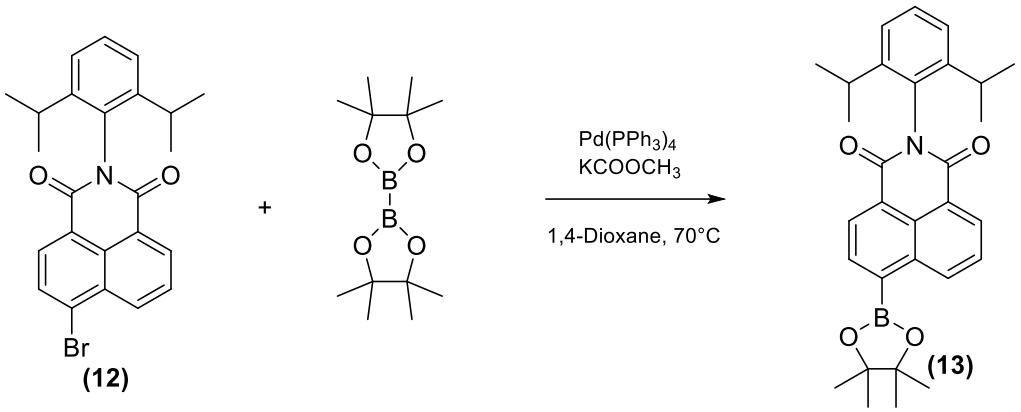

2-(2,6-diisopropylphenyl)-6-(4,4,5,5-tetramethyl-1,3,2-dioxaborolane-2-yl)-1H-benzo[de]isoquinoline-1,3(2H)-dione (13): The reaction was carried out under argon atmosphere and dry conditions according to literature[35], analogously to the synthesis of **(8)** yielding 286 mg of the yellowish solid (81 %). Purification was conducted via column chromatography (Cy/DCM; Educt: 6+4 to 1+1; Product: 3 % MeOH).

^{1}H NMR (300 MHz, Methylene Chloride-d_2) δ 9.22 (s, 1H), 8.62 (s, 2H), 8.35 (s, 1H), 7.85 (s, 1H), 7.49 (s, 1H), 7.35 (s, 2H), 2.73 (s, 2H), 1.23 (s, 21H), 1.12 (s, 3H).

MS of **(13)** m/z: [MH^+] calc. for $C_{30}H_{34}BNO_4$: 483.3; found: 484.3

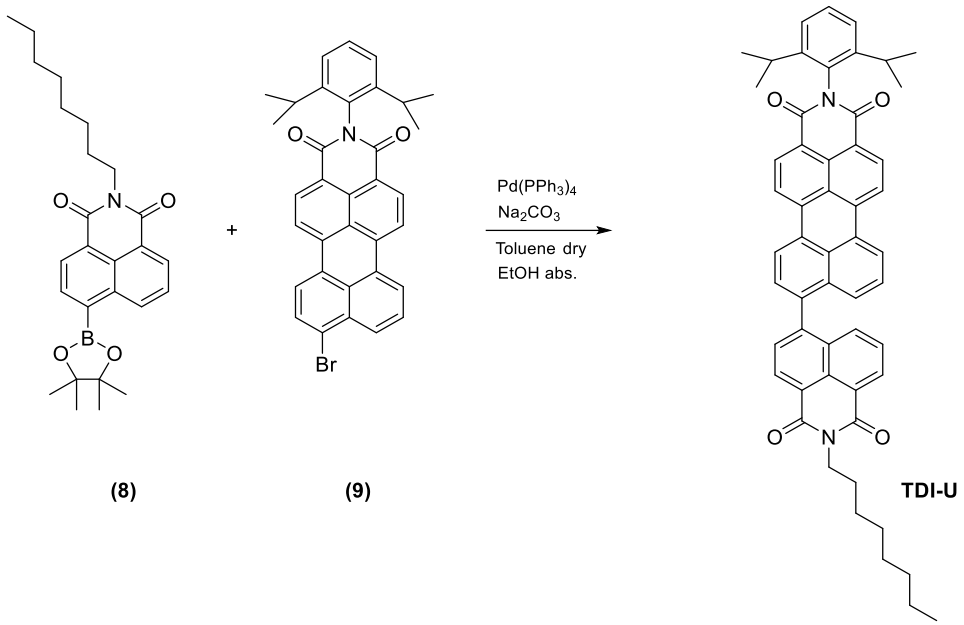

(8) (9) TDI-U

2-(2,6-diisopropylphenyl)-8-(2-octyl-1,3-dioxo-2,3-dihydro-1H-benzo[de]isoquinolin-6-yl)-1H-benzo[10,5]anthra[2,1,9-def]isoquinoline-1,3(2H)-dione (TDI-U): The reaction was carried out under argon atmosphere according to literature.[35] A 10 mL. A Schlenk tube was charged with **(8)** (40.0 mg, 2.30 eq.), **(9)** (22.6 mg, 1.00 eq.) and 2 mL of dry toluene. In addition, 0.2 mL of 0.5 M Na_2CO_3 and 0.1 mL of ethanol abs. were added to the suspension. The reaction mixture was bubbled with argon for 20 min, before a catalytic amount of the air sensitive catalyst $Pd(PPh_3)_4$ was added. The suspension was heated to 80 °C for 42 h, allowed to cool down to room temperature, washed with H_2O and extracted with DCM. The solvent was removed under reduced pressure and the residue purified by column chromatography (silica gel, Cy/DCM, 2:3 to DCM + 1% MeOH) to obtain 10 mg (32 %) of the product.

Furthermore, another way for the synthesis of **TDI-U** was tested. A Schlenk flask was charged with **(9)** (40.0 mg, 1.00 eq.), bis(pinacolato)diboron (19.9 mg, 1.10 eq.), **(7)** (28.0 mg, 1.00 eq.) and potassium acetate (21.7 mg, 3.10 eq.). The reagents were dissolved in 1.5 mL DMSO. Subsequently, a catalytic amount of $Pd(dppf)_2Cl_2$ was added and the solution was stirred for 18 h at a temperature of 70 °C. Reaction control via TLC and MS showed no formation of the desired product but formation of the naphthalene dimer **(23)**.

^{1}H NMR (300 MHz, Chloroform-*d*) δ 8.57 (s, 8H), 7.78 (s, 2H), 7.59 (s, 2H), 7.41 (s, 3H), 7.29 (s, 1H), 7.18 (s, 1H), 4.17 (s, 2H), 2.70 (s, 2H), 1.71 (s, 2H), 1.16 (d, *J* = 33.2 Hz, 25H).

MALDI-TOF-MS of **TDI-U** m/z: [M^+] calc. for $C_{54}H_{48}N2O_4$: 788.3614; found: 788.3293.

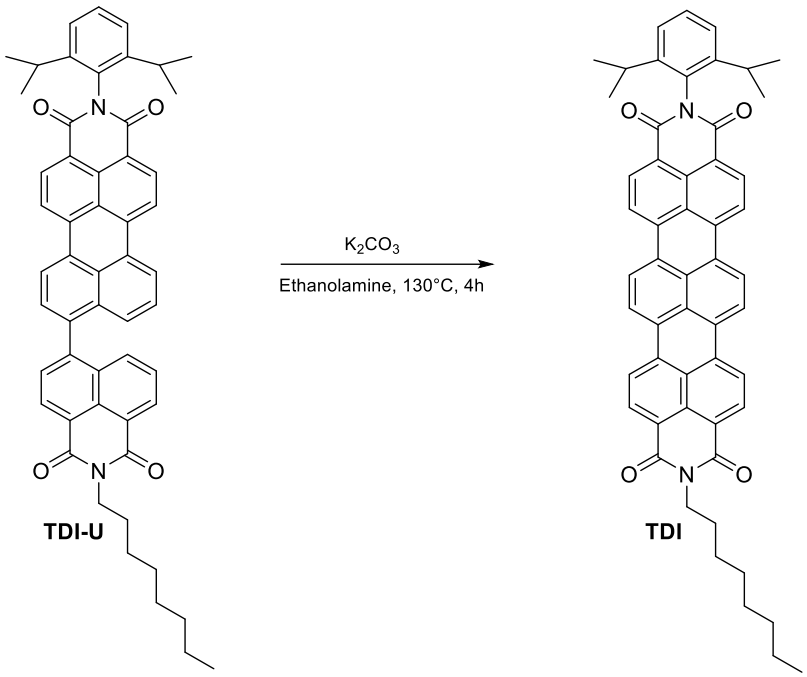

N,N'- (2,6-diisopropylphenyl)(5-octyl)terrylen-3,4:11,12-tetracarboxiimide (TDI): The following reaction was carried out under argon atmosphere according to literature.[35] A 10 mL Schlenk tube was charged with **TDI-U** (119 mg, 1.00 eq.) and potassium carbonate (1.21 g, 58.0 eq.). Afterwards, 1.8 mL of ethanolamine were added and the reaction mixture was heated to 130°C. When the temperature was reached, the components dissolved and the colour changed from red to blue within a few minutes. After 4 h complete conversion of the reactants was observed via TLC. Purification of the crude product was conducted by washing the reaction mixture with cold H_2O. The blue precipitate was separated by centrifugation. The residue was washed several times with MeOH and a 1:2 mixture of DCM and MeOH until no more orange colour was observed (100 mg, 84 %). Due to low solubility, only mass spectrometry was used for analytical characterization.

MALDI-TOF-MS of **TDI** m/z: [M^+] calc. for $C_{54}H_{46}N_2O_4$: 786.3458; found: 786.5284.

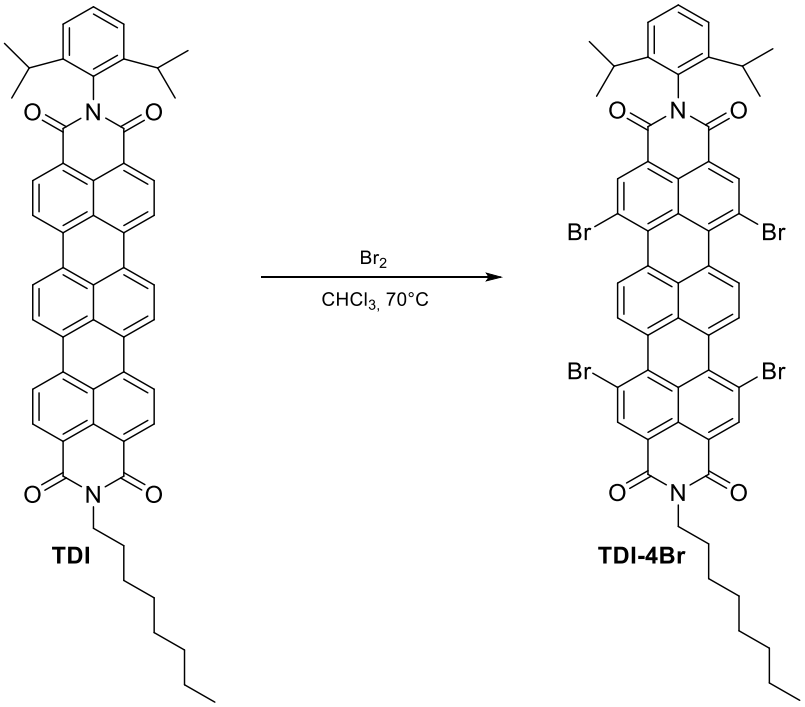

N,N'-(2,6-diisopropylphenyl)-(5-octyl)-1,6,9,13-tetrabromoterrylene-3,4:11,12-tetracarboxdiimide (TDI-4Br): The synthesis of **TDI-4Br** was carried out according to literature under argon atmosphere and exclusion of light.[37] In a dry 25 mL Schlenk tube, **TDI** (100 mg, 1.00 eq.) was suspended in 10 mL $CHCl_3$. 0.04 mL bromine (5.00 eq.) were added in one portion. The reaction mixture was heated to reflux and stirred overnight (17 h). The reaction was allowed to cool down to room temperature. Not reacted bromine was quenched by addition of saturated Na_2SO_3 solution. The product was extracted with $CHCl_3$ and concentrated under reduced pressure. The resulting blue solid was purified via column chromatography (Cy/DCM; 10/90 (fraction 1); educt at 1 % MeOH) yielding 89.8 mg (65 %). The in addition resulting mono-, di-, and trisubstituted **TDI** can be converted to **TDI-4Br** under the same reaction conditions due to the fact, that overbromination was not observed.

^{1}H NMR (300 MHz, Methylene Chloride-d_2) δ 9.14 (s, 4H), 8.89 (s, 2H), 8.60 (s, 2H), 7.56 (p, J = 9.4, 8.3 Hz, 1H), 7.40 (d, J = 7.8 Hz, 2H), 4.15 (t, J = 7.7 Hz, 2H), 2.88 (hept, J = 7.3 Hz, 2H), 1.75 (q, J = 7.8, 7.4 Hz, 2H), 1.50 – 1.01 (m, 25H).

MALDI-TOF-MS of **TDI-4Br** m/z: [M^+] calc. for $C_{54}H_{42}Br_4N_2O_4$: 1101.9847; found: 1102.1965.

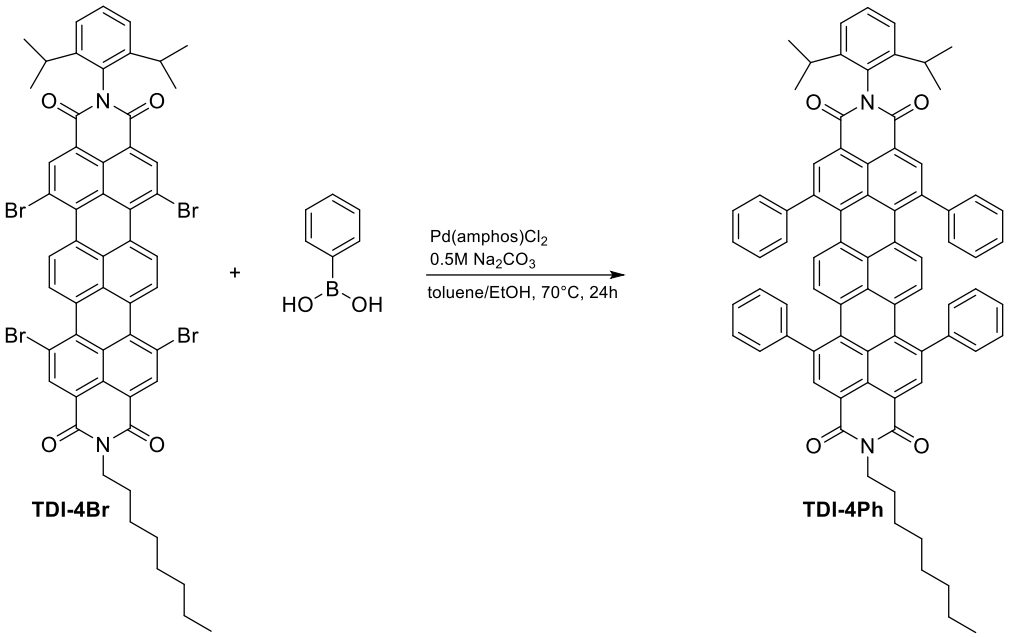

N,N'-(2,6-diisopropylphenyl)-(5-octyl)-1,6,9,13-tetraphenylterrylene-3,4:11,12-tetracarboxdiimide (TDI-4Ph): The synthesis of **TDI-4Ph** was carried out under argon atmosphere according to literature.[38] A 10 mL Schlenk flask was charged with **TDI-4Br** (20.0 mg, 1.00 eq.) and phenylboronic acid (14.4 mg, 6.50 eq.). A catalytic amount of Pd(amphos)Cl_2 was added. The reaction mixture was stirred for 24 h at 70 °C. The crude product was extracted using DCM/H_2O and dried over Na_2SO_4. Purification was conducted via column chromatography (Cy/DCM; product: 0.5 % MeOH) yielding a green solid (10.2 mg; 52 %).

^{1}H NMR (300 MHz, Methylene Chloride-d_2) δ 8.49 (d, J = 14.7 Hz, 4H), 7.45 (s, 27H), 4.16 (s, 2H), 2.76 (s, 2H), 1.73 (s, 2H), 1.20 (d, J = 47.9 Hz, 25H).

MALDI-TOF-MS of **TDI-4Ph** m/z: [M^+] calc. for $C_{78}H_{62}N_2O_4$: 1090.4709; found: 1090.4076.

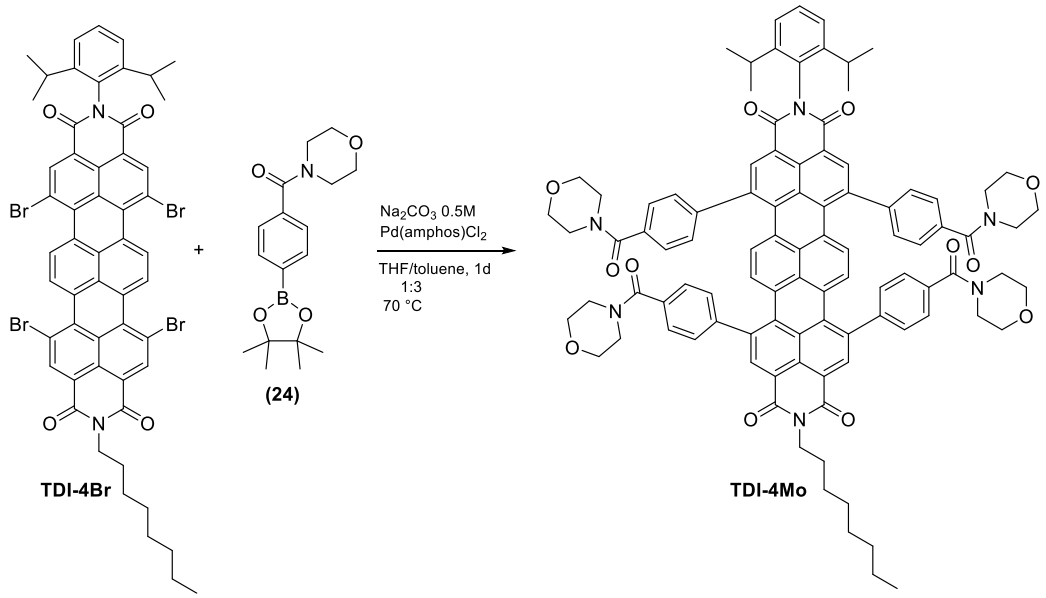

N,N'-(2,6-diisopropylphenyl)-(5-octyl)-1,6,9,13-tetra-4-benzoylmorpholinoterrylene-3,4:11,12-tetracarboxdiimide (TDI-4Mo): The following reaction was carried out under argon atmosphere. **TDI-4Br** (50.1 mg, 1.00eq.) and 4-(morpholine-4-carbonyl)phenylboronic acid pinacol ester **(24)** (86.4 mg, 6.00 eq.) were combined in a 15 mL Schlenk tube and dissolved in 0.5 mL THF and 2.5 mL toluene. As base, a 0.5 M Na_2CO_3 solution (3.00 eq.) was added to the reaction mixture. The blue solution was heated to 70 °C. A catalytic amount of the oxygen resistant catalyst Pd(amphos)Cl_2 was added. After stirring the reaction mixture for 27 h a complete conversion of **TDI-4Br** was observed. The colour had changed to green. Work-up was conducted by adding water and extraction of the product with DCM. The green solution was dried over Na_2SO_4 and concentrated under reduced pressure. Separation of the mono-, di-, tri- and tetra substituted compound was performed via column chromatography (DCM/MeOH; product: 4 % MeOH). (67 % yield)

^{1}H NMR (300 MHz, Methylene Chloride-d_2) δ 8.75 – 8.33 (m, 3H), 8.09 (h, J = 8.5, 7.8 Hz, 1H), 8.00 – 7.86 (m, 1H), 7.81 – 7.40 (m, 17H), 7.34 (t, J = 7.6 Hz, 2H), 7.08 – 6.82 (m, 2H), 6.74 (d, J = 8.1 Hz, 0H), 4.15 (dt, J = 15.6, 7.3 Hz, 2H), 3.62 (dd, J = 54.3, 27.2 Hz, 30H), 3.00 (s, 1H), 2.75 (td, J = 15.5, 13.9, 8.5 Hz, 2H), 2.01 (d, J = 16.7 Hz, 1H), 1.81 – 1.64 (m, 2H), 1.44 – 1.06 (m, 25H).

MALDI-TOF-MS of **TDI-4Mo** m/z: [MNa^+] calc. for $C_{98}H_{90}N_6O_{12}$: 1566.6547; found: 1566.6859.

The same reaction was carried out with 4-acetamidophenylboronic acid pinacol ester. Due to the much faster reaction rate using 4-(Morpholine-4-carbonyl)phenylboronic acid pinacol ester, this pathway was discarded.

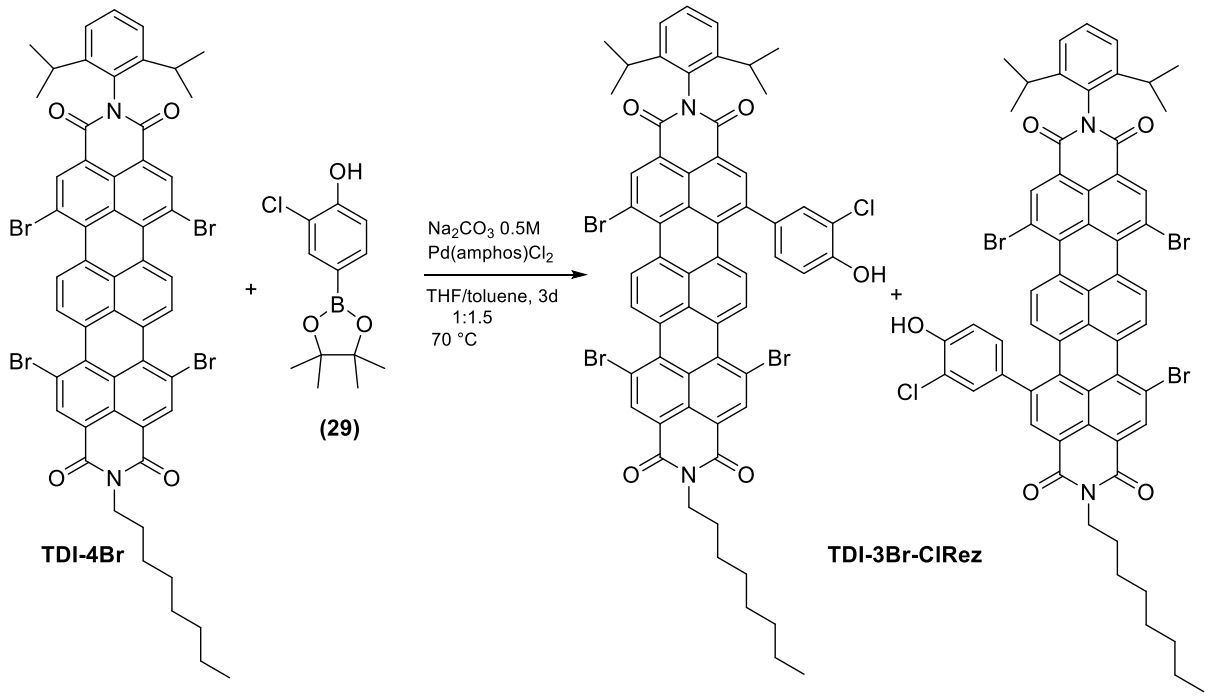

TDI-3Br-ClRez: The following reaction was carried out under argon atmosphere. A 10 mL Schlenk tube was charged with **TDI-4Br** (30.0 mg, 1.00 eq.) and 3-chloro-4-hydroxyphenyl boronic acid pinacol ester **(29)** (4.45 mg, 0.95 eq.). In addition, 0.16 mL THF, 2.5 mL toluene and 0.12 mL of a 0.5 M Na_2CO_3 solution (3.00 eq.) were added. Subsequently, a catalytic amount of Pd(amphos)Cl_2 was added. The reaction mixture was heated to 70 °C and stirred for 1 day. Due to the fact that Suzuki coupling did not work after one day of stirring, the temperature was set to 80 °C and after another day to 90 °C. After 20 hours at 90 °C, no further conversion of reactants was observed and the reaction was allowed to cool to room temperature. Prior to further work-up, THF was removed via rotary evaporation to obtain defined phase separation during extraction. After extraction with DCM/H_2O the organic layer was dried over Na_2SO_4 and concentrated under reduced pressure. The crude product was purified via column chromatography (silica gel; Cy/DCM/MeOH). Exact determination of the received product amount was not possible due to the low yield.

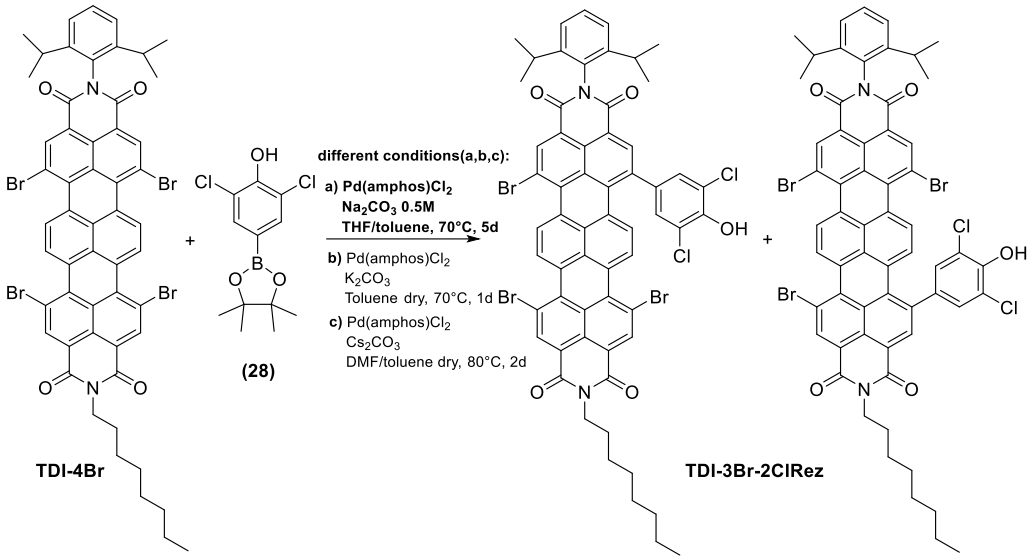

TDI-3Br-2ClRez: Different attempts to achieve pH sensitivity via Suzuki coupling of the desired receptor to the dye were conducted, using the same educts under different reaction conditions (**a, b, c**). The reactions were carried out under argon atmosphere.

Trial a) A 10 mL Schlenk flask was charged with **TDI-4Br** (30.0 mg, 1.00 eq.) and 3,5-dichloro-4-hydroxyphenylboronic acid pinacol ester **(28)** (5.50 mg, 0.70 eq.) and dissolved in 0.8 mL THF and 1.5 mL toluene. In addition, 0.16 mL of a 0.5 M Na_2CO_3 solution was added as a base. The reaction mixture was heated to 70 °C and a catalytic amount of Pd(amphos)Cl_2 was added. After the blue solution was stirred for 3 days, reaction control showed low conversion of the dye. Thus, no more pinacol ester **(28)** was left in the reaction mixture 3.30 mg were added additionally (0.42 eq.). Furthermore, 0.2 mL of THF were added to achieve better solubility of the pinacol ester. The reaction mixture was stirred for 2 days at a temperature of 70 °C. Reaction control via TLC showed no further conversion since day 2. The reaction mixture was allowed to cool down, and the dye was extracted with DCM/H_2O. The water phase contained a dark oil. After drying of the organic layer over Na_2SO_4, the blue solution was concentrated via rotary evaporation and purified via column chromatography (Cy/DCM; Educt: 3+7; Product: right after educt) yielding a very low amount of a blue solid (5 %).

Trial b and c): The reaction was repeated twice under different conditions. The described procedure under conditions **a)** showed highest yields. The reaction carried out under conditions **b)** was conducted under total exclusion of water but did not show adequate formation of product. By utilization of conditions **c)** the formation of side products was preferred. The reaction was also carried out under total exclusion of water. All crude products were purified

via column chromatography and combined, yielding 4.5 mg of a blue solid, which could not be identified.

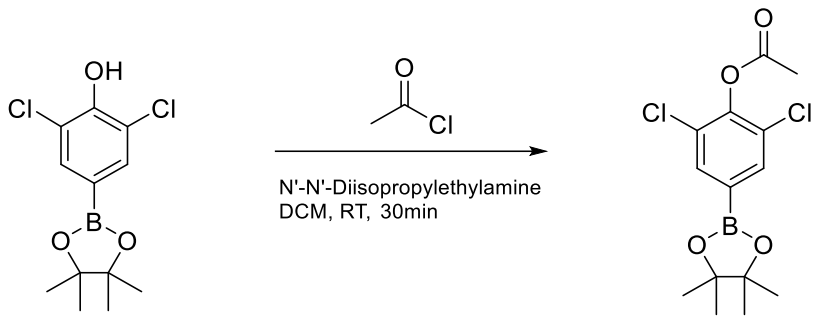

(28) **(28)-OAc**

2,6-dichloro-4-(4,4,5,5-tetramethyl-1,3,2-dioxaborolan-2-yl)phenyl acetate (28-OAc): The reaction was carried out under argon atmosphere according to literature.[39] In a 10 mL Schlenk tube **(28)** (100.4 mg, 1.00 eq.) was placed and dissolved in 2 mL DCM. Subsequently, 0.09 mL (1.50 eq.) DIPEA were added. After the reaction mixture was stirred for 5 min, 0.04 mL (1.50 eq.) acetyl chloride were added. The solution was stirred for 25 min. The work up was conducted by silica filtration (DCM) yielding the product as a colourless solid (89,3 mg, 78 %).

^{1}H NMR (300 MHz, Chloroform-*d*) δ 7.77 (s, 2H), 2.40 (s, 3H), 1.33 (s, 12H)

MS of **(28)-OAc** m/z: [M^+] calc. for $C_{14}H_{17}BCl_2O_4$: 331.0; found: 331.1

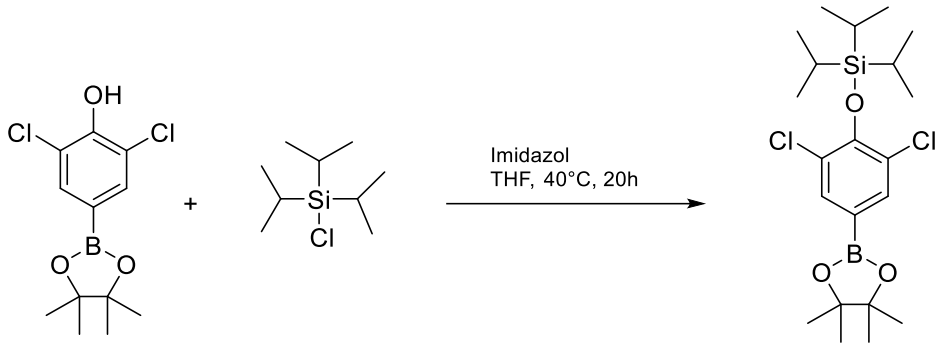

(28) **(28)-TIPS**

((2,6-dichloro-4-(4,4,5,5-tetramethyl-1,3,2-dioxaborolan-2-yl)phenoxy)triisopropylsilane (28-TIPS): The reaction was carried out under argon atmosphere according to literature.[40] A 10 mL Schlenk tube was charged with imidazole (30 mg, 1.34 eq.), compound **(28)** (101 mg, 1.00 eq.) and 3 mL THF. Subsequently, triisopropylsilyl chloride (TIPS-Cl; 67 mg, 1.00 eq.) was added and the reaction mixture was heated to 40 °C and stirred for 20 h. The work-up was conducted via silica filtration using DCM. The solvent was evaporated, yielding a colourless oil. The oil crystallized during drying at the Schlenk line, resulting in a colourless solid (quantitative yield, 155 mg)

^{1}H NMR (300 MHz, Chloroform-*d*) δ 7.66 (s, 2H), 1.45 (s, 3H), 1.33 (s, 12H), 1.13 (s, 17H).

MS of **(28)-TIPS** m/z: [M^+] calc. for $C_{21}H_{35}BCl_2O_3Si$: 445.3; found: 445.1

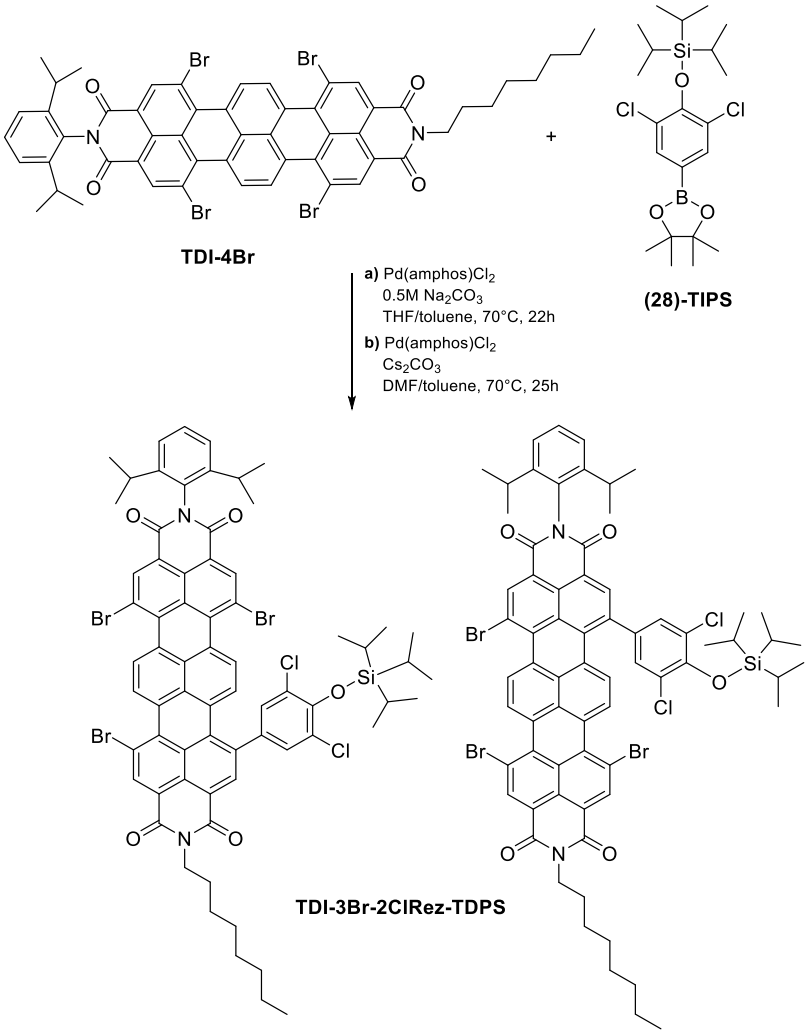

TDI-3Br-2ClRez-TIPS: The following reactions were carried out under argon atmosphere.

Trial a)

TDI-4Br (10.1 mg, 1.00 eq.) and (2,6-dichloro-4-(4,4,5,5-tetramethyl-1,3,2-dioxaborolan-2-yl)phenoxy)triisopropylsilane **(28-TIPS)** (4.7 mg, 1.15 eq.) dissolved in a mixture of 0.4 mL THF and 0.8 mL toluene (in a 10 mL Schlenk tube). In addition, 0.03 mL of a 0.5 M Na_2CO_3 were added as base. The reaction mixture was heated to 70 °C. When the temperature was reached, a catalytic amount of Pd(amphos)Cl_2 was added. After stirring for 17 h, reaction control via TLC showed low conversion and no remaining protected pinacol ester. Thus, further **28-TIPS** (3.2 mg, 0.78 eq.) was added to the reaction mixture. After stirring for 5 h the reaction was stopped due to the formation of new side product. Purification was conducted via column chromatography (Cy/DCM; 8+2 to DCM + 0.5 % MeOH). The amount of the resulting blue solid was too low to identify the product but was directly used in the next step (deprotection reaction).

Trial b)

The reaction was repeated with DMF/toluene as solvents and Cs_2CO_3 as a base under argon atmosphere and total exclusion of water. **TDI-4Br** (29.9 mg, 1.00 eq.) and the **28-TIPS** (15.9 mg, 1.32 eq.) were dissolved in 1 mL DMF and 2 mL toluene. Cs_2CO_3 (26.7 mg, 3.02 eq.) and the catalyst Pd(amphos)Cl_2 were added. The reaction mixture was heated to 100 °C and stirred for 48 h. Because no further conversion to the desired product was observed after 2 days, the reaction was allowed to cool down to RT. Before extraction was performed, DMF was evaporated. The crude product was extracted with DCM/H_2O, the organic layer dried over Na_2SO_4 and solvent was removed via rotary evaporation. Due to the challenging synthesis the pure product could not be isolated and therefore no characterization was possible.

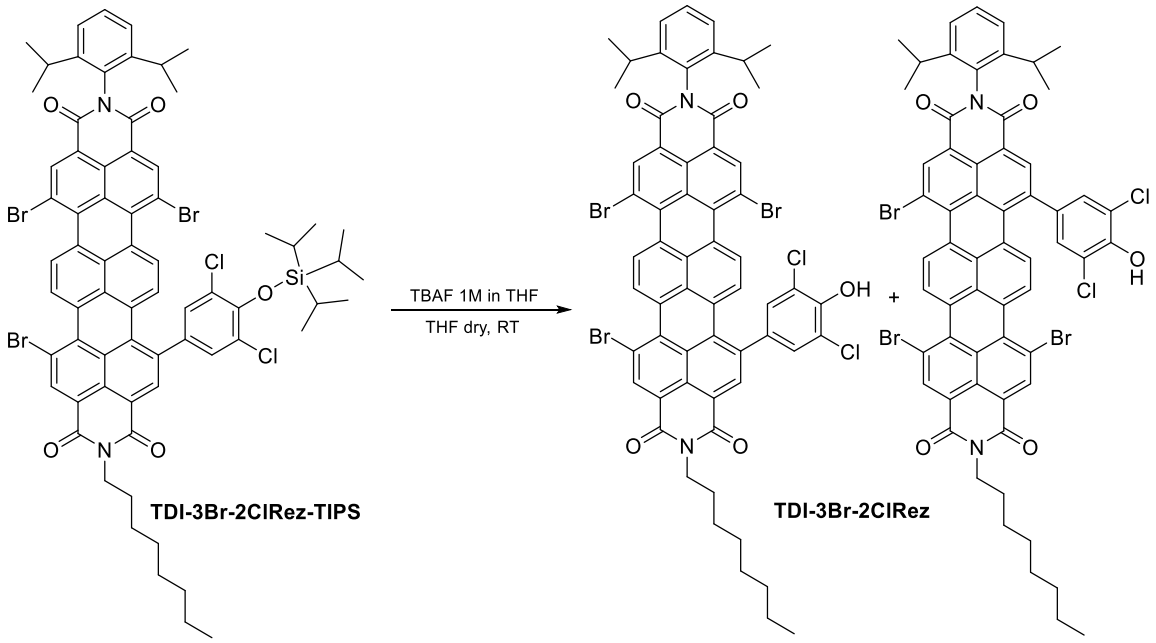

Deprotection of TDI-3Br-2ClRez-TIPS: The deprotection of **TDI-3Br-2ClRez-TIPS** was conducted under argon atmosphere and exclusion of light according to literature[40] with tetrabutylammonium fluoride (TBAF). In a 10 ml Schlenk tube, **TDI-3Br-2ClRez-TIPS** (30.0 mg, 1.00 eq.) was dissolved in 3 ml THF. Subsequently, 30 µL of a 1 M TBAF solution in THF (1.5 eq.) were added dropwise. The reaction mixture was stirred at RT for 40 min. When the reaction was stopped, ethyl acetate was added and the deprotected product was extracted with EA/H_2O/sat. NaCl. In the next step, purification was conducted via column chromatography (Cy/DCM/0.5 % HAc; TDI-4Br: 3+7; supposed product: 3+7). The yield of the resulting blue solid was very low. (4.9 mg, 18 %) and no characterization was possible.

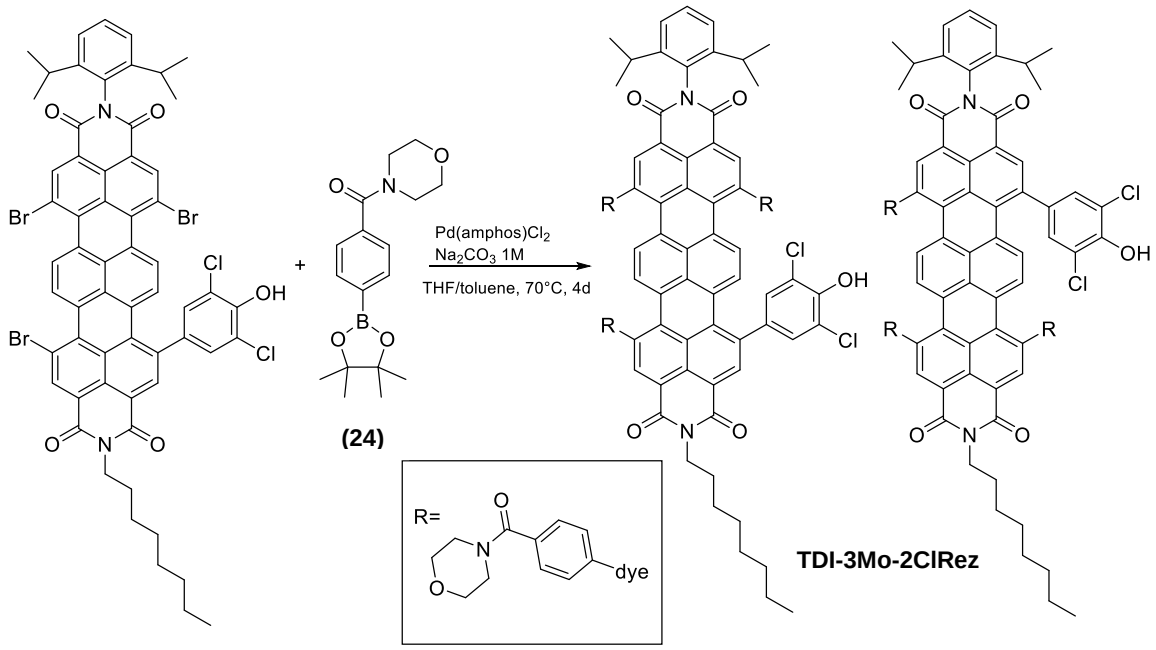

TDI-3Mo-2ClRez: TDI-3Br-2ClRez (4.90 mg, 1.00 eq.) and **(24)** (6.70 mg, 5.10 eq.) was dissolved in a mixture of THF and toluene and 0.02 mL of a 1 M Na_2CO_3 solution and the catalyst Pd(amphos)Cl_2 were added. The reaction mixture was heated to 70 °C and stirred for 4 days. No further conversion could be observed and the reaction was stopped. The crude product was extracted with DCM/H_2O and the organic layer was dried over Na_2SO_4. Purification was conducted via column chromatography (Cy/DCM/MeOH;). Due to the low yields no determination of the resulting products was possible.

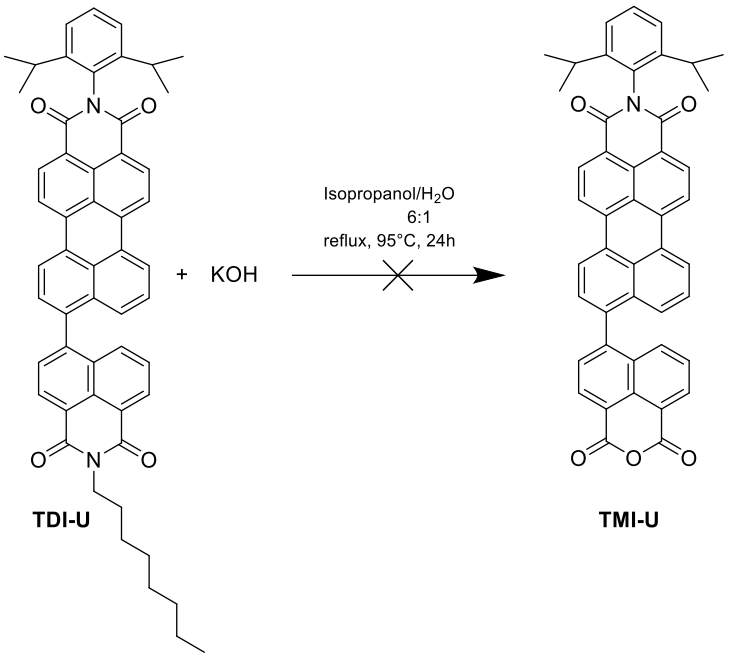

Attempt of saponification of TDI-U: The following reaction was carried out under ambient atmosphere A 10 mL Schlenk tube was charged with **TDI-U** (20.1 mg, 1.00 eq) and dissolved in a 6:1 (V:V) mixture of isopropanol and water . Subsequently, 71.2 mg KOH (50.0 eq.) were added and the reaction mixture was heated to 95 °C. After stirring for 24 h, no conversion to **TMI-U** was observed. Extraction of the educt was conducted with DCM/H_2O. The orange organic layer was dried (Na_2SO_4) and concentrated under reduced pressure. The substance identified was pure **TDI-U**, indicating that saponification did not occur.

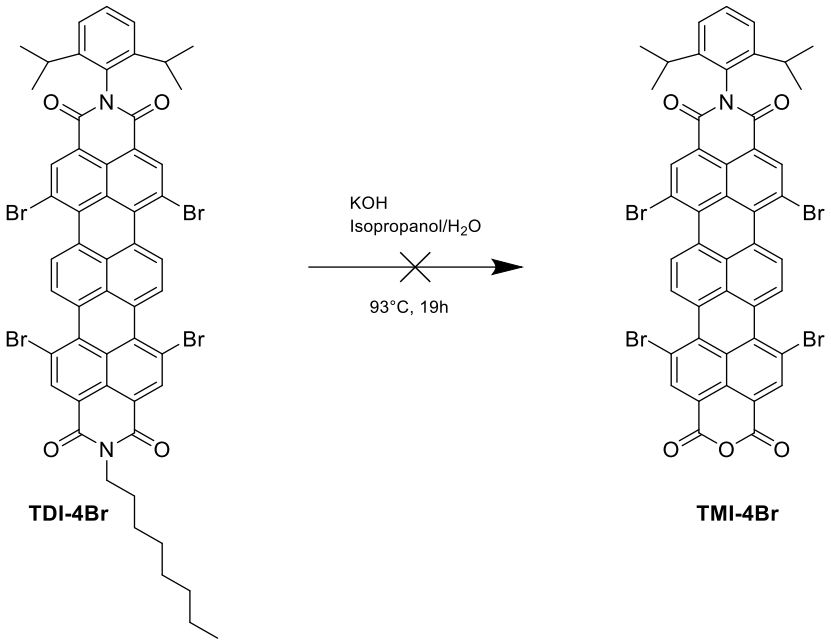

Attempt of saponification of TDI-4Br: The reaction was carried out analogously to the attempt of saponification of **TDI-U** according to literature[26].

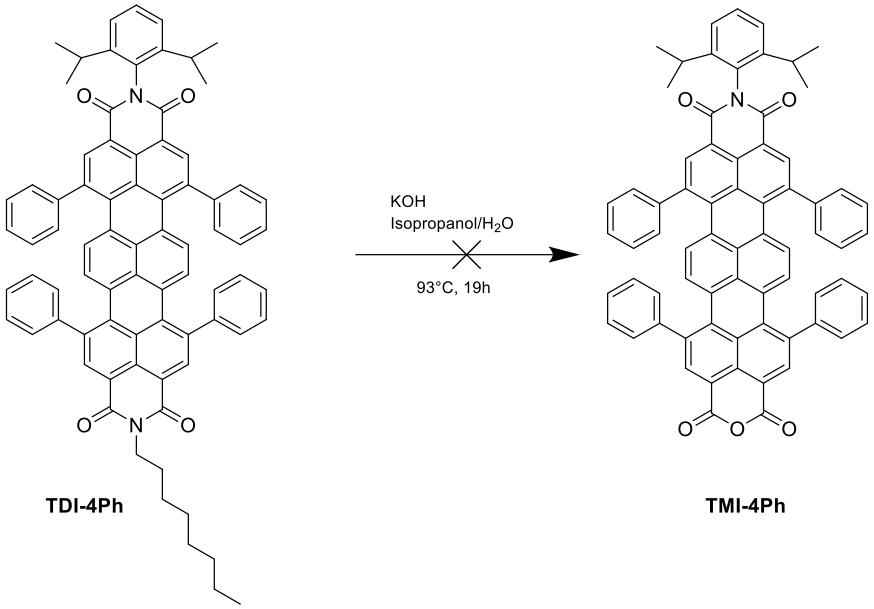

Attempt of saponification of TDI-4Ph: The reaction was carried out analogously to the attempt of saponification of **TDI-U** according to literature[26].

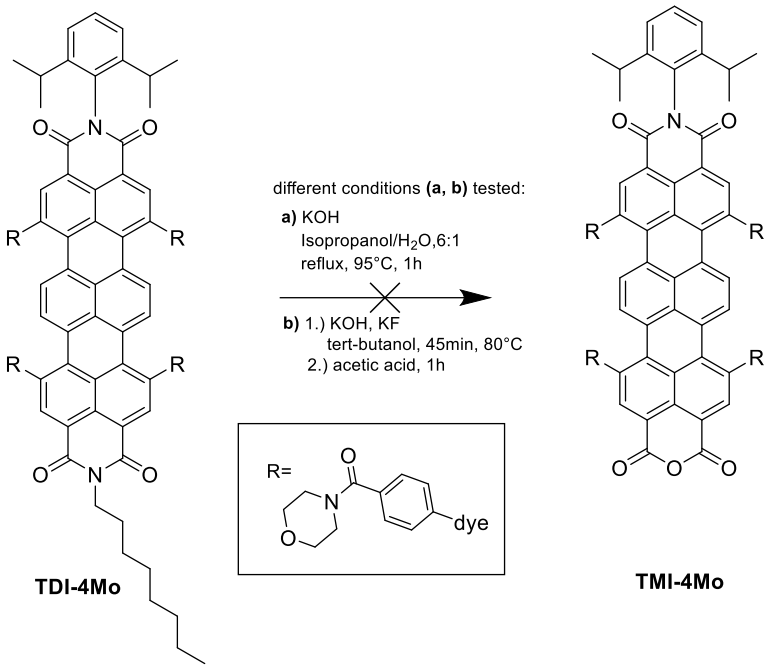

Attempt of one sided saponification of TDI-4Mo:

Trial a)

The following reaction was carried out according to literature[26]. A 10 mL Schlenk tube was charged with **TDI-4Mo** (14.9 mg, 1.00 eq) and as solvent a 6:1 (V:V) mixture of isopropanol and water was added. In addition, KOH (27.3 mg, 50.0 eq.) was added and the mixture was heated to 93 °C. After stirring for 1h, the reaction was allowed to cool down and 5 mL of glacial acetic acid was added. Reaction mixture was extracted with DCM/H_2O. After drying the solution with Na_2SO_4, the solvents were evaporated under reduced pressure. The crude product was purified via column chromatography (DCM/MeOH; Educt: DCM+ 3% MeOH, second spot: 6-10 % MeOH). The second spot could not be identified as desired product via NMR and HR-MS.

Trial b) The second trial of the one sided saponification was carried out according to literature[41]. In a 10 mL Schlenk tube, potassium fluoride (18.8 mg, 50.0 eq.) and potassium hydroxide (18.2 mg, 50.0 eq.) were dissolved in 2 mL tert-butanol. In another Schlenk tube, **TDI-4Mo** (10.0 mg, 1.00 eq.) was placed and 1.5 mL of tert-butanol were added. The mixture was also heated to 80°C. When the temperature was reached, the hot KF/KOH solution was added to the dye solution and stirred for 45 min. The reaction was stopped by adding a 1:1 (V:V) mixture of acetic acid and water. The reaction mixture was stirred for 1h at RT. In the next step, the dye was extracted with DCM/H_2O, dried with Na_2SO_4 and concentrated under reduced pressure. TLC showed no conversion of **TDI-4Mo**.

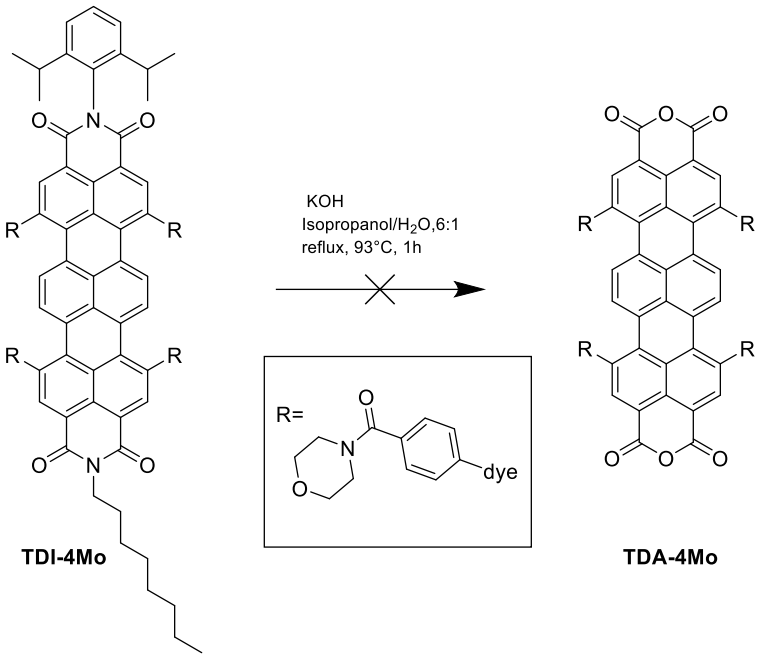

Attempt of total saponification of TDI-4Mo: The reaction was carried out analogously to the one sided saponification of **TDI-4Mo**.[26] The only difference is the used amount of potassium hydroxide (100 eq.). The reaction did not work out. No product could be isolated.

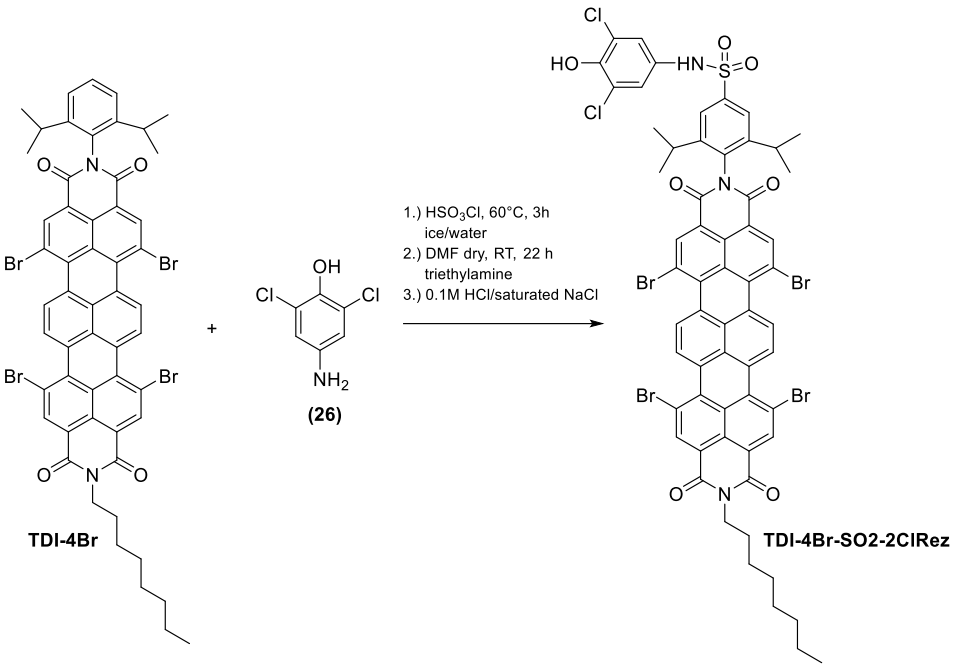

TDI-4Br-SO2-2ClRez: The following reaction was carried out under argon atmosphere in adaption to literature.[23] In an inert 10 mL Schlenk flask **TDI-4Br** (20.1 mg, 1.00eq.) was dissolved in 0.2 mL chlorosulfonic acid. After the completed addition of the acid the mixture was heated to 60 °C and stirred for 3 h. The red reaction mixture was allowed to cool down to RT and was then dropped onto crushed ice very slowly. The resulting bluish/greenish precipitate was washed with ice water until neutral. Afterwards, the precipitate on the filter was dried at the Schlenk line for 2 h. In the next step, the blue precipitate was transferred into a 10 mL Schlenk tube and 1.5 mL dry dimethylformamide were added as solvent. Afterwards, the receptor 4-amino-2,6-dichlorophenol **(26)** (6.70 mg, 2.00 eq.) and 25 µL triethylamine were added. The reaction mixture was stirred overnight (16 h) at RT under exclusion of light. The solution was then poured into 20 mL of a 0.1 M HCl/ saturated NaCl (1:1; v:v) mixture. The blue precipitate was separated by centrifugation. Purification by column chromatography was not possible due to the bad solubility of the product in all solvents except DMF and DMSO. Purification was conducted by washing the precipitate with cyclohexane, THF, DCM, EtOH and water, which is not sufficient.

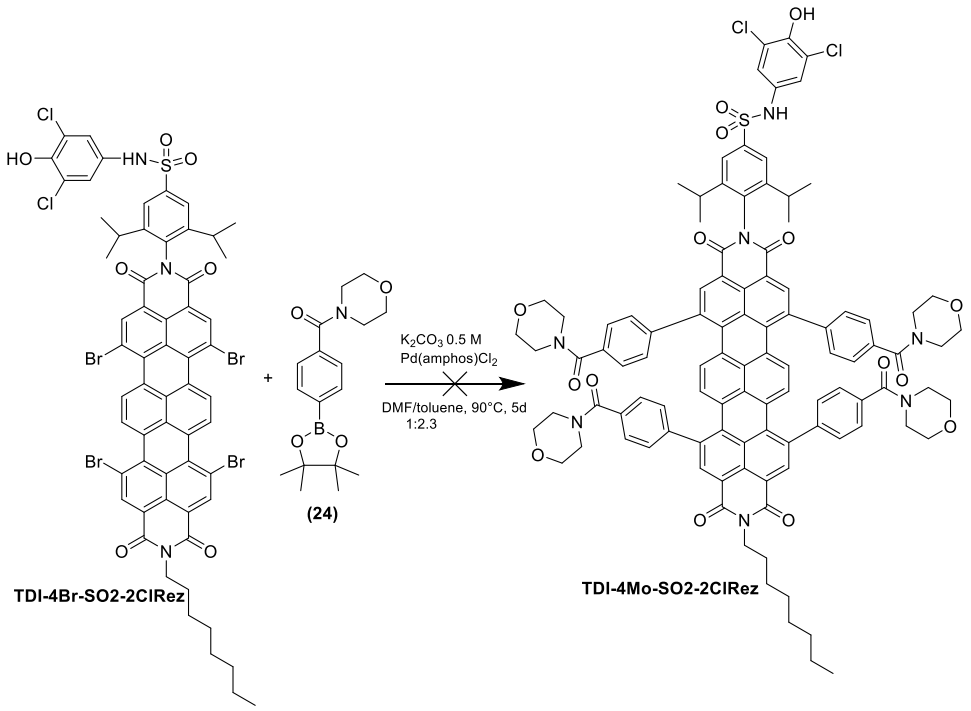

TDI-4Mo-SO2-2ClRez: A 10 mL Schlenk tube was charged with the washed **TDI-4Br-SO_2-2ClRez** (5.10 mg, 1.00 eq.), **(24)** (7.10 mg, 6.00 eq.) and 0.3 mL of DMF and 0.7 mL of toluene. Additionally, 0.1 mL of 0.5 M K_2CO_3 (3.00 eq.) and a catalytic amount of the catalyst Pd(amphos)Cl_2 were added. Subsequently, the reaction mixture was heated to 90 °C and turned green after 20 min. The reaction mixture was stirred for 5 days but no reaction to the desired product was observed. The green suspension was cooled down to RT and toluene was added to precipitate the product. The green solid was separated by centrifugation and then washed with water. Isolation of the very fine precipitate was not possible by centrifugation anymore. The precipitate was dissolved by adding EtOH to the suspension. Afterwards, the solvents were removed by rotary evaporation yielding a bluish residue which was only soluble in DMSO. Absorption spectra in DMSO showed a shift to higher wavelengths (763nm) but due to the bad solubility in water immiscible solvents purification was not possible.

4.2. Perylene

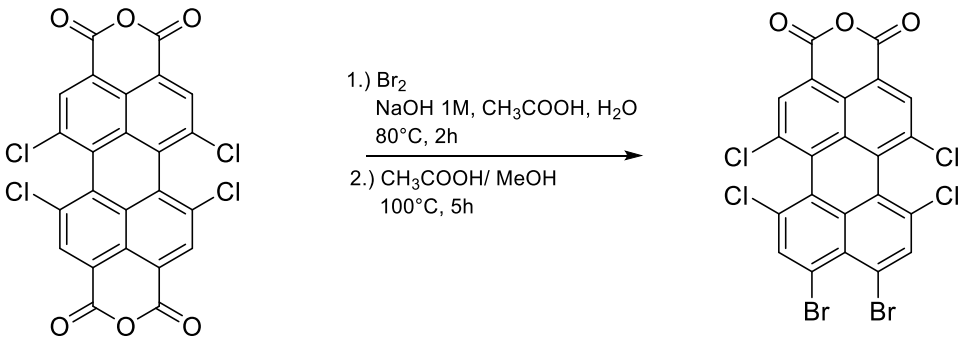

(14) **(15)**

9,10-dibromo-1,6,7,12-tetrachloro-3,4-perylenecarboxylic acid anhydride (15): The following reaction was carried out according to literature[42] under ambient conditions. Compound 1,6,7,12-tetrachloro-3,4-perylenedicarboxylic acid anhydride **(14)** (510 mg, 1.00 eq.) was suspended in 40 ml H_2O. To the orange suspension 5.6 ml of 1M NaOH (6.00 eq.) were added and stirred until a limpid solution was obtained (30 min). The solution was heated to 80 °C and 0.3 ml acetic acid conc. were added. In the next step, 0.1 ml of bromine were added and the mixture was stirred for 2h. The reaction mixture was allowed to cool down to RT and an orange solid precipitated. The precipitate was separated by centrifugation, washed with water twice and dried in the vacuum oven at 70 °C overnight.

In the next step, the dry orange solid was suspended in 40 ml of a 1:1 (V:V) mixture of MeOH and acetic acid, heated to 100 °C and stirred for 5 h. Afterwards, the product was precipitated in 80 ml MeOH, separated by filtration and washed with cold MeOH (3x20 ml) yielding 404 mg (69%) of a red solid. Characterization via NMR spectroscopy was not possible due to the low solubility of the product.

MS of **(15)** m/z: [MH^+] calc. for $C_{22}H_4Br_2Cl_4O_3$: 618; found: 618.8

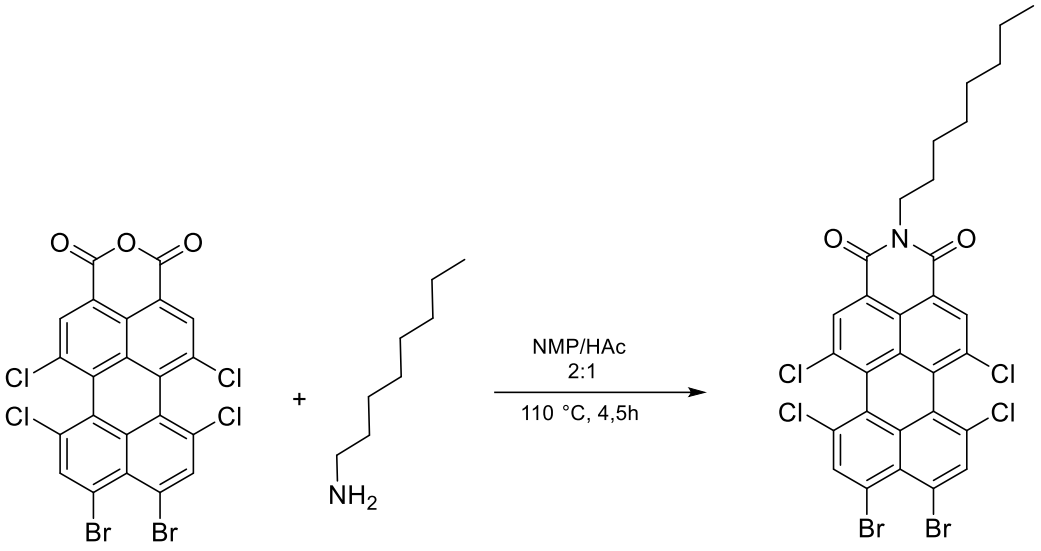

(15) **(16)**

8,9-dibromo-5,6,11,12-tetrachloro-2-octyl-1H-benzo[5,10]anthra[2,1,9-def]isoquioline-1,3(2H)dione (16): The following reaction was carried out under argon atmosphere according to literature[43]. Under inert atmosphere in a 25 mL Schlenk tube **(15)** was suspended in 10 mL NMP and 5 mL acetic acid. Subsequently, n-octylamine (0.8 mL, 1.13 eq.) was added. The reaction mixture was heated to 110 °C and stirred for 4.5 h. The reaction mixture was poured into 200 mL H_2O. The red precipitate was separated by centrifugation and dried. Purification was conducted by column chromatography (Cy/DCM; Product: 1+1 to 3+7) yielding 86 mg of an orange solid (29%). Characterization via NMR spectroscopy was not possible due to the low solubility of the product.

MS of **(16)** m/z: [MH^+] calc. for $C_{30}H_{21}Br_2Cl_4NO_3$: 729.1; found: 729.8

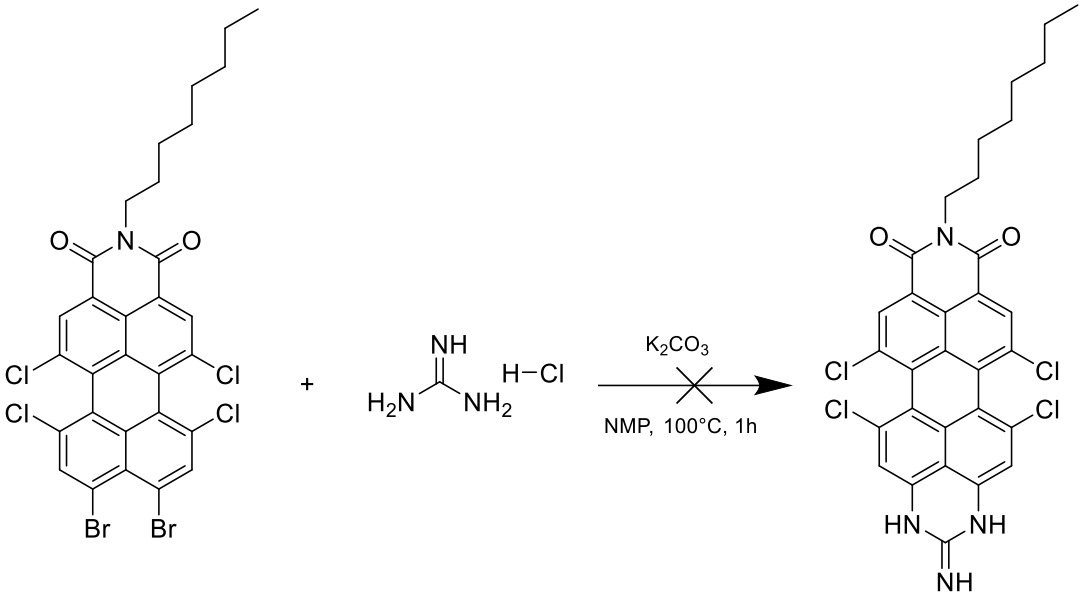

(16) **(17)**

5,6,12,13-tetrachloro-2-imino-9-octyl-2,3-dihydropyrido[3',4',5':6,7]phenaleno[1,2,3-gh] perimidine-8,10(1H,9H)-dione (17): The following reaction was carried out under argon atmosphere according to literature.[43] A 10 mL Schlenk tube was charged with **(16)** (20.2 mg, 1.00 eq.), guanidine hydrochloride (12.7 mg, 3.32 eq.) and potassium carbonate (6.40 mg, 2.42 eq.). The reactants were suspended in 2 mL NMP, stirred and heated to 105 °C for 3 h. The reaction mixture was allowed to cool down to RT and was then poured into 20 mL H_2O. The mixture was acidified with 0.1 M HCl and the resulting precipitate was separated by filtration. Purification of the orange solid was conducted via column chromatography (Cy/DCM) resulting in different fractions. The mass of the desired product was not found in any of these fractions.

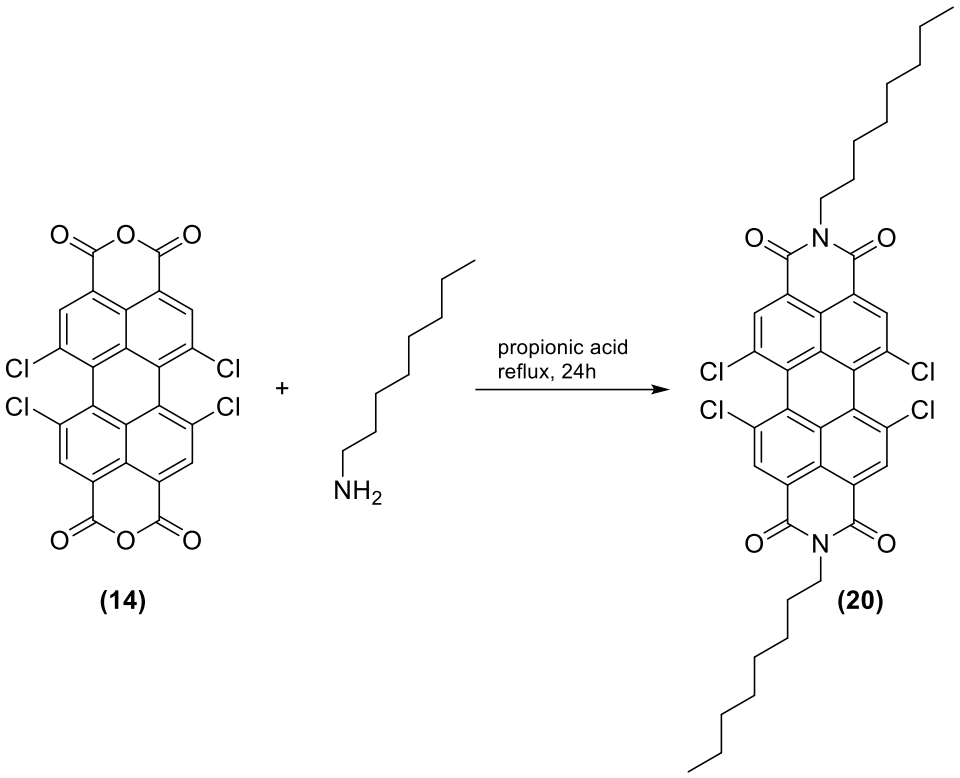

PDI-4Cl (20): The following reaction was carried out under ambient conditions according to literature[44]. In a 150 mL Schlenk tube compound **(14)** (1.00 g, 1.00 eq.) was suspended in 40 mL propionic acid. Additionally, n-octylamine (1.57 mL, 5.00eq.) was added and the reaction mixture was stirred for 24 h at 160 °C. The mixture was allowed to cool down to room temperature and an orange solid precipitated. The precipitate was washed with water until neutral. The orange precipitate was dissolved in DCM and dried over Na_2SO_4. The solvent was evaporated and the crude product was purified via column chromatography (silica gel, Cy/DCM; product: 6+4) yielding 1.28 g of the orange solid (90 %).

^{1}H NMR (300 MHz, Chloroform-*d*) δ 8.68 (s, 4H), 4.21 (s, 4H), 1.74 (s, 4H), 1.28 (s, 20H), 0.88 (s, 7H).

MS of **(20)** m/z: [M^+] calc. for $C_{40}H_{38}Cl_4N_2O_4$: 752.6; found: 752.3

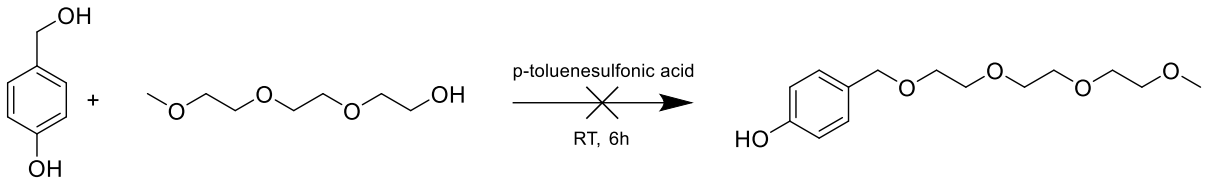

(18) (19)

4-(2,5,8,11-tetraoxadodecyl)phenol (19): The reaction was carried out under ambient conditions according to literature[45]. A 25 mL round bottom flask was charged with **(18)** (502 mg, 1.00 eq.) and 3 mL of triethylene glycol monomethyl ether. A catalytic amount of p-Toluenesulfonic acid was added and the reaction mixture was stirred for 6 h at RT. Work-up of the crude product was conducted via extraction with $CHCl_3/H_2O$ and subsequently bulb-to-bulb-distillation. At a pressure of 600 mbar the temperature was slowly increased until 180 °C. The product decomposed during distillation. The reaction was repeated and extraction with H_2O/DCM/sat. NaCl was performed to remove the high excess of TEG. After removal of DCM under reduced pressure, a yellowish oil was received. The product could not be found in this oil. The residue was dissolved in acetone and concentrated under reduced pressure. Extraction with chloroform/H_2O (20 x 30 mL H_2O) was performed but the excess of triethylene monomethyl ether could not be removed. A further trial of the work-up was conducted. Therefore, the crude product was poured into 150 mL H_2O. The solution was stirred for 1 h and then put to rest overnight to allow precipitation of the desired product. The resulting turbid mixture was centrifuged and a colourless residue was received. The residue was identified as triethylene monomethyl ether. The water phase contained product and triethylene monomethyl ether. Due to the challenging separation of the product and the excess of triethylene monomethyl ether the product could not be isolated.

MS of **(19)** m/z: $[MH^-]$ calc. for $C_{14}H_{22}O_5$: 270.3; found: 269.1

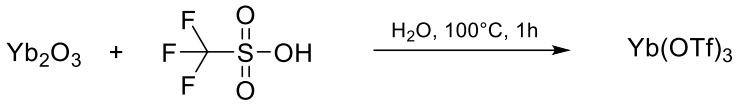

Ytterbium triflate: The reaction was carried out under ambient atmosphere according to literature.[46] A Schlenk tube was charged with ytterbium oxide (700 mg, 1.50 eq.) and the solid was suspended in 700 µL H_2O. Subsequently, 600 µL trifluorosulfonic acid anhydride (1.00 eq.) were added and the suspension was stirred at 100 °C for 1 h. Unreacted oxide was removed by filtration. Water was removed under reduced pressure and the resulting colourless solid was dried under vacuum at 200 °C. (702 mg, 96 %)

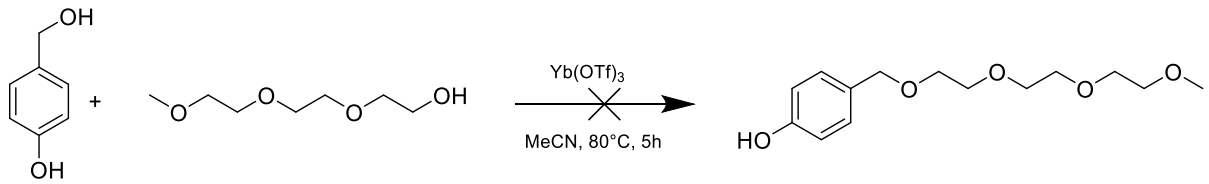

(18) **(19)**

4-(2,5,8,11-tetraoxadodecyl)phenol (19): The reaction was carried out under ambient atmosphere according to literature.[47] A 100 mL round bottom flask was charged with **(18)** (1.00 g, 1.00 eq.), 6.4 mL triethylene glycol monomethyl ether and $Yb(OTf)_3$ (51.6 mg, 0.01 eq.). As a solvent, 10 mL acetonitrile were added. A condenser was attached to the round bottom flask and the mixture was heated to 80 °C. After the reaction mixture was stirred for 5 h the reaction was stopped and ACN was removed via rotary evaporation. Subsequently, extraction was conducted with $H_2O/CHCl_3$. Due to the TEG excess, isolation of the desired product was not possible.

MS of **(19)** m/z: $[MH^-]$ calc. for $C_{14}H_{22}O_5$: 270.3; found: 269.0

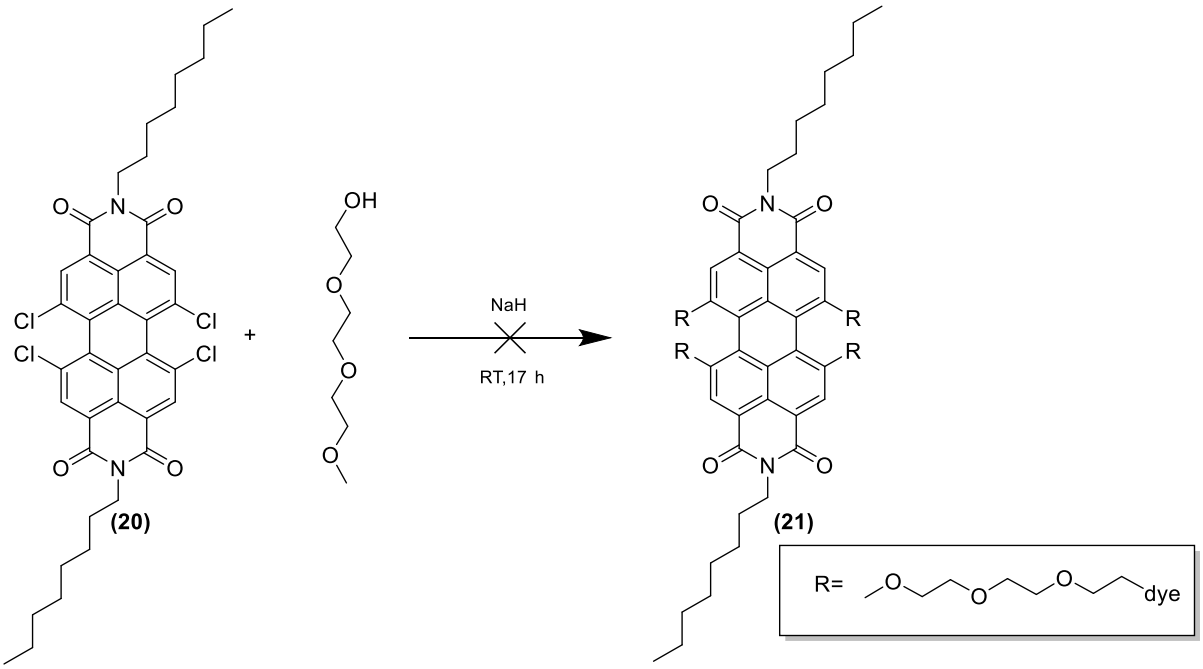

5,6,12,13-tetrakis(2-(2-(2-methoxyethoxy)ethoxy)ethoxy)-2,9-dioctylanthra[2,1,9-def:6,5,10-d'e'f']diisoquinoline-1,3,8,10(2H,9H)-tetraone (21): The following reaction was carried out under argon atmosphere according to the principle of the Williamson ether synthesis.[48] A 10 mL Schlenk tube was charged with NaH 60 % in mineral oil (17 mg, 10.0 eq.) and 1.3 mL triethylene monomethyl ether were added. The reaction takes place immediately under formation of hydrogen gas. After stirring the reaction mixture for 10 min, no more gas formation was observed and the dye **(20)** (30.4 mg, 1.00 eq.) was added. The mixture was stirred at RT overnight (17 h). The reaction was stopped by adding water to the violet solution. The reaction was extracted with EA/H_2O/sat. NaCl. Due to challenging work-up and the excess of TEG, isolation of the desired product was not possible.

5. Results and Discussion

5.1. Synthesis of terrylene chromophores

5.1.1. Synthetic considerations

The aim of this work was the synthesis of new pH-sensitive terrylene diimide dyes (**TDI)**, emitting in the deep red range of the electromagnetic spectrum. Terrylene diimide dyes belong to the dye class of rylenes and are the higher homologues of the widely used perylene diimides. It is known that the blue coloured terrylene diimide features very good photophysical properties over many other deep-red emitting fluorophores.[16] By extending the π-conjugated system of the perylene core the terrylene diimide ground structure **(TDI)** (**Figure 13**) can be achieved.[17] However, the terrylene ground structure has limited solubility in organic solvents and synthetic modifications are necessary. Therefore, solubility improving groups can be attached at the terminal imide position and at the bay region of the ground structure. The chemical modification at the terminal imide position does not significantly affect the optical and electronic properties of **TDI** due to nodes in the LUMO and HOMO orbitals of the imide nitrogen atoms. However, the optical properties are strongly affected by modification at the bay region of the terrylene. By extending the π-conjugated system and introduction of electron donor or acceptor groups at this position, the emission band of **TDI** (680 nm) can be shifted to higher wavelengths in the deep red range of the electromagnetic spectrum. [26]

The functionalization of the terrylene core can be achieved by synthetic modifications of the halogenated **TDI** derivate **(TDI-4Br)**. To reach the goal of pH sensitivity, different modification strategies were investigated. First, attempts of introducing the pH-sensitive receptor at the terminal imide position were conducted. Second, the introduction of the pH-sensitive group at the bay region was carried out.

First of all, the basic core of the terrylene diimide molecule **TDI** was synthesized. On that basis, attempts to achieve pH-sensitivity and further modifications to improve solubility and to extend the π-conjugated system were conducted by modifying the terminal imide position and the red marked positions at the bay region of the core (**Figure 13**).

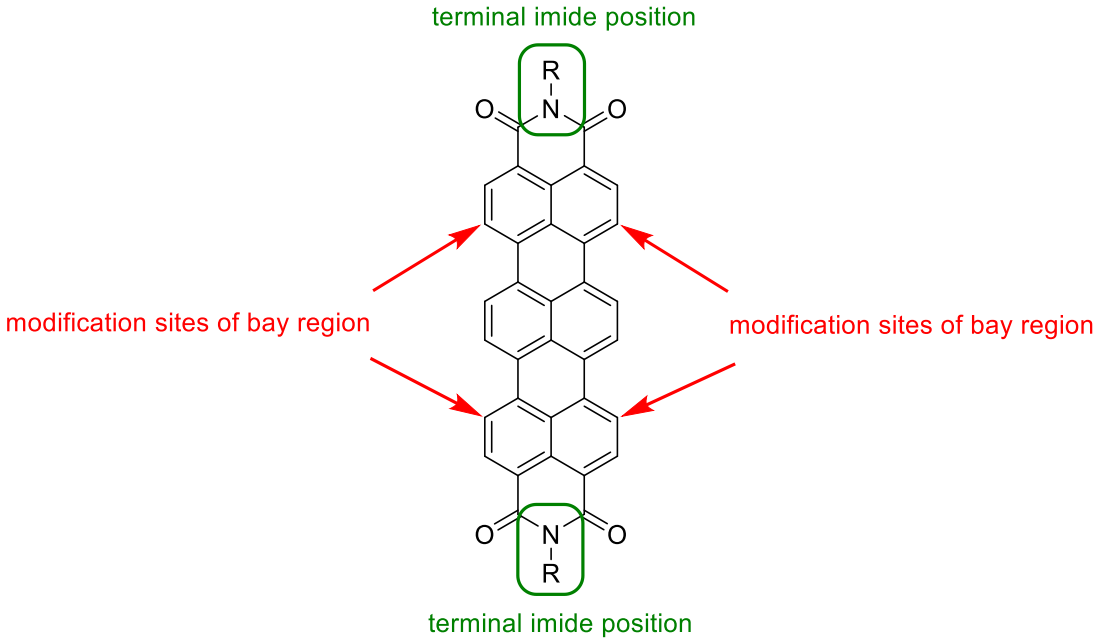

Figure 13: Basic structure of terrylene diimide

5.1.2. Initial plan of TDI synthesis

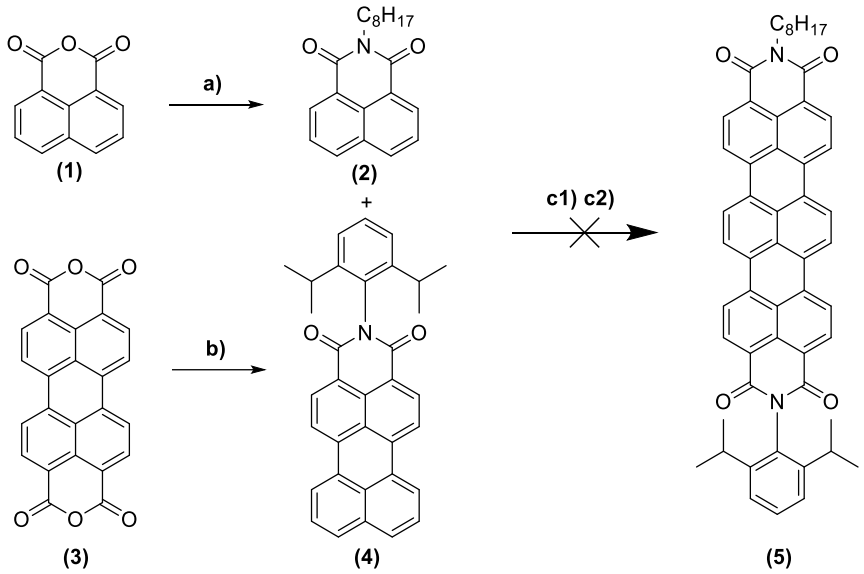

Figure 14: Originally planned synthesis pathway of TDI; a) n-octylamine, HAc, reflux, 12h (53 %); **b)** diisopropylaniline, $Zn(CH_3COO)_2 \cdot 2H_2O$, imidazole, H2O, 190 °C, bomb reactor, 24 h (73 %); **c1)** 1,5-diazabicyclo[4.3.0]non-5-ene, tBuNaO, diglyme,130°C, 3 h **c2)** 1,5-diazabicyclo[4.3.0]non-5-ene, $(CH_3)_3COK$, toluene dry,130 °C, 3 h

The initial plan to synthesize the terrylene core was conducted corresponding to the work published by the group of Müllen in 2005 (**Figure 14**).[17] The first step was the synthesis of the building blocks **(2)** and **(4)**, required for the synthesis of **TDI (5)**. Introduction of the imide group in terminal position of the starting materials was necessary to improve the solubility in organic solvents and therefore facilitate handling of the compounds. Amination of the starting

material 1,8-naphtalic anhydride **(1)** with n-octylamine was successful (53 %).[35] The second building block was synthesized according to a procedure developed by Langhals and co-workers, which is used as starting point in most routes for substituted perylene and terrylene dyes.[49] Conversion of perylene-3,4-dicarboxylic anhydride **(3)** was conducted under high pressure and elevated temperature in a bomb reactor. During the condensation reaction the primary amine diisopropylaniline is attached in imide position and the molecule undergoes partial decarboxylation forming compound **(4)**. The reaction is carried out in molten imidazole and the presence of water and zinc acetate. The presence of water and the closed system of the bomb reactor enables the partial carboxylation reaction. In an opened system and in absence of water, the full carboxylation of the perylene dominates.[49] The reaction was followed by time-consuming purification steps resulting in high yields (93 %) of the product.

The aryl-aryl fusion reaction of the two building blocks **(3)** and **(4)** to **TDI** was carried out several times as published in literature.[13,16,17,35] This reaction is described as an alternative method to the rough alkaline-fusion method and enables aryl fusion reaction under mild conditions. Two different reaction conditions were tested. First, the reaction was carried out using the base tBuNaO and diglyme as a solvent. In literature, diglyme is described as the most effective solvent for this type of reaction. In the second attempt to achieve aryl fusion, the base t-BuKO and toluene were used.[50] However, the desired terrylene product could not be obtained using the above mentioned conditions. During every attempt of this synthesis (both conditions), the colour of the reaction mixture turned from red to blue under inert atmosphere. When the resulting bluish mixture was exposed to ambient atmosphere, the mixture turned red again. The appearance of the blue colour cannot indicate the formation of the desired product since **TDI** is stable at ambient atmosphere. Due to this, degradation of this product cannot be the issue in this reaction. As potential side-reaction, this one-pot synthesis can be accompanied by saponification reactions at the imide position, which can lead to the formation of byproducts such as quaterrylenes or perylene monoanhydrides.[16] After several trials, this synthesis pathway was abandoned and an alternative route towards **TDI** was investigated.

5.1.3. Alternative synthesis pathway of TDI

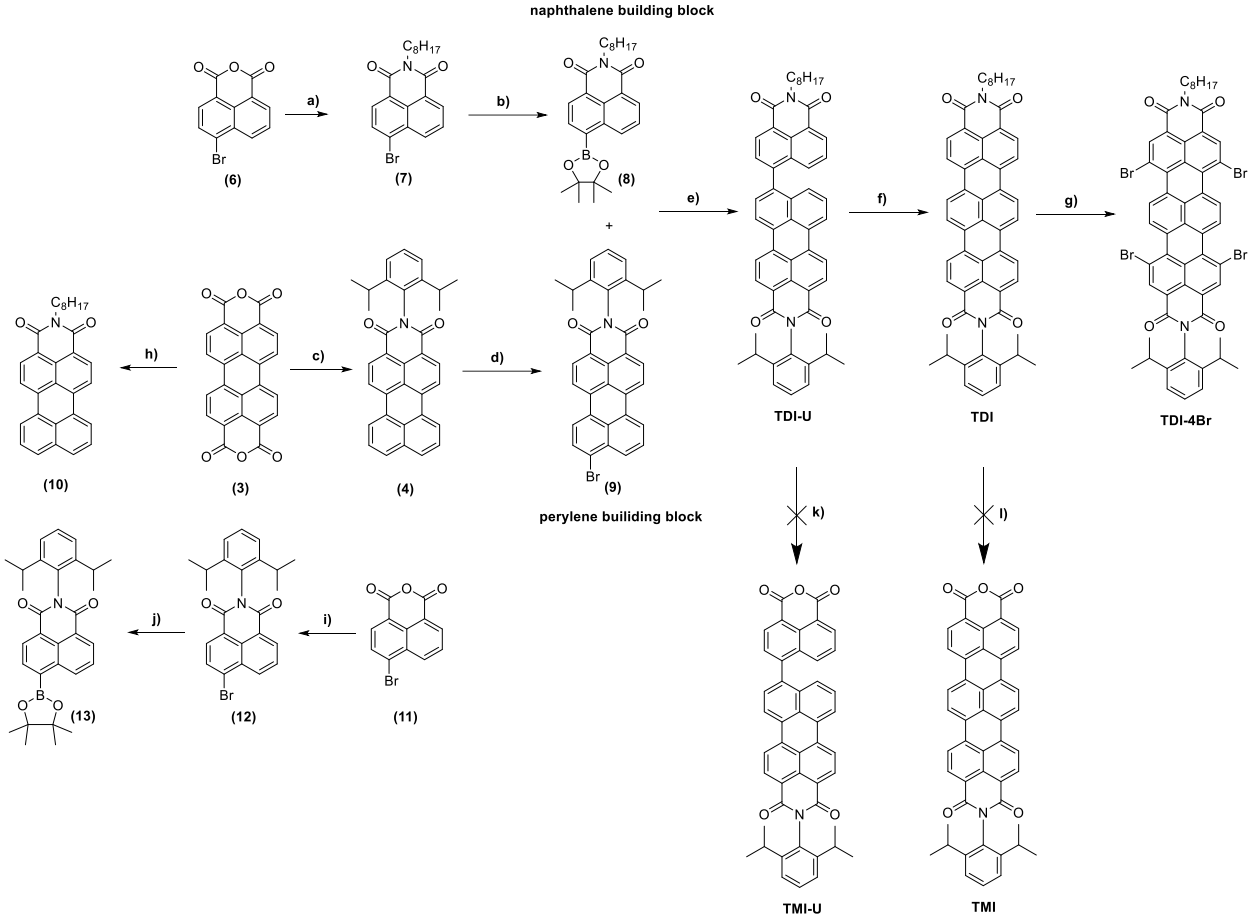

Figure 15: Alternative synthesis pathway of TDI-4Br; **a)** n-octylamine, HAc, reflux, 17h (92 %); **b)** bis(pinacolato)diboron, $Pd(PPh_3)_4$, $KCOOCH_3$, 1,4-dioxane, 70°C, 94 h (35 %); **c)** diisopropylaniline, $Zn(CH_3COO)_2 \cdot 2H_2O$, imidazole, H_2O, 190 °C, bomb reactor, 24 h (93 %); **d)** Br_2, DCM, reflux, 3 h (76 %); **e)** $Pd(PPh_3)_4$, Na_2CO_3, toluene/EtOH, 80°C, 42 h (32 %); **f)** K_2CO_3, ethanolamine, 130 °C, 4 h (84 %); **g)** Br_2, $CHCl_3$, 70 °C, 17 h (65 %); **h)** n-octylamine, $Zn(CH_3COO)_2 \cdot 2H_2O$, imidazole, H_2O, 190 °C, bomb reactor, 24 h (73 %); **i)** diisopropylaniline, HAc, 120 °C, 17 h (78 %); **j)** $Pd(PPh_3)_4$,$KCOOCH_3$, 1,4-dioxane, 70°C (81 %); **k,l)** 50eq. KOH, 2-propanol/H_2O, reflux, 24 h

The alternative way to synthesize terrylenes was also described by the group of Müllen.[17,37,51] The pathway is illustrated in **Figure 15**. As a starting material the commercially available brominated 1,8-naphtalic anhydride **(6)** was used and n-octylamine was introduced at the terminal region of the naphthalene resulting in compound **(7)** in good yield (92 %).

In the next step, Miyaura-borylation was conducted to receive the naphthalene boronic ester **(8)**. The Miyaura-borylation enables the synthesis of boronates by cross-coupling of aryl halides with bis(pinacolato)diboron.[52,53] The borylation reaction was one of the most time-consuming steps of the terrylene synthesis due to low yields. The low conversion rates to the desired product can be explained by the formation of a dimer side product due to appearance of Suzuki coupling.[54] As shown in **Figure 16**, formation of coupled naphthalene **(23)** building blocks was

observed. The formed product **(8)** reacts with the reactant **(7)** catalysed by the palladium catalyst. Separation of this side product and the desired product **(8)** was achieved via column chromatography.

.

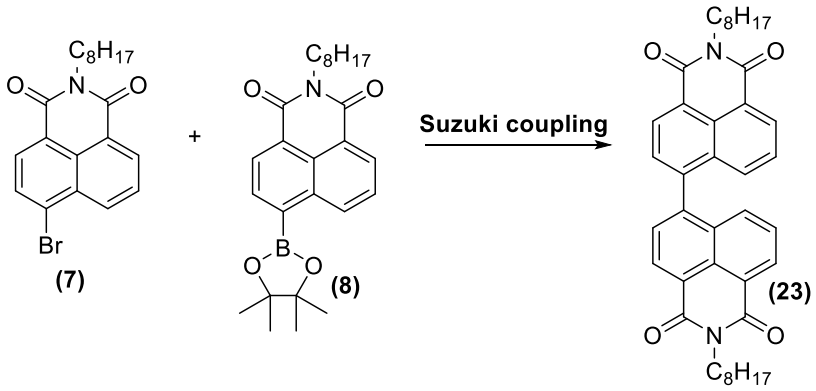

Figure 16: Side reaction during Miyaura-borylation, Suzuki coupling to naphthalene dimer (23)

The first step of the synthesis of the perylene building block was conducted analogous to the reaction in the originally planned synthesis pathway (**Figure 14**). The reaction was carried out in a bomb reactor under high pressure and elevated temperature (190 °C). Due to the closed system and the presence of water, the partial carboxylation of **(3)** occurs and compound **(4)** is obtained. [49] The crude product was purified via Soxhlet extraction and subsequent column chromatography. This method was a very time-consuming part to obtain high quantities of the product. To reduce expenditure of time, the reaction in the bomb reactor was carried out 3 times, prior to the purification of the crude products. Preparation of compound **(9)** for the usage in Suzuki cross-coupling via bromination of (**4**) in dichloromethane (DCM) was conducted resulting in good yields (76 %).[35,55] Unfortunately, the resulting 9-bromoperylene-3,4-dicarboximide **(9)** is poorly soluble in organic solvents and therefore characterization via NMR spectroscopy was not possible. Purification by column chromatography was possible, using high amounts of DCM. The purity of the received orange solid was confirmed by mass spectrometry. Subsequently, palladium catalyzed Suzuki cross-coupling of **(8)** and **(9)** was conducted yielding in terrylene diimide precursor **TDI-U**.[29] In this coupling reaction the usage of an excess of **(8)** is necessary to minimize homo-coupling reactions.[56] The purified **TDI-U** was cyclized to terrylene diimide **TDI** by cylcodehydrogenation in ethanolamine using potassium carbonate as a base. The advantage of cyclization with help of a mild base is the prevention of possible saponification of the terminal N-substituents.[17] Purification of **TDI** via column chromatography was not possible due to the low solubility of the blue solid in organic

solvents. However, the educt **TDI-U** is soluble in methanol and DCM whereas the product **TDI** is not. Hence, the blue solid could be washed several times with MeOH and DCM/MeOH (v:v, 1:2) until no more orange educt **TDI-U** dissolved in the washing solution. The fine blue solid was separated from the washing solution via centrifugation in good yield (84 %).

The last step to obtain tetrabromoterrylene diimide **TDI-4Br** was the introduction of reactive bromine groups at the bay region of **TDI**. The reaction was carried out in chloroform under reflux yielding mainly **TDI-4Br** (65 %). As side products, partially brominated terrylene diimides can occur such as **TDI-Br**, **TDI-2Br**, **TDI-3Br**. These side products can be converted into 4-fold brominated **TDI** via the same reaction conditions due to the fact, that no overbromination was observed (**Figure 17**). This approach was performed several times receiving **TDI-4Br** as product. The attachment of the bromine at the bay region improves the solubility of the compound in organic solvents significantly. This is attributed to the distortion of the skeletal structure of the terrylene diimide.[17]

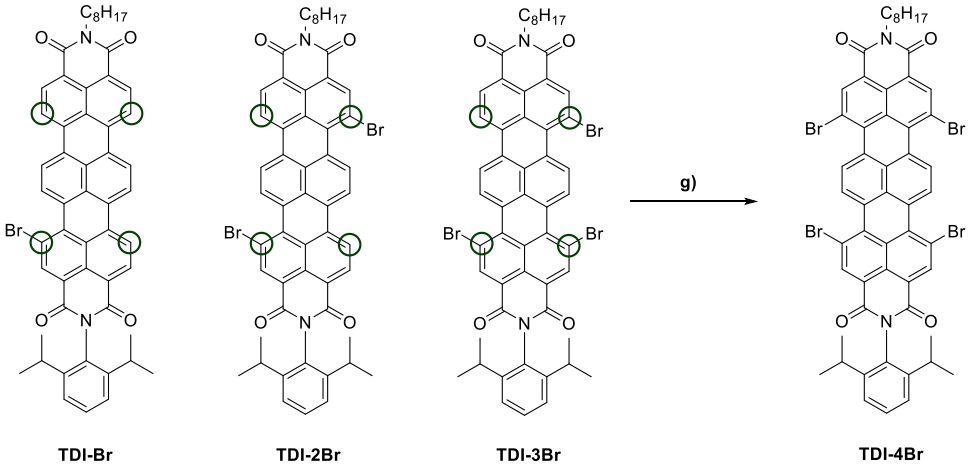

Figure 17: Conversion of side products TDI-3Br, TDI-2Br, TDI-Br to TDI-4Br with reaction conditions g) Br_2, $CHCl_3$, 70 °C, 17 h; bromine can be attached at marked positions; regioisomeres of each structure are possible

Within the synthesis of **TDI-4Br**, the solubility of the terrylene ground structure was already improved in organic solvents by the substitution of the bay region with bromine and introduction of bulky substituents such as 2,6-diisopropylaniline and n-octylamine at the terminal imide position of the terrylene. The introduction of these two different groups at the terminal positions led to an unsymmetrical terrylene diimide. The brominated unsymmetrical **TDI-4Br** was used as starting material for further synthetic modifications to influence optical properties and to introduce pH-sensitivity. In

Figure18 all conducted strategies of modification are shown.

5.1.4. Modification attempts originating of TDI-4Br

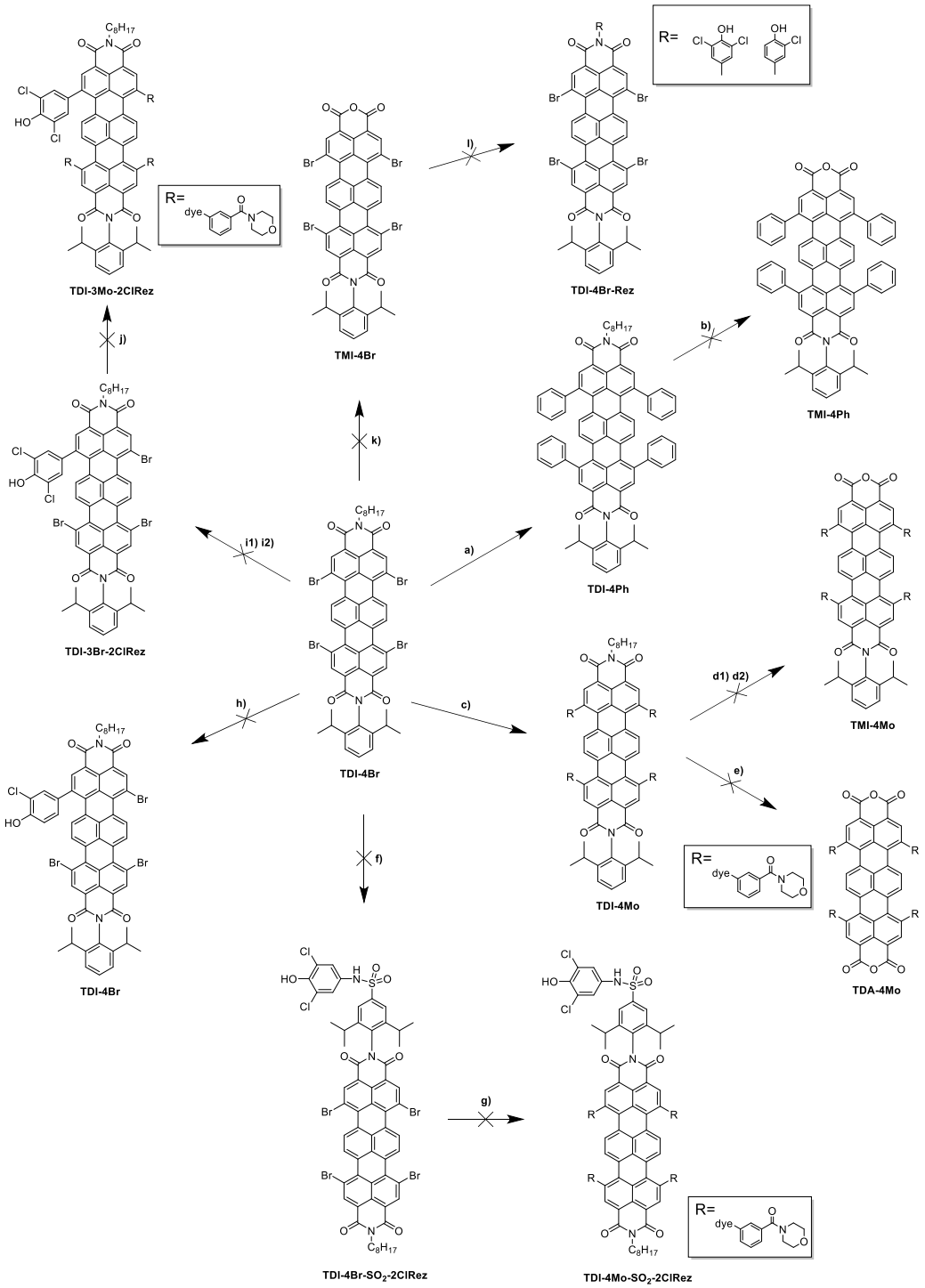

Figure18:Attempts to introduce pH-sensitivity and improve solubility of TDI a) phenylboronic acid, Na_2CO_3, tol/EtOH, 70 °C, 24 h (52 %); **b)** 50 eq. KOH, 2-propanol/H_2O, 93 °C, 19h; c) morpholino(4-(4,4,5,5-tetramethyl-1,3,2-dioxaborolan-2-yl)phenyl)methanone, Na_2CO_3, Pd(amphos)Cl_2, THF/tol, 70 °C, 1d (67 %); **d1)** 50eq. KOH, 2-propanol/H_2O, 95 °C, 1 h; **d2)** KOH, KF, tert-butanol, 80 °C, 45 min, acetic acid; **e)** 100 eq. KOH, 2-propanol/H_2O, 93 °C, 1 h **f)** 1) HSO_3Cl, 60 °C, 3 h 2) DMF dry, trimethylamine, 22 h, RT 3) 0.1M HCl/ sat. NaCl; **g)** morpholino(4-(4,4,5,5-tetramethyl-1,3,2-dioxaborolan-2-yl)phenyl)methanone, K_2CO_3, Pd(amphos)Cl_2, DMF/tol, 90 °C, 5 d **h)** 3-chloro-4-hydroxyphenyl boronic acid **i1)** (2,6-dichloro-4-(4,4,5,5-tetramethyl-1,3,2-dioxaborolan-2-yl)phenoxy)triisopropylsilane, Na_2CO_3, Pd(amphos)Cl_2, THF/tol, 70 °C, 22 h; **i2)** (2,6-dichloro-4-(4,4,5,5-tetramethyl-1,3,2-dioxaborolan-2-yl)phenoxy)triisopropylsilane, Cs_2CO_3, Pd(amphos)Cl_2, DMF/tol, 70 °C, 25 h; **j)** morpholino(4-(4,4,5,5-tetramethyl-1,3,2-dioxaborolan-2-yl)phenyl)methanone, Na_2CO_3, Pd(amphos)Cl_2, THF/tol, 70 °C, 4 d; **l)** 3,5-dichloro-4-hydroxyaniline, propionic acid, 140°C, 10 h

In **Figure18** all conducted attempts to modify **TDI-4Br** are illustrated.

On the basis of **TDI-4Br**, attempts to achieve a bathochromic shift of the emission band to the deep-red range were carried out. Two different dyes **(TDI-4Ph, TDI-4Mo)** with an extended π-conjugated core were successfully synthesized.

First, the literature known synthesis of **TDI-4Ph** was successfully performed. Brominated terrylene diimide and phenyl boronic acid were converted via Suzuki cross-coupling to **TDI-4Ph**, catalyzed by the air stable Pd(amphos)Cl_2 catalyst.[38] The reaction resulted in a good yield of a green solid (52 %). As expected, the received **TDI-4Ph** showed a bathochromic shift compared to **TDI-4Br** of about 90 nm (em_{max}**(TDI-4Ph)** = 750 nm) to the deep-red range of the electromagnetic spectrum (for more details see section 5.2.3/ page 85) . As this reaction worked out well, attempts to attach new types of functional group at the bay region were conducted. Therefore, two different boronic acid pinacol esters **(24)** and **(25)** were tested (**Figure 19**).

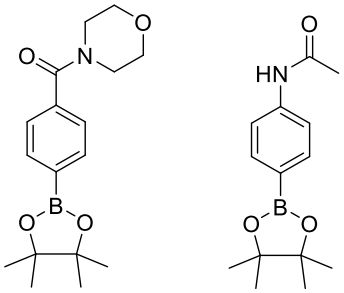

(24) **(25)**

Figure 19: (24) 4-(Morpholine-4-carbonyl)phenylboronic acid pinacol ester

(25) 4-Acetamidophenylboronic acid pinacol ester

Attachment of 4-(morpholine-4-carbonyl)phenylboronic acid pinacol ester **(24)** to the **TDI** core was performed via Suzuki cross-coupling reaction. Utilization of an excess of **(24)** ensures 4-fold substitution of bromine. As **TDI-4Br** shows good solubility in THF and the pinacol ester **(24)** is soluble in toluene, the reaction was carried out in a mixture of THF and toluene, using Na_2CO_3 as base. A good conversion rate to the desired product was observed after a reaction time of 24 hours. The reaction resulted in mainly 4-fold substituted terrylene diimide (**TDI-4Mo,** 67 %). As side products less substituted derivates were formed. which could be easily separated via column chromatography. Simultaneously, the reaction using 4-acetamidophenylboronic acid pinacol ester **(25)** under same conditions to examine which

pinacol ester is the more suitable reactant, was carried out. The reaction did not show an adequate conversion after several days, thus 4-morpholine-4-carbonyl)phenylboronic acid pinacol ester **(24)** was chosen as the more suitable substituent for this modification strategy. After modification of the bay region with **(24)** the emission band was shifted bathochromically from 680 nm (**TDI-4Br**) to 750 nm (**TDI-4Mo**) (for more details see section 5.2.4/ page 88). As the goal of a bathochromic shift to the deep-red range of the electromagnetic spectrum was reached, the next step was the introduction of a pH-sensitive group. The plan compromised a one sided saponification of the terminal imide position of **TDI** and subsequent attachment of an amine, bearing a phenol, at this position (**Figure 20**).

5.1.5. pH receptors used to gain pH sensitivity

Introduction of pH-sensitivity can be realized by introduction of phenolic groups into the fluorescent dye. Receptors **(26)** and **(27)** carry a phenolic group which causes a photoinduced electron transfer (PET), when deprotonated (**Figure 20**). According to literature, the fluorescence quenching is extremely efficient which makes these receptors suitable for the usage in pH-indicator dyes.[57] Receptor **(26)** differs from receptor **(27)** in the pK_a-value of the hydroxyl group. The pK_a can be shifted by substituents attached to the aromatic ring. The effect is called inductive effect. By bonding of electron withdrawing groups such as chlorine, the pK_a can be shifted to lower values, thus to a more acidic pH range (-I-effect). If electron donating groups (e.g. CH_3) are attached the pK_a is shifted to higher values, thus to a more basic pH range (+I-effect). 4-Aminophenol has a pK_a of 10.17. By adding one chlorine atom to the aromatic ring in ortho position, the pK_a is shifted to 8.75. Attachment of a second chlorine atom in ortho position shifts the pK_a to 7.29.

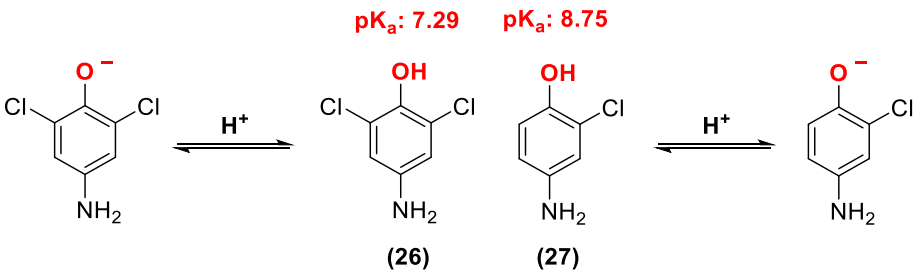

Figure 20: pH-sensitive groups (26) 3,5-dichloro-4-hydroxyaniline and (27) 3-chloro-4-hydroxyaniline protonated and deprotonated form

5.1.6. Introduction of the pH-sensitive group via partial saponification and subsequent amination

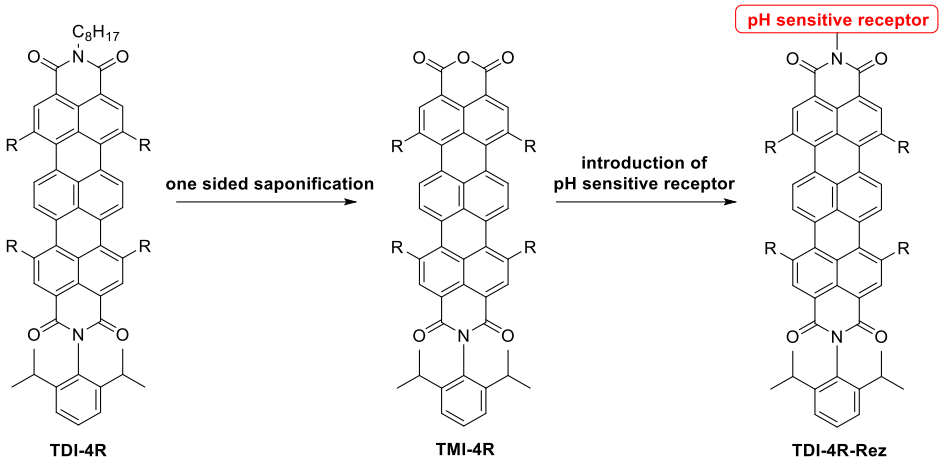

Figure 21: Initial plan of synthesis pathway for the introduction of pH-sensitive receptor

Saponification reactions of terrylene diimides and perylene diimides are described in literature several times. [17,26,41,58] First, partially saponification of terrylene diimide (**TDI-4Mo)** was carried out using a strong base, such as KOH, resulting in a terrylene monoimide (**TMI-4Mo)**. This is illustrated in **Figure 21.** According to literature, using an excess of 50 eq. KOH in a 6:1 (v:v) mixture of 2-propanol and water should result in one sided saponification. To obtain full saponification, an excess of 100 eq. KOH is required.[26] To facilitate the one sided saponification, the asymmetric terrylene diimide was synthesized as ground structure (**TDI,** Figure 15). The n-octylamine substituent was assumed to be removed easier than the 2,6-diisopropylaniline substituent. However, partial saponification did not work out for **TDI-4Mo**. No conversion was observed. For this reason, a full saponification of **TDI-4Mo** was attempted to enable a comparison of this reaction and the already conducted partial saponification reaction. The reaction mixtures of both attempts (partial and full saponification) were compared with the educt **TDI-4Mo** via TLC and no conversion of the reactant was observed. Hence, partial saponification of **TDI-U, TDI, TDI-4Br** was carried out under same conditions. During every attempt, no conversion of the reactants was observed via TLC.

The challenge of the saponifications was the low solubility of KOH in 2-propanol. A possible reason for the unsuccessful reaction was the insufficient solubility of the required amount of KOH to obtain high basicity.

Due to this, another method to obtain a partial saponification of **TDI-4Mo** was performed, according to literature.[41] The attempt of an alkaline hydrolysis of **TDI-4Mo** was carried out in

t-butanol using KOH as a base. Additionally, potassium fluoride was added. However, the reaction did not work either. The solubility of KOH in t-butanol was very low and even at elevated temperature (80 °C) not sufficient for the reaction. No conversion of the reactant **TDI-4Mo** to **TMI-4Mo** was observed via TLC and HR-MS measurements of both conducted methods did not show formation of desired product.

To gain pH sensitivity a pH-receptor had to be introduced to the terrylene molecule. Introduction of a pH-sensitive amine **(26)** (**Figure 20**) was attempted even without confirmation of successful saponification. Therefore, one sided saponification was conducted as described and the resulting mixture was used without further purification for the reaction with the amine. The amination was carried out in propionic acid according to literature.[35] Reaction control via TLC showed no conversion of the amine. Due to this, this strategy to obtain pH sensitivity was abandoned.

5.1.7. Attempt of introduction of the pH receptor at the bay region of TDI-4Br

Due to the fact that saponification of all terrylene diimide derivates failed, another way to attach the pH-sensitive receptor to the dye was aimed. The idea was to achieve coupling of the receptor and the dye at the brominated bay region via Suzuki cross-coupling. Two different pH receptors featuring a phenolic PET group were utilized **(28, 29)** (**Figure 22**). The receptors differ in the pK_a-value of the hydroxyl group caused by the different substitution with chlorine (-I-effect).

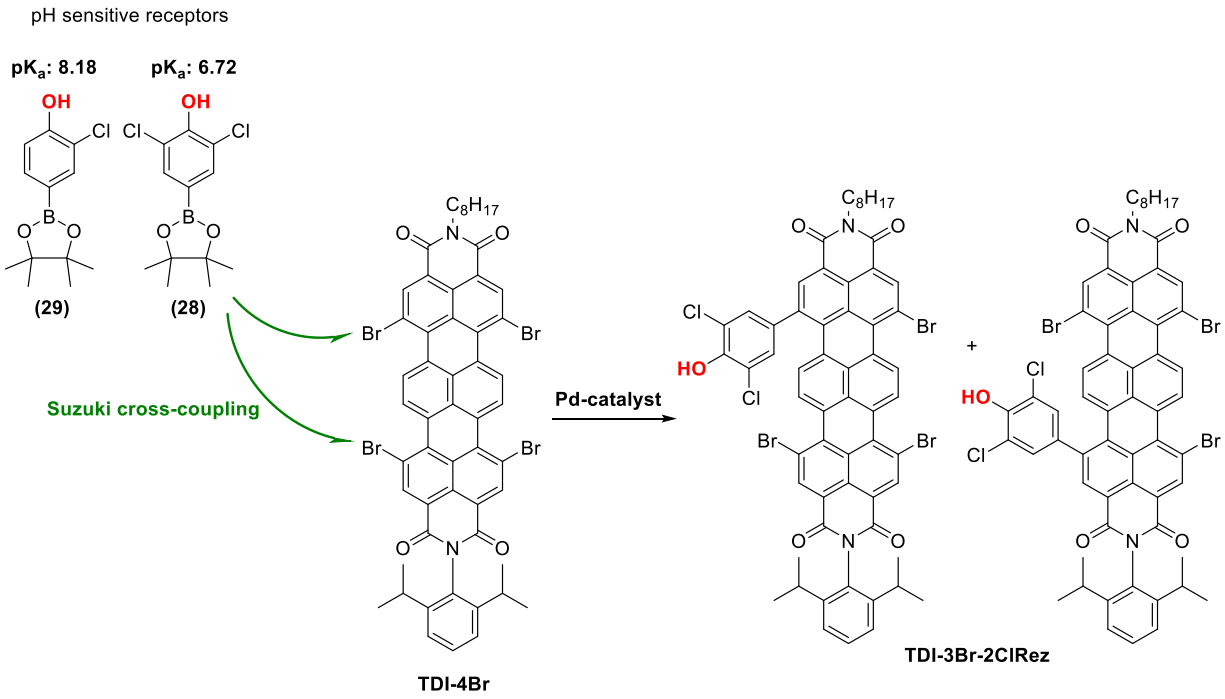

Figure 22: Positions for introduction of pH-sensitive group via Suzuki coupling; due to asymmetric TDI-4Br the formation of regioisomeres is possible; (28) 3,5-Dichloro-4-hydroxyphenylboronic acid pinacol ester, (29) 3-Chloro-4-hydroxyphenylboronic acid pinacol ester; pKa values: calculated using Advanced Chemistry Development (ACD/Labs) Software V11.02 (© 1994-2020 ACD/Labs)

First, Suzuki coupling of commercially available monochlorophenol pinacol ester **(29)** and **TDI-4Br** to **TDI-3Br-ClRez** was attempted. The issue of this strategy was the possible formation of two isomers due to the asymmetric character of the synthesized terrylene diimide (**Figure 22**). Therefore, the utilization of a symmetric **TDI-4Br** would have been the better choice for this modification strategy. However, in the case of the initial modification strategy via the one-sided saponification, the asymmetric terrylene diimide was the compound of choice. Due to this reason, the asymmetric **TDI-4Br** was synthesized. Due to the time consuming synthesis of **TDI-4Br** the difficulties accompanied by using the asymmetric **TDI-4Br** for this reaction were neglected.

The reaction was carried out in a mixture of toluene and THF as **TDI-4Br** shows good solubility in THF and **(29)** in toluene using Na_2CO_3 (aq.) as base. To avoid time consuming degassing and to facilitate handling of the reaction mixture, the air stable catalyst Pd(amphos)Cl_2 was used. After one day of stirring at elevated temperature (70 °C) C-C coupling of the receptor and the terrylene could not be obtained in an adequate amount. Therefore, the temperature was first increased to 80 °C and after further 20 hours to 90 °C. Even at this temperature, the conversion rate was very low. TLC showed mainly unreacted **TDI-4Br** and a new light blue spot beneath the educt spot. (Rf_{educt}=0.81, $Rf_{newspot}$=0.59 (Cy/EE; 4+1)). This new spot was assumed to be the desired product. Separation was easily achieved by column chromatography. However, determination via NMR spectroscopy was not possible due to the very low yields (< 2 mg) and HR-MS did not confirm the assumption.

Final introduction of pH sensitivity, was carried out using the pH-sensitive receptor dichlorophenol pinacol ester **(28)**. Suzuki cross-coupling was carried out in the same way as described in the previous section. During the work-up, a high amount of a brown viscous oil emerged at the bottom of the Schlenk tube which was found to be a degradation product of the receptor **(28).** This indicated decomposition of the boronic acid pinacol ester. In general, boronic acid pinacol esters are described as relatively stable compared to boronic acids and other boronic acid esters but are still not completely stable against hydrolysis. It is known, that phenylboronic pinacol esters with a hydroxyl group at para position can be hydrolyzed more easily explaining the decomposition to the brown oil. [59,60] The small amount of formed crude product was easily separated from unreacted **TDI-4Br** via column chromatography. (Rf_{ed}=0.83; $Rf_{newspot}$=0.68; Cy/EE;4+1).

To verify the introduction of the pH-sensitive group, fluorescence measurements in basic and acidic environment were performed. No pH dependency in fluorescence was observed which indicated an unsuccessful synthesis of the desired product.

A potential side reaction could be the substitution of bromine with a hydrogen atom. However, this reaction is implausible due to the conducted TLC. The newly formed product is more polar compared to the educt **TDI-4Br**. If one bromine substituent was exchanged with a hydrogen atom the polarity would decrease.

Another and more plausible reaction which could have occurred, is the palladium catalyzed C-O cross coupling of primary alcohols and aryl halides. This reaction is catalyzed by a palladium catalyst and occurs in the presence of a base, a primary alcohol and an aryl halide. The general catalytic cycle is illustrated in **Figure 12** on page 22.[61] Therefore, bonding of the

hydroxyl group of the receptor to bay region of terrylene diimide can occur in the conducted reaction. When the pH-sensitive OH-group forms an ether the pH-sensitivity is lost. This could be an explanation for the pH insensitivity of the formed product. The formation of the ether (**Figure 23**) was not confirmed.

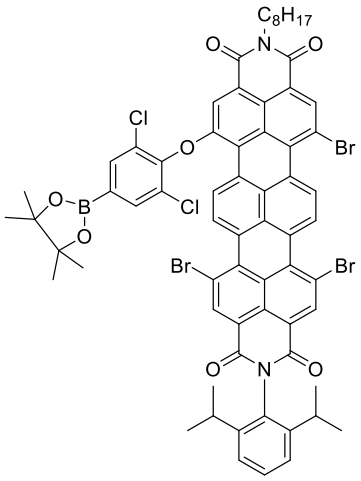

Figure 23: Possible formed side product during Suzuki cross-coupling attempt; Ether formation via C-O cross-coupling reaction

To avoid hydrolysis of the receptor **(28)**, Suzuki cross-coupling was performed again under exclusion of water. Therefore, a mixture of dry dimethylformamide (DMF) and dry toluene was used. Due to its solubility in DMF, Cs_2CO_3 was chosen as a base. The reaction was carried out at 80 °C. Reaction control via TLC showed the formation of several new compounds similar to the Suzuki cross-coupling carried out in THF/toluene. However, mainly unreacted **TDI-4Br** remained in the mixture and no product could be identified via TLC and MS measurement. Furthermore, the reaction was carried out in dry toluene using potassium carbonate as a base. This combination of base and solvent did not work out neither.

Table 2: Combinations of solvents and base used in attempts of Suzuki cross-coupling of TDI-4Br and (28); Rf values; eluent Cy/EE 4+1

solvent	base	temperature / °C	R_f-value$_{educt}$	R_f-value $_{new\ spot}$
toluene/THF/H_2O	Na_2CO_3	70	0.83	0.68
DMF/toluene (dry)	Cs_2CO_3	80	0.70	0.44
toluene (dry)	K_2CO_3	70	0.68	0.51

5.1.8. Protection of hydroxyl-group of the pH-sensitive receptor

Due to the possible C-O cross coupling reaction, two different protection methods of the hydroxyl group were conducted.

The first protection strategy was the acetylation of the primary alcohol of the receptor **(28)** via conversion with acetyl chloride. The reaction is described as a simple and selective method when carried out in the presence of a sterically hindered amine (base).[39] Separation of formed side products was easily achieved by silica filtration using DCM as solvent. The acetylated receptor **(28-OAc)** was obtained in high yields as a colorless solid (78 %).

The second approach to protect the hydroxyl group was performed using triisopropylsilane (**TIPS**), which is a common and widely used hydroxyl-protecting group. Deprotection can be achieved under mild conditions using tetrabutylammonium fluoride in THF.[62,63] The protection reaction worked out well, resulting in quantitative yield of the protected receptor **(28-TIPS)**. Due to the simple deprotection procedure, **(28-TIPS)** was chosen for further reactions.

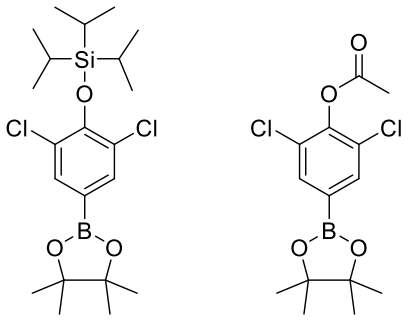

(28)-TIPS **(28)-OAc**

Figure 24: Protected hydroxyl group of pH-sensitive receptor with different protecting groups

5.1.9. Introduction of protected pH-sensitive group

In the next step, introduction of the pH-sensitive receptor was attempted again, using the **TIPS** protected receptor **(28-TIPS)** as reactant. Suzuki cross-coupling reaction was carried out as described previously. In the first approach, aqueous Na_2CO_3 solution and a mixture of toluene and THF was utilized. Reaction control was conducted via TLC. TLC confirmed that the conversion rate did not increase compared to the attempt using the unprotected receptor **(28)**. The newly formed compound was separated from unreacted educts by column chromatography. A second approach in a water-free environment was conducted. Formation of a new compound was observed, but yields were too low to identify the compound. The R_f value of the formed compound (R_f=0.90) was very similar to the one formed in the aqueous environment (R_f= 0.83) Owing to the very low yields, the newly formed and isolated products from each attempt were combined. In the next step, deprotection was performed without knowledge about the success of the cross coupling reaction. Due to the very low yields of the reactions, no determination via NMR spectroscopy was possible.

Table 3: Conducted Suzuki cross-coupling reactions in different solvent/base combinations; Rf values of educt TDI-4Br and the new formed compound

solvent	base	Temperature / °C	R_f-value$_{educt}$	R_f-value $_{new\ spot}$
toluene/THF/H_2O	Na_2CO_3	70	0.83	0.59
DMF/toluene (dry)	Cs_2CO_3	80	0.90	0.68

5.1.10. Deprotection of pH-sensitive group

Due to the possible C-O coupling reaction, the hydroxyl moiety of the pH-sensitive group was protected with TIPS **(28-TIPS)**. After Suzuki cross-coupling of the receptor and the dye was performed, deprotection had to be done to recover pH-sensitivity. The reaction scheme is illustrated in **Figure 25**.[40]

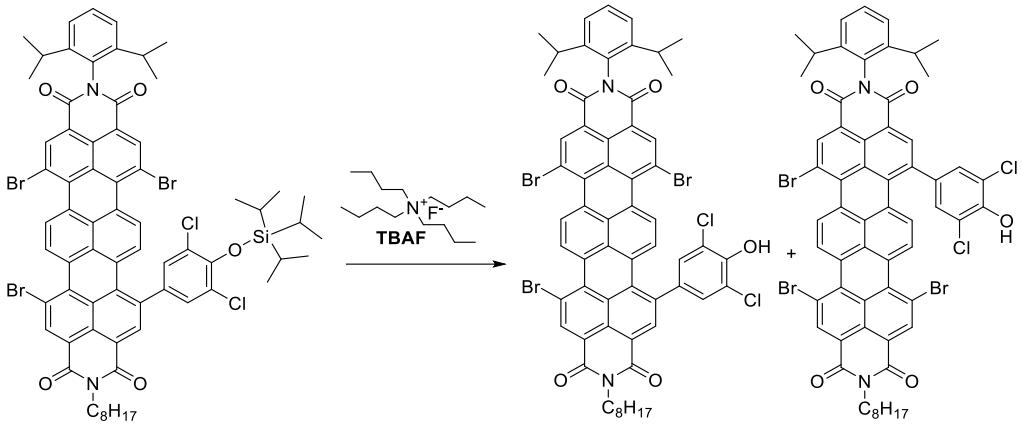

Figure 25: Reaction scheme of deprotection reaction with TBAF

Determination if introduction of the receptor was successful or not is easier when the hydroxyl group is deprotected. Therefore, deprotection was carried out subsequently after Suzuki-cross-coupling without further purification. Fluorescence measurements of the deprotected dye were performed in acidic (addition of acetic acid) and basic (addition of triethylamine) environment. However, no significant differences in fluorescence intensities were obtained, indicating unsuccessful Suzuki cross-coupling.

Due to the challenging synthesis and many unsuccessful attempts to introduce pH sensitivity via Suzuki cross coupling this pathway was considered to be not expedient.

To conclude this synthetic route, the used boronic acid pinacol ester seemed to be not suitable for Suzuki cross-coupling reaction conditions. Probably, hydrolysis of the boronic acid pinacol ester occurs and makes further reaction impossible. Furthermore, dry Suzuki reactions did not work out most likely due to the low solubility of the used bases in other solvents than water. Caused by the low yields (<5%) no product characterization could be performed.

5.1.11. Attempt to introduce pH-sensitive group via chlorosulfonation

The next synthetic pathway to introduce pH-sensitivity to the terrylene diimide dye was adapted from a procedure published by Aigner in 2013 applied for perylene diimides to introduce a polymerizable functionality.[23] It was assumed to be a promising method for terrylene diimides too. The desired product is shown in **Figure 26**. However, formation of the product could not be confirmed within this work.

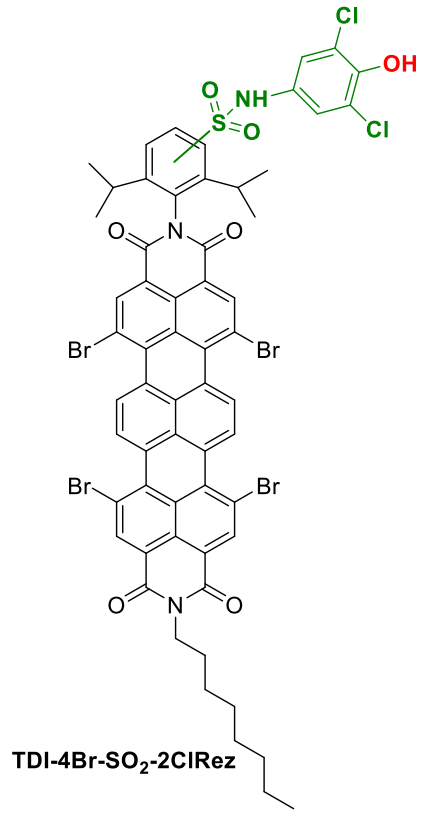

Figure 26:TDI-4Br-SO2-2ClRez, desired product of chlorosulfonation reaction

The brominated terrylene diimide **TDI-4Br** was stirred in chlorosulfonic acid at 60 °C. After 3 h the reaction mixture was slowly dropped onto crushed ice. This neutralization is strongly exothermic and during dropping on the crushed ice, the temperature should be kept low to avoid hydrolysis of the product. The formed precipitate was washed with ice water until neutral and dried at the rotary vane pump. The sulfonyl chloride derivate was allowed to react with the amine group of **(26) (Figure 27)** in the presence of a tertiary base such as triethylamine. It is preferable to perform the reaction in water-free media to avoid base catalyzed hydrolysis. As solvent dry DMF was chosen.

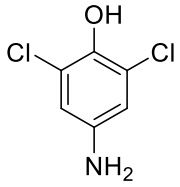

(26)

Figure 27: (26) 4-Amino-2,6-dichlorophenol

In **Figure 28** the mechanism of the reaction between an amine and a sulfonyl chloride attached to an aryl is illustrated. The reaction follows a bimolecular S_N2 mechanism wherein the chlorine is substituted by the nucleophilic amine.[64]

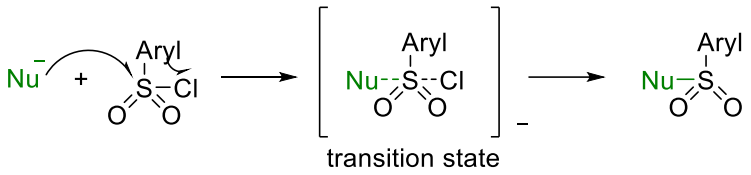

Figure 28: Reaction mechanism of the reaction between an amine (nucleophile) and a sulfonyl chloride attached to an aryl

As an amine, the pH-sensitive 4-amino-2,6-dichlorophenol **(26)** was used. The resulting bluish solid was only soluble in dimethyl sulfoxide (DMSO) which made purification via classical column chromatography impossible. Alternatively, multiple washing steps with different solvents from the polarity scale (H_2O, EtOH, MeOH, DCM, THF, ACN, DMF) were performed. However, this purification was not sufficient and conversion to the desired product could not be confirmed via HR-MS or NMR spectroscopy.

Once, direct conversion of not purified **TDI-4Br-SO_2-2ClRez** with 4-(morpholine-4-carbonyl)phenylboronic acid pinacol ester **(24)** was attempted to improve the solubility and thus enable column chromatography for purification. However, Suzuki cross-coupling between **TDI-4Br-SO_2-2ClRez** and **(24)** did not work out probably due to the solubility behavior of the chlorosulfonated terrylene dye.

As conclusion it can be said, that even the synthesis of the basic terrylene diimide structure (**TDI**) is very time-consuming. The pathway to gain the basic structure includes many challenging synthesis steps which leads to low yields of **TDI**. Therefore, the pathway had to be repeated several times to gain sufficient amounts of the precursor **TDI** which enables further

functionalization attempts. Improvement of the solubility of **TDI** was successfully conducted by introduction of bulky substituents such as n-octylamine and diisopropylaniline at the terminal imide positions and modification of the bay region. The successful four-fold functionalization of the bay region with the morpholino moiety and with phenyl groups also lead to significant bathochromic shifts of the emission bands compared to **TDI-4Br**. Optical properties of the modified terrylene diimides **TDI-4Br**, **TDI-4Mo**, **TDI-4Ph**, are discussed in detail in chapter 5.2 starting on page 81.

All attempts to achieve pH-sensitivity via saponification and subsequent introduction of the receptor were not successful. Further experiments to introduce the pH-sensitive receptor were performed via Suzuki cross-coupling. Even the conducted reactions using a receptor with a protected hydroxyl group did not work out.

The introduction of the pH-sensitive group in an earlier step of the synthesis pathway could be a possible way to gain the desired result. For example, introduction of the receptor at the naphthalene or perylene building block could be performed right before coupling to **TDI-U**. This pathway was not pursued in the course of this work.

5.2. Photophysical properties of synthesized terrylene diimide dyes

As described in the previous chapter, the challenging synthesis of a pH-sensitive terrylene diimide dye was not successful. However, three bay functionalized terrylene diimides were successfully synthesized **(TDI-4Br**, **TDI-4Ph**, **TDI-4Mo**).

Within this work, optical properties of **TDI-4Br**, **TDI-4Ph** and **TDI-4Mo** (**Figure 29**) were investigated mainly focused on influences caused by environments differing in polarity. Measurements were performed in solvents, covering a broad range of the polarity scale (EtOH, DCM, THF, toluene). The dependence of quantum yield, fluorescence lifetime and molar absorption coefficient on the polarity of the environment was examined and therefore the applicability of the dyes in different polarities. Furthermore, photostability of the three dyes was surveyed and compared to dibutoxy-aza-BODIPY. In the following figures and tables all determined optical properties are illustrated and listed, respectively.

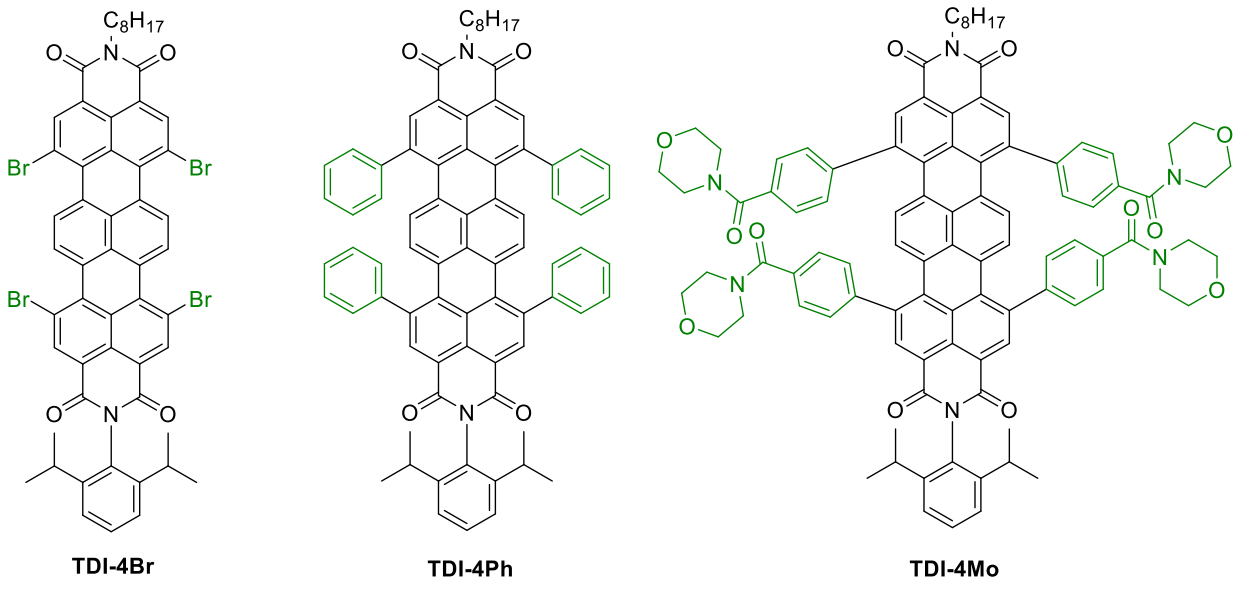

Figure 29: Investigated bay-functionalized terrylene diimide dyes (TDI-4Br, TDI-4Ph, TDI-4Mo)

5.2.1. Change of absorption spectra during TDI synthesis

Within this work, the first step was the synthesis of **TDI-4Br** which was used as platform for further modification of the bay region. An overview of absorption spectra of intermediate stages of the **TDI-4Br** synthesis is shown in **Figure 30**. Absorption spectra of the naphthalene building block **(8)** and the perylene building block **(9)**, the linked terrylene precursor **TDI-U**, the conjugated terrylene **TDI** and the fourfold brominated terrylene **TDI-4Br** are illustrated. Linkage of **(8)** and **(9)** via Suzuki cross-coupling leads to the formation of **TDI-U**. This can be seen when the absorption spectrum of **TDI-U** is contemplated. It corresponds to the combination of the absorption spectra of compounds **(8)** and **(9)** with the expected difference in the molar absorption coefficient of the naphthalimide and perylene chromophore. After conjugation of the system to **TDI** the shape of the absorption spectrum changes to the typical spectrum shape of rylene dyes. After four-fold bromination at the bay region the absorption spectrum changed as described in literature.[17] The absorption maximum remains unaffected. However, the shoulder of the absorption band changes and gets less distinct. The difference between **TDI** and **TDI-4Br** is presented in more detail in **Figure 31**.

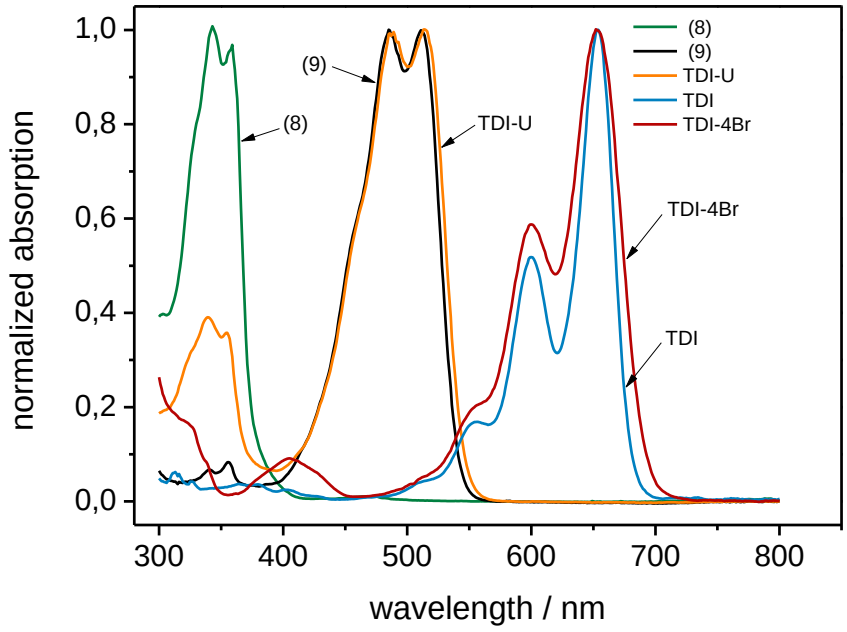

Figure 30: Overview of absorption spectra in $CHCl_3$ of intermediate products within the synthesis of TDI-4Br

In **Figure 31** absorption and emission spectra of **TDI** and **TDI-4Br** in chloroform are compared. As can be seen, the form of the spectra is characteristic for rylene dyes. The absorption maximum at 652 nm stays unaffected when the bay region of **TDI** is substituted with four bromine atoms. In contrast to the absorption maximum, the emission maximum of **TDI-4Br** is bathochromically shifted from 670 nm to 684 nm. Absorption and emission bands of **TDI** are relatively narrow and exhibiting a Stokes shift of 18 nm, while **TDI-4Br** shows slightly enlarged Stokes shift of 32 nm. Furthermore, the shoulder of the absorption as well as the shoulder of the emission bands gets less distinct. In addition, the spectra of **TDI-4Br** are slightly broader compared to the unmodified terrylene. **TDI** possesses a dark blue color, whereas **TDI-4Br** has a violet color.

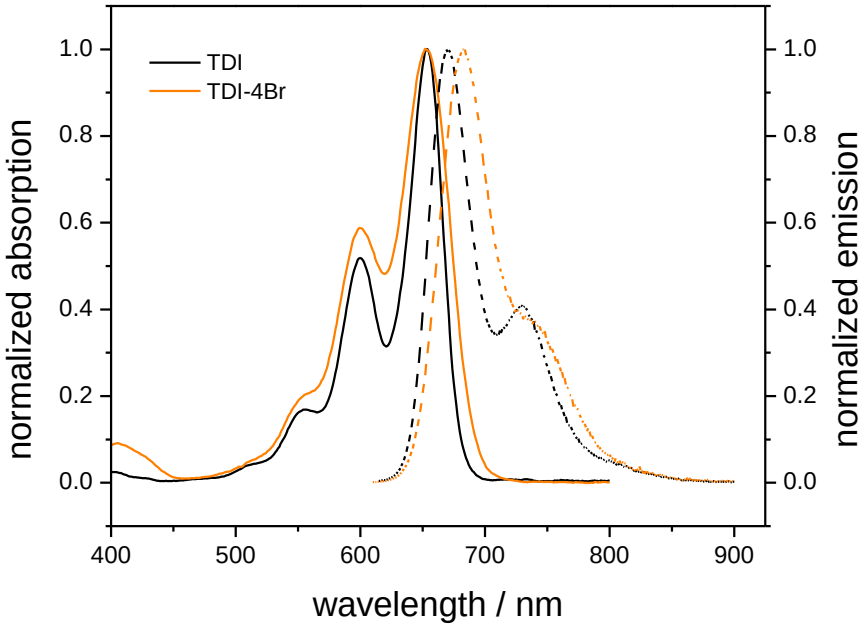

Figure 31: Differences of absorption (continuous lines) and emission (dashed lines) spectra of TDI and TDI-4Br

5.2.2. Photophysical properties of TDI-4Br

The influence of the polarity of the used solvent on the photophysical properties of **TDI-4Br**, **TDI-4Ph** and **TDI-4Mo** was investigated. Therefore, relative quantum yield, fluorescence lifetime and molar absorption coefficient were determined in toluene, THF, and $CHCl_3$. **TDI-4Br** is insoluble in ethanol and therefore no measurements were conducted within this solvent. All results are listed in **Table 4.**

Table 4: Photophysical properties of TDI-4Br in different solvents at 25 °C

TDI-4Br

solvent	λ_{abs} [nm]	λ_{em} [nm]	ε [L mol^{-1} cm^{-1}]	Φ	τ [ns]
toluene	651	680	68000	0.43	3.6
THF	644	676	94000	0.35	3.1
$CHCl_3$	653	683	82000	0.43	3.5

The absorption maximum of **TDI-4Br** is located at about 650 nm and the emission maximum at about 680 nm with a slight variance in different solvents due to solvatochromic effects.[65] The values correspond to the values listed in literature.[51]

The highest molar absorption coefficient was determined in THF (94 000 L mol^1 cm^{-1}), while the highest quantum yield (QY) was measured in $CHCl_3$ and toluene (Φ = 0.43). The quantum yield for **TDI-4Br** reported in literature is 64 %[34] and is therefore higher than the value determined within this work. The quantum yield was measured relative to 3,3'-diethylthiadicarbocyanine iodide which has a known quantum yield of 35 % in ethanol.[34]

Fluorescence lifetimes were determined via time-correlated single photon counting and are in the same range between 3 ns to 4 ns within different solvent environments.

5.2.3. Photophysical properties of TDI-4Ph

The goal of a bathochromic shift of emission bands to the deep red range of the electromagnetic spectrum was reached via modification of **TDI-4Br** at the bay region by substitution of the four bromine atoms with phenyl groups resulting in compound **TDI-4Ph**. The modification affords a green coloured product instead of the violet coloured **TDI-4Br**. Thereby, the absorption maximum shifted bathochromically to 702 nm (in chloroform) as well as the emission maximum shifted to 748 nm (**Figure 32**). Characterization of **TDI-4Ph** was conducted in toluene, THF, $CHCl_3$ and EtOH. Determination in EtOH was now possible due to the improved solubility in polar solvents of **TDI-4Ph** compared to **TDI-4Br**. The increased solubility can be explained by the nonplanar conformation of **TDI-4Ph** which furthermore leads to a decreased aggregation behavior.[38] The quantum yield of **TDI-4Ph** was determined relative to dibutoxy aza-BODIPY which has a known quantum yield of 36 % in chloroform.[33] All results are listed in **Table 5**.

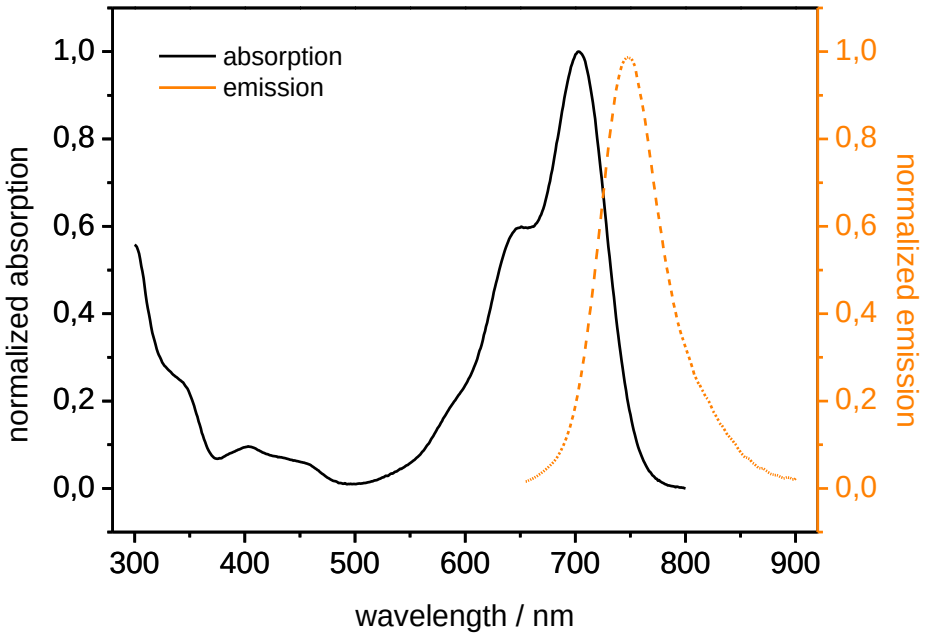

Figure 32: Absorption and emission spectra of TDI-4Ph in chloroform

Table 5: Photophysical properties of TDI-4Ph in different solvents

TDI-4Ph

solvent	λ_{abs} [nm]	λ_{em} [nm]	ε [L mol^{-1} cm^{-1}]	Φ	τ [ns]
toluene	696	738	52000	0.30	3.8
THF	689	738	40000	0.17	2.4
$CHCl_3$	702	748	44000	0.18	2.6
EtOH	697	748	42000	0.019	0.47

Examination of the results shows the dependency of the photophysical properties on the polarity of the solvent. The absorption maximum and emission maximum is only slightly affected by solvent polarity and stays in the same range about 700 nm and 750 nm, respectively. The slight variance between the maxima does not correlate well with increase in solvent polarity (e.g. the absorption maximum in THF is located at 689 nm, but in less polar toluene and more polar EtOH it shifts bathochromically to 696 nm and 697 nm, respectively). In

Figure 33**,** absorption and emission spectra of **TDI-4Ph** in different solvents are illustrated. The highest molar absorption coefficient was measured in the most nonpolar solvent toluene (52 000 L mol^{-1}cm^{-1}). However, the value is even lower than expected. A possible explanation could be that the measured compound was not completely pure and contained grease residues which affects the weight of the taken sample. This has a huge impact on the determination of the molar absorption coefficient. The quantum yield of **TDI-4Ph** strongly depends on the used solvent. As can be seen in **Table 5**, the fluorescence quantum yield decreases dramatically with increasing polarity. The highest value of 30 % was determined in toluene whereas the lowest quantum yield of 1.9 % was determined in the most polar environment ethanol, which is 15-fold lower.

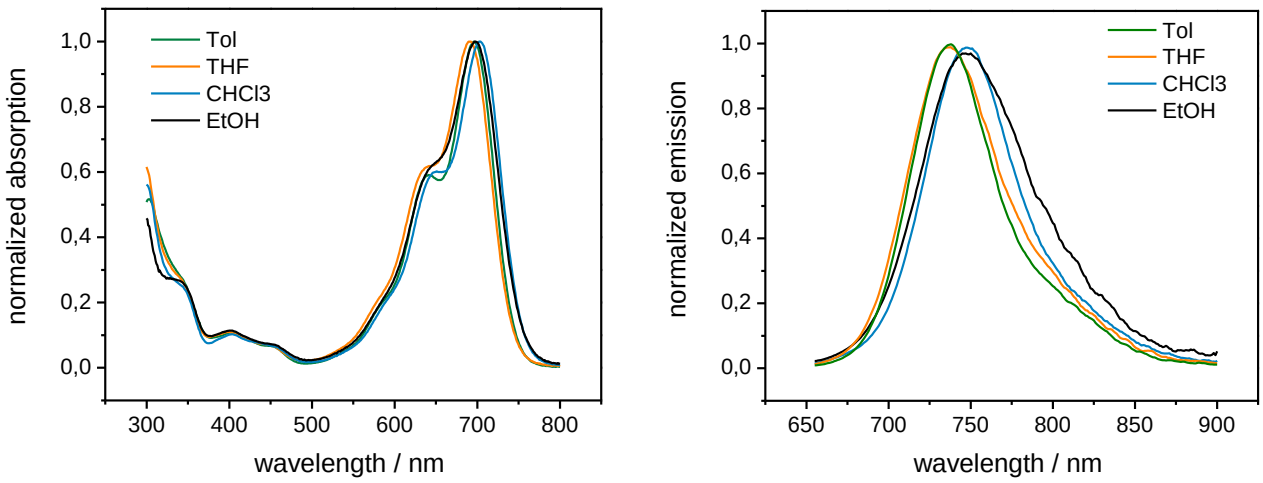

Figure 33: Absorption spectra (left) and emission spectra (right) of TDI-4Ph in different solvents

Furthermore, the fluorescence lifetime is affected by the polarity of the environment too. The longest lifetime of 3.8 ns was measured in toluene. Measurements in chloroform and THF showed slightly decreased values. However, the fluorescence lifetime in ethanol decreases drastically to the picosecond range (470 ps). In **Figure 34** an example of a decay function is shown.

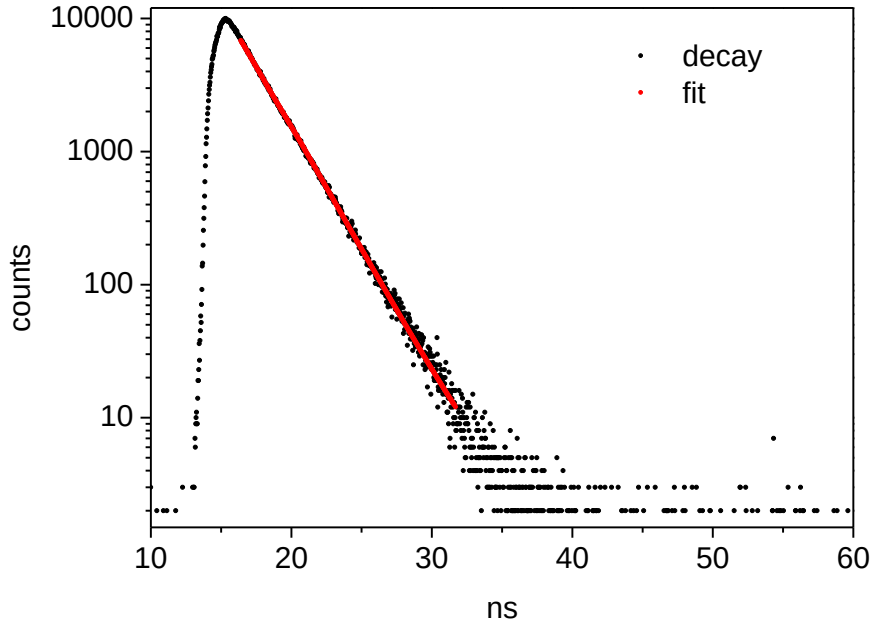

Figure 34: Fluorescence intensity decay of TDI-4Ph in THF

5.2.4. Photophysical properties of TDI-4Mo

The second successful modification of **TDI-4Br** was performed via substitution of the four bromine atoms with 4-(morpholine-4-carbonyl)phenylboronic acid pinacol ester resulting in **TDI-4Mo** (**Figure 29**). Absorption and emission bands bathochromically shifted to 700 nm and 743 nm, respectively. The absorption and emission spectra in chloroform are illustrated in **Figure 35**.

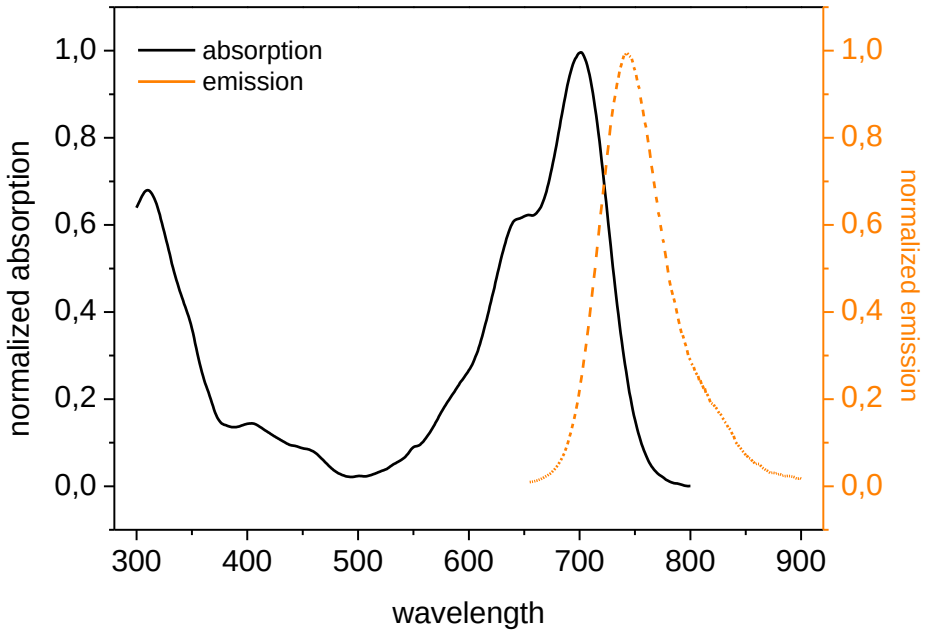

Figure 35: Absorption (continuous line) and emission (dashed line) spectrum of TDI-4Mo in chloroform

Table 6: Photophysical properties of TDI-4Mo

TDI-4Mo

solvent	$\lambda_{max,\ abs}$ [nm]	$\lambda_{max,\ em}$ [nm]	ε [L mol^{-1} cm^{-1}]	Φ	τ [ns]
toluene	697	739	61000	0.27	3.7
THF	693	738	70000	0.14	2.5
$CHCl_3$	700	743	76000	0.18	2.9
EtOH	694	746	68000	0.019	0.57

TDI-4Mo was as well characterized in different solvents to investigate the influence of different polarities on the photophysical properties of the dye. Measurements were conducted in toluene, THF, $CHCl_3$ and EtOH and the results are listed in **Table 6**. The influence of the solvent on the photophysical properties is similar to that observed for **TDI-4Ph**. Molar absorption coefficients

are in the range of 70000 $Lmol^{-1}cm^{-1}$ and do not differ much in different solvents, only the spectrum recorded in ethanol become slightly broader. The highest molar absorption coefficient was determined in chloroform. In **Figure 36** absorption and emission spectra of **TDI-4Mo** recorded in different solvents are illustrated.

Highest quantum yield of **TDI-4Mo** was observed in toluene with a fluorescence quantum yield of 27 %. The quantum yield decreases with increasing polarity of the environment. The determined quantum yield in ethanol is 14-fold lower than in toluene. The quantum yields of the dye in THF and chloroform are similar and about the half of the QY value in toluene. The obtained results correspond to those obtained for **TDI-4Ph**. Quantum yields were also determined relative to dibutoxy-aza-BODIPY (Φ=0.36 in $CHCl_3$).

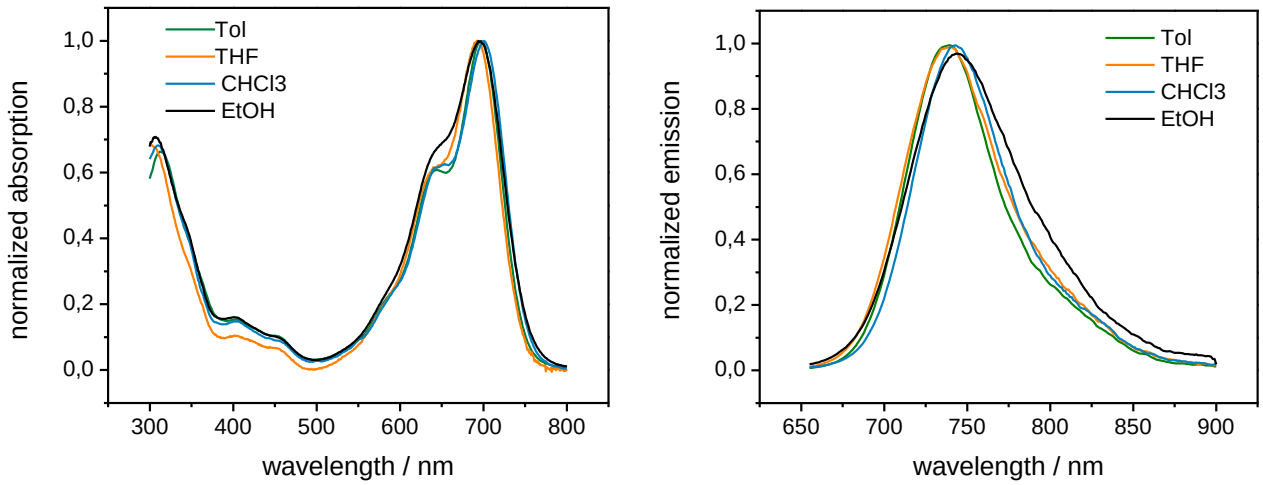

Figure 36: Absorption spectra (left) and emission spectra (right) of TDI-4Mo in different solvents

Furthermore, a decrease of the fluorescence lifetime of **TDI-4Mo** with increasing polarity was observed. The correlation between the fluorescence lifetime and the polarity of the environment confirms the trend observed in **TDI-4Ph** characterization. In toluene, THF and chloroform the fluorescence lifetime is in the typical range of rylene dyes of 3.7 ns to 2.5 ns. However, the determined fluorescence lifetime in ethanol showed a drastic decrease to 0.57 ns. **TDI-4Mo** showed monoexponential decays and the decay function of **TDI-4Mo** in THF is illustrated in **Figure 37**.

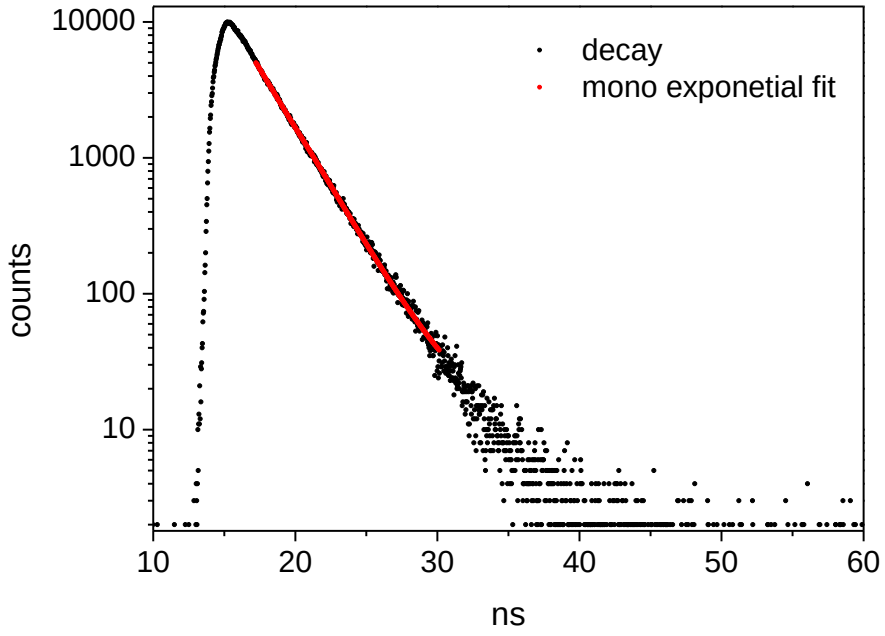

Figure 37: Fluorescence intensity decay of TDI-4Mo in THF

5.2.5. Overview of absorption and emission spectra

Here, all obtained absorption and emission spectra of the successfully synthesized dyes (**TDI-4Br**, **TDI-4Ph**, **TDI-4Mo**) are compared. The shown spectra (**Figure 38**) were recorded in chloroform.

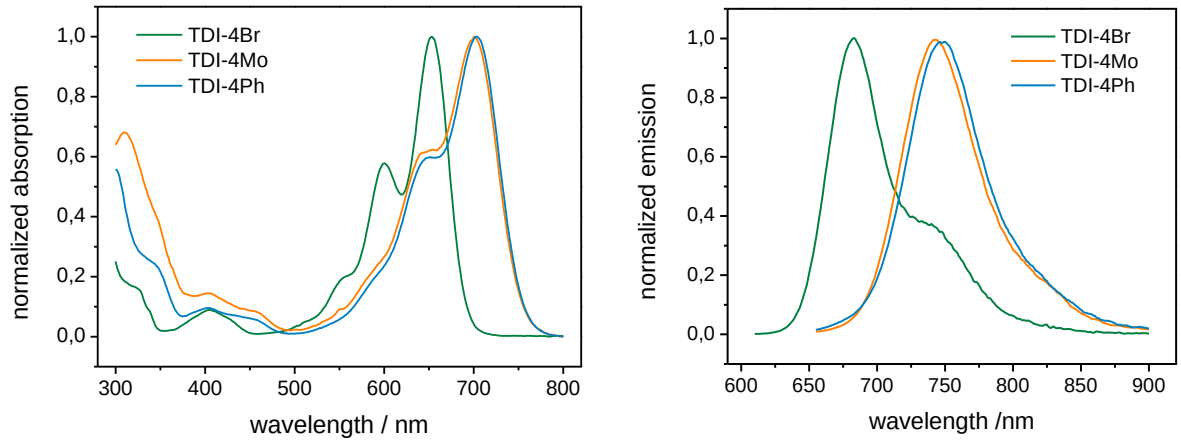

Figure 38: Absorption (left) and emission spectra (right) of synthesized dyes (TDI-4Br, TDI-4Mo, TDI-4Ph) in $CHCl_3$

All investigated photophysical properties of **TDI-4Br**, **TDI-4Ph** and **TDI-4Mo** measured in chloroform are listed in **Table 7**.

Table 7: Photophysical properties of TDI-4Br, TDI-4Ph and TDI-4Mo in chloroform

dye	$\lambda_{max,\ abs}$ [nm]	$\lambda_{max,\ em}$ [nm]	ε [L mol^{-1} cm^{-1}]	Φ	τ [ns]
TDI-4Br	653	683	82000	0.43	3.5
TDI-4Ph	702	748	44000	0.18	2.6
TDI-4Mo	700	743	76000	0.18	2.9

5.2.6. Photostability of synthesized dyes

Another very important parameter for the application of dyes in optical sensors is the photostability. In order to estimate the photostability of the synthesized dyes (**TDI-4Mo**, **TDI-4Ph**, **TDI-4Br**), solutions of the dyes in THF were irradiated and the photodegradation profiles were recorded via UV-Vis spectroscopy. As a light source, a metal halogen lamp was used. Absorption spectra were recorded every 30 min. Photodegradation can be quantified via the decrease of the absorbance. As reference dye, dibutoxy aza-BODIPY dissolved in THF was used. This dye is rated as a highly photostable dye, emitting in the far red range of the electromagnetic spectrum.[66]

Rylene dyes, such as perylenes and terrylenes, are known as very photostable compounds. [22,51] The high photostability was confirmed for the synthesized dyes. In **Figure 39**, photodegradation profiles of synthesized dyes compared to the reference are shown.

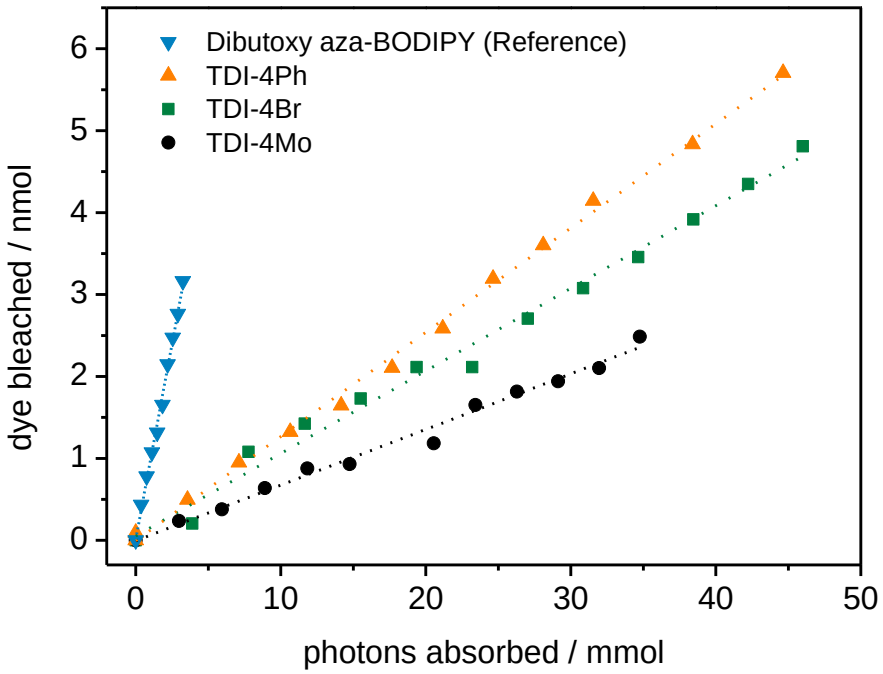

Figure 39: Photostability of the synthesized dyes compared with highly photostable dibutoxy aza-BODIPY

As can be seen, the synthesized terrylene diimide dyes are more stable compared to the reference dibutoxy aza-BODIPY. Quantification of the photodegradation was conducted via calculation of the photobleaching quantum efficiency Φ_{bl}, which equals the slopes of the individual curves. Thereby, the number of photons absorbed in the cuvette is plotted versus the moles of bleached dye. Calculated photobleaching quantum efficiencies are listed in **Table 8**.

Table 8: Photobleaching quantum efficiencies Φ_{bl} of TDI-4Mo, TDI-4Ph, TDI-4Br and dibutoxy aza-BODIPY

dye	Φ_{bl}
TDI-4Mo	6.8×10^{-8}
TDI-4Ph	1.3×10^{-7}
TDI-4Br	1.0×10^{-7}
dibutoxy aza-BODIPY	9.5×10^{-7}

Photostabilities measured for terrylene diimide dyes **TDI-4Mo**, **TDI-4Ph** and **TDI-4Br** are about one order of magnitude higher compared to the reference dibutoxy aza-BODIPY with the Φ_{bl} in the range of 1.0×10^{-7}-6.8×10^{-8}. The highest stability against photodegradation showed **TDI-4Mo**. **TDI-4Ph** and **TDI-4Br** have a similar photodegradation behavior. However, the photostability is slightly lower compared to TDI-4Mo.

The examined photostabilities of terrylene diimide dyes are in the same range when compared with pH-sensitive BODIPY dyes used for carbon dioxide imaging, emitting in the red part of the electromagnetic spectrum. The investigated BODIPY dyes, bearing different receptors, showed photostabilities in the range of 1.0×10^{-7} – 5.7×10^{-8}.[67] It can be concluded that the photostability of the terrylene dyes synthesized within this work is remarkable and sufficient for applications in optical sensing. However, the decreasing brightness and the decreasing fluorescence lifetime in polar environments make the dyes inappropriate material for application in optical sensors.

5.3. Summary and outlook

To conclude, the synthesis of terrylene dyes is very challenging and time consuming. Although the terrylene dyes with certain substituents have been successfully prepared, the chosen pathways for the synthesis of a pH-sensitive terrylene diimide were not accomplished successfully. Another possible way to synthesize a pH-sensitive terrylene dye could be the introduction of the pH-sensitive group at an earlier stage of the synthesis. Attachment of the pH-sensitive group instead of the n-octylamine at the naphthalene building block or the perylene building block before linkage to the terrylene precursor **TDI-U** may be possible. Therefore, protection of the hydroxyl group would be also necessary. Within this pathway the unsuccessfully conducted one sided saponification reaction or the Suzuki coupling of the pH-sensitive receptor to the terrylene diimide core would not be longer necessary to yield pH-sensitive terrylene dyes.

The limiting reaction within the chosen pathway was the Miyaura-borylation. Thereby, the naphthalene building block was converted to a boronic acid pinacol ester. Once, the borylation was performed with the perylene building block. The yield of this borylation reaction was significantly higher than the borylation reaction of the naphthalene building block. Due to this, the synthesis of **TDI** could have been more effective when executed via a perylene boronic acid pinacol ester.

Overall, a tetra-brominated terrylene dye and two bay substituted terrylene diimide dyes emitting in the deep red range of the electromagnetic spectrum were synthesized. The solubility of the terrylene ground structure was improved by introduction of bulky substituents at the terminal imide position and the bay region. Furthermore, the emission bands shifted bathochromically by extension of the π-conjugated system of the terrylene structure. This was reached by modification of the terrylene bay region with four phenyl groups or with four 4-(morpholine-4-carbonyl)phenyl groups resulting in **TDI-4Ph** and **TDI-4Mo**, respectively. Investigation of photophysical properties revealed excellent photostability, long wavelength absorption and emission, appropriate fluorescence lifetimes and adequate quantum yields. Unfortunately, the strong decrease of the brightness and the fluorescence lifetime of the dyes in polar solvents was observed. This makes them poorly suitable for applications in hydrophilic environments and thus prevents the application of these chromophores as potential pH indicators.

Another possible way to synthesize a pH-sensitive terrylene dye could be the introduction of the pH-sensitive group at an earlier stage of the synthesis. Attachment of the pH-sensitive group

instead of the n-octylamine at the naphthalene building block or the perylene building block before linkage to the terrylene precursor **TDI-U** could be possible. Therefore, protection of the hydroxyl group would be also necessary. Within this pathway the unsuccessfully conducted one sided saponification reaction or the Suzuki coupling of the pH-sensitive receptor to the terrylene diimide core would not be longer necessary to yield pH-sensitive terrylene dyes.

The limiting reaction within the chosen pathway was the Miyaura-borylation. Thereby, the naphthalene building block was converted to a boronic acid pinacol ester. Once, the borylation was performed with the perylene building block. The yield of this borylation reaction was significantly higher than the borylation reaction of the naphthalene building block. Due to this, the synthesis of **TDI** could have been more effective when executed via a perylene boronic acid pinacol ester.

5.4. Modification attempts of a perylene chromophore

Within this work modification of perylenes was pursued additionally. Perylenes belong to the dye class of rylenes such as terrylenes. Perylene derivates have gained much attention in research over the last decades and are promising for the usage as indicators for optical sensors. Perylenes exhibit optical properties desirable for the application in optical sensing, such as excellent photostability, high molar extinction coefficients and high brightness.[24] Hence, different modification approaches of tetrachloroperylene tetracarboxylic acid anhydride **(PDI-4Cl (14)**, shown in **Figure 40** were performed. Modifications were attempted at the terminal anhydride position and the chlorinated bay region of the chromophore.

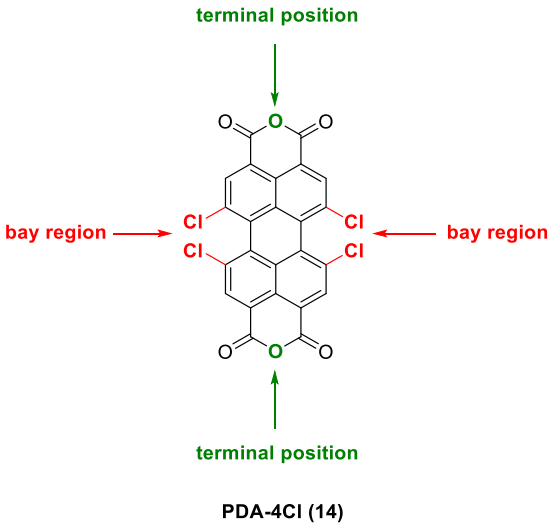

Figure 40: Starting material for attempted modifications; tetrachloroperylene tetracarboxylic acid anhydride PDA-4Cl

The first modification strategy was focused on introduction of a pH-sensitive group at the terminal position of the perylene with the idea, to obtain a pH indicator via an easy and short synthesis pathway.

The second modification strategy was focused on introduction of four triethylene glycol monomethyl ether groups (**TEG**) in bay region, to enhance solubility in polar media such as polyurethane hydrogels used as matrices for pH sensing. Two different attempts were performed. First, direct attachment of **TEG** via Williamson ether synthesis. Second, attaching **TEG** group to a 4-hydroybenzyl alcohol first and to introduce this group at the bay region of the perylene. However, these modification strategies were not accomplished successfully.

All experiments are described in more detail in the following sections.

5.4.1. Introduction of a pH-sensitive group at the terminal position

The approach of introduction of a pH-sensitive group at the terminal position of **PDI-4Cl** was conducted according to a procedure published in 2016. [43] The reaction pathway is illustrated in **Figure 41**.

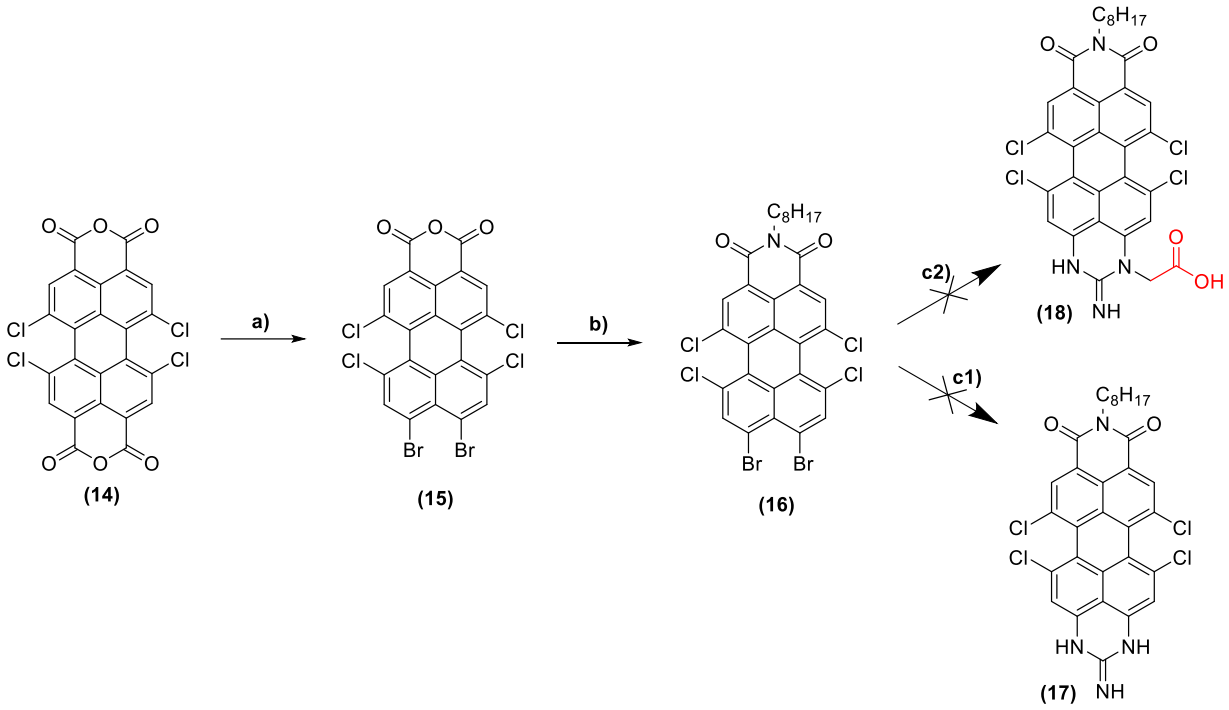

Figure 41: Synthesis pathway of perylene dye; a)1) Br_2, NaOH, HAc, H2O, 80 °C, 2 h, 2) HAc/MeOH, 100 °C, 5h (69 %) **b)** n-octylamine, NMP/HAc, 110°C, 4.5 h (29 %) **c1)** guanidine hydrochloride, K_2CO_3, NMP, 100 °C, 1h **c2)** guanidine acetic acid, K_2CO_3, NMP, 100 °C

As first step, **PDI-4Cl** was brominated according to literature.[42] Identification of the received product was not possible via NMR spectroscopy due to the low solubility of the product. However, the 2-fold brominated product was confirmed via mass spectroscopy. Due to the low solubility, purification of the crude product via column chromatography was not possible and therefore the precipitate was washed several times with methanol. The resulting red solid **(15)** was used in the next step without further purification.

Subsequently, the introduction of n-octylamine at the second terminal position was performed to improve the solubility of the dye resulting in compound **(16)**, which could be purified via column chromatography. However, identification via NMR spectroscopy could not be conducted, due to the still very low solubility in common solvents. The product was confirmed by mass spectroscopy.

By introduction of a guanidine substituent at the brominated positions of the perylene, a chromophore emitting in the far-red part of the electromagnetic spectrum **(17)** could be obtained. In addition, the solubility of the dye should increase significantly.[43] With respect to the published reaction, the plan consisted of introduction of guanidine, bearing a pH-sensitive group. The planned synthesis is illustrated in **Figure 41**.

The reaction was first carried out using guanidine hydrochloride. The crude product was separated via column chromatography and several byproducts were obtained. The product **(17)** could not be identified via mass spectroscopy and the largest bathochromic shifted absorption maximum was located at 630 nm which does not correspond to the published absorption maximum of **(17)** at 720 nm.[43] The reaction was repeated several times, but formation of product **(17)** could not be obtained in any trial. Thus, functionalization with guanidine acetic acid was not attempted which would have enabled further coupling of a pH receptor.

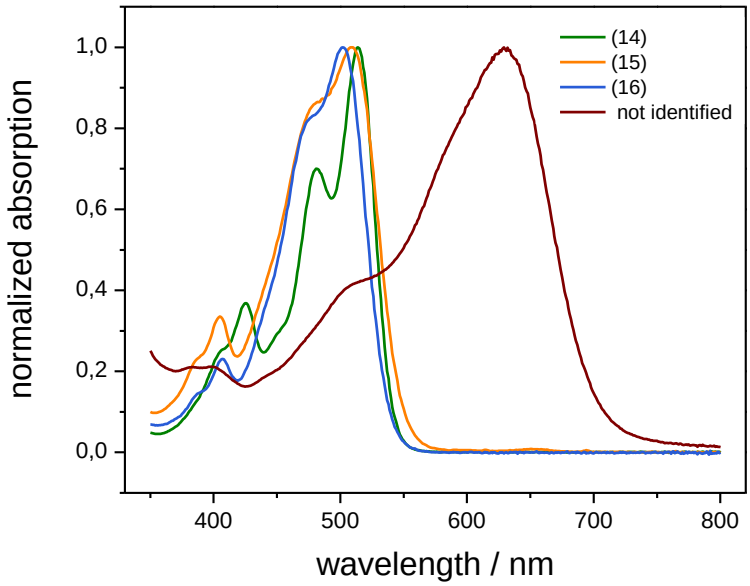

Figure 42: Absorption spectra of intermediate products and the byproduct exhibiting the largest bathochromic shift

5.4.2. Introduction attempt of TEG groups at the bay region of a perylene

The second approach of a perylene modification was attaching **TEG** groups (triethylene glycol monomethyl ether) at the bay region. Two different strategies were pursued.

The first strategy is illustrated in **Figure 43**. As starting material **PDA-4Cl (14)** was utilized. To enable the reaction, the solubility of **PDA-4Cl** had to be improved, by attachment of n-octylamine groups at the terminal positions yielding a symmetric product **(20)**.[44]

In the next step, a Williamson ether synthesis was performed. In this reaction the formation of an ether out of an alcoholate and a halogenated compound takes place. The alcoholate is formed out of an alcohol by a base such as sodium hydride (NaH).[48] The first trial was a one pot synthesis using an excess of the liquid **TEG**, which also acted as solvent in this reaction. Alcoholate formation (release of hydrogen gas) was completed after several minutes and the mixture was stirred overnight. Separation was very challenging due to the high excess of **TEG** and the many different components, which had formed within the reaction. Hence, isolation of the desired product was not possible.

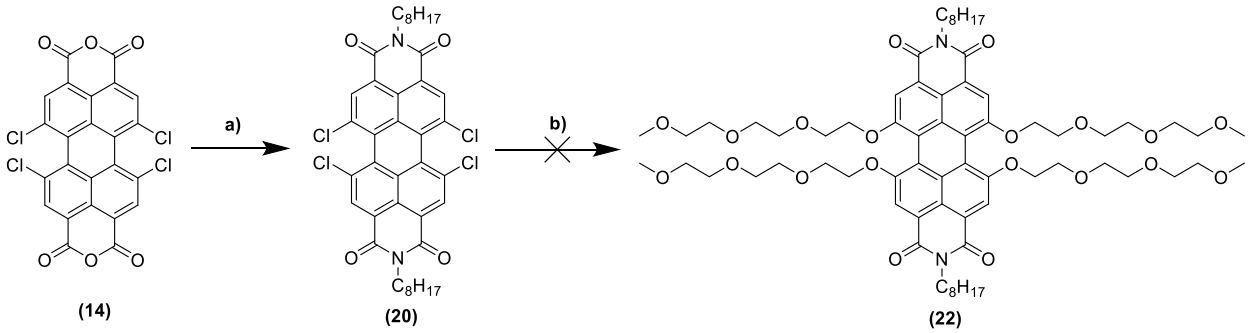

Figure 43: Synthesis pathway to improve solubility of perylene dye a) n-octylamine, propionic acid, reflux, 24 h **b)** triethylene monomethyl ether, NaH, RT, 17 h

In another attempt, activation of **TEG** via NaH was conducted before **(20)** was added to the reaction mixture. In **Figure 44** absorption spectra of isolated fractions, which showed defined absorption bands, are illustrated. Fraction 2 (orange line) contained a compound with the molar mass corresponding to a 2-fold substituted perylene diimide. However, identification via NMR was not possible due to very low yields. The fraction 2 has an absorption maximum located at 570 nm which is bathochromically shifted compared to the absorption maximum of the educt **(20)**, which is located at 520 nm. The absorption maximum of fraction 3 (blue line) is further bathochromically shifted and located at 592 nm. The compound within fraction 3 was not

identified due to low yields. It can be assumed, that the desired product **(22)** could be obtained via this reaction pathway after further optimization of the reaction conditions.

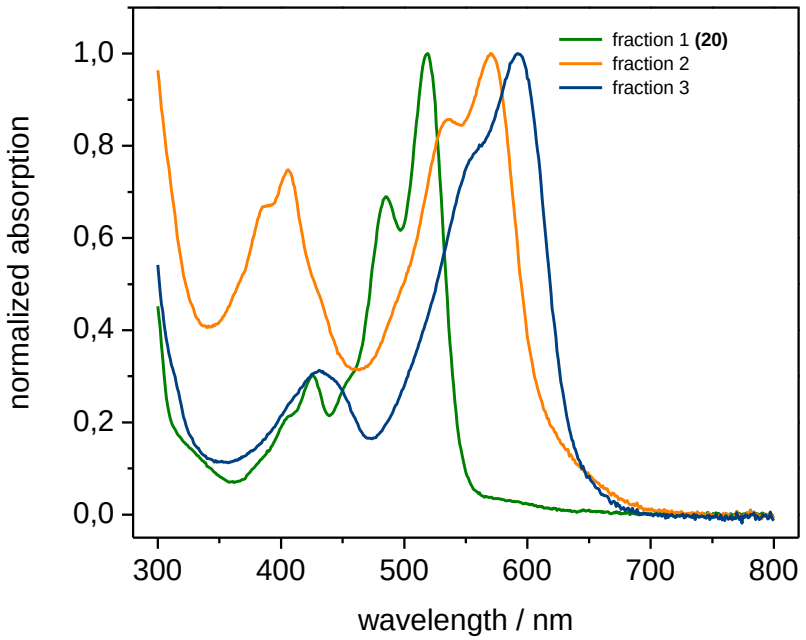

Figure 44: Absorption spectra of obtained fractions during purification of crude product (22) via column chromatography

The second plan to introduce four **TEG** groups at the bay region was conducted according to the same synthetic principle. Bonding of TEG and the perylene core should occur under formation of an ether. In contrast to the first attempt, the TEG group was linked to 4-hydroxybenzyl alcohol before attaching at the chlorinated bay region. The synthetic pathway is shown in **Figure 45**.

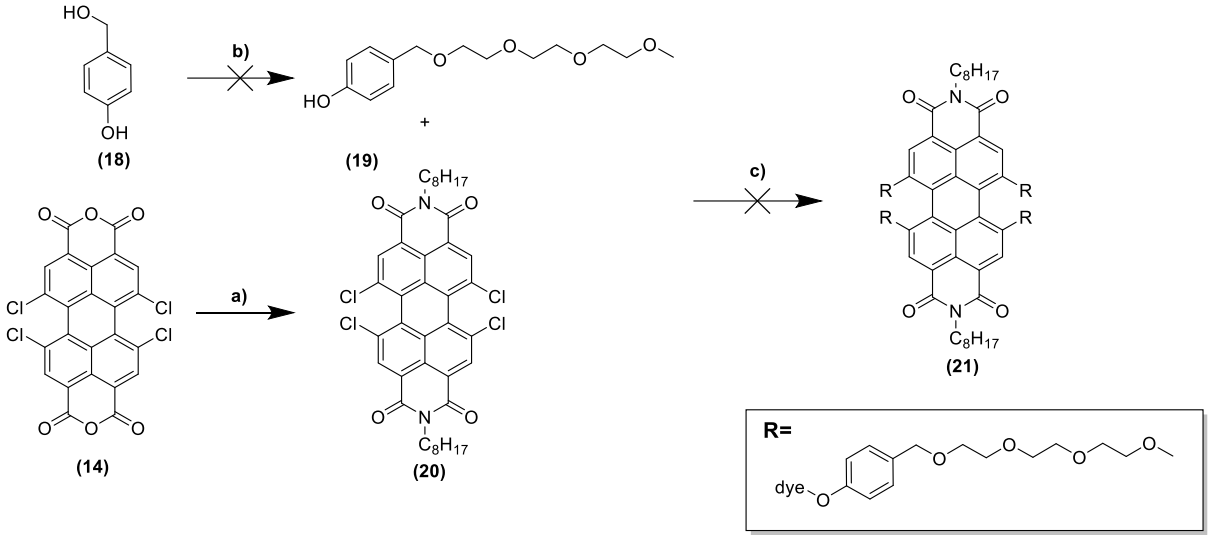

Figure 45: Synthesis pathway for introduction of TEG groups at the bay region of a perylene

As starting material, 1,6,7,12-tetrachloroperylene-3,4-dicarboxylic anhydride **(14)** was chosen and the functionalization with n-octylamine at the terminal anhydride positions was realized to gain a better solubility of **(20)**. Subsequently, preparation of the functional group bearing the TEG group **(19)** was attempted.

Within the reaction, **TEG** was used in high excess and no further solvent was used. The tosylation reaction was performed in situ. The tosylation reagent p-toluene sulfonic acid was added to a mixture of the educts and after stirring at RT for 6 h the product **(19)** was formed. The successful formation was confirmed by mass spectrometry. However, isolation of the product was challenging and could not be realized. The issue of purification was, that the product **(19)** and **TEG** have similar physical and chemical properties, which makes separation difficult. Different purification methods were conducted. First, extraction with $CHCl_3$ /water and subsequent bulb to bulb distillation was performed. However, no separation was reached and at a temperature of 180 °C and a pressure of 600 mbar the product decomposed. Extraction via DCM/H_2O/sat. NaCl did not work out neither. Furthermore, removal of the **TEG** excess

was tried by pouring the reaction mixture into water. However, the product did not precipitate and therefore isolation was not possible. Thus, synthesis of **(21)** could not be conducted.

The last attempt to synthesize and isolate compound **(19)** was conducted using ytterbium triflate as catalyst. The rare earth metal triflate acts as Lewis acid catalyst in etherification of alcohols even in aqueous environment.[47] Ytterbium triflate was successfully synthesized according to literature by conversion of ytterbium oxide and trifluorosulfonic acid anhydride in water.[46] The formation of **(19)** was confirmed by mass spectrometry, However, isolation of the product **(19)** was not possible due to the difficult separation of the **TEG** excess and the product. Therefore, linkage of **(19)** and **(20)** could not be performed.

6. References

(1) Valeur. *Molecular Fluorescence.*; Wiley VCH: Somerset, 2002.

(2) Lakowicz, J. R. *Principles of Fluorescence Spectroscopy*, 3rd ed.; Springer: New York, 2006.

(3) Gründler, P. *Chemical Sensors: An Introduction for Scientists and Engineers*; Springer: Berlin ; New York, 2007.

(4) Absolute Measurements of Photoluminescence Quantum Yields of Solutions Using an Integrating Sphere | SpringerLink https://link.springer.com/article/10.1007/s10895-005-0054-8 (accessed Mar 26, 2020).

(5) Rodrigues, L. *Bioinspired Materials for Medical Applications.*; Elsevier Science, 2016.

(6) Miró, M.; Worsfold, P.; Poole, C.; Townshend, A. *Encyclopedia of Analytical Science. Volume 1 Volume 1*; 2019.

(7) Nagl, S.; Wolfbeis, O. S. Classification of Chemical Sensors and Biosensors Based on Fluorescence and Phosphorescence. In *Standardization and Quality Assurance in Fluorescence Measurements I: Techniques*; Resch-Genger, U., Ed.; Springer Series on Fluorescence; Springer: Berlin, Heidelberg, 2008; pp 325–346. https://doi.org/10.1007/4243_2008_022.

(8) Optical Biosensors | Chemical Reviews https://pubs.acs.org/doi/10.1021/cr068105t (accessed Apr 16, 2020).

(9) Wolfbeis, O. S. Materials for Fluorescence-Based Optical Chemical Sensors. *J. Mater. Chem.* **2005**, *15* (27–28), 2657–2669. https://doi.org/10.1039/B501536G.

(10) Wencel, D.; Abel, T.; McDonagh, C. Optical Chemical PH Sensors. *Anal. Chem.* **2014**, *86* (1), 15–29. https://doi.org/10.1021/ac4035168.

(11) Strobl, M.; Rappitsch, T.; Borisov, S. M.; Mayr, T.; Klimant, I. NIR-Emitting Aza-BODIPY Dyes – New Building Blocks for Broad-Range Optical PH Sensors. *Analyst* **2015**, *140* (21), 7150–7153. https://doi.org/10.1039/C5AN01389E.

(12) Jung, H. S.; Verwilst, P.; Kim, W. Y.; Kim, J. S. Fluorescent and Colorimetric Sensors for the Detection of Humidity or Water Content. *Chem. Soc. Rev.* **2016**, *45* (5), 1242–1256. https://doi.org/10.1039/C5CS00494B.

(13) Jung, C.; Müller, B. K.; Lamb, D. C.; Nolde, F.; Müllen, K.; Bräuchle, C. A New Photostable Terrylene Diimide Dye for Applications in Single Molecule Studies and Membrane Labeling. *J. Am. Chem. Soc.* **2006**, *128* (15), 5283–5291. https://doi.org/10.1021/ja0588104.

(14) Design und Synthese maßgeschneiderter funktioneller Rylenfarbstoffe, Johannes Gutenberg-Universität Mainz, Mainz, 2011.

(15) Avlasevich, Y.; Li, C.; Müllen, K. Synthesis and Applications of Core-Enlarged Perylene Dyes. *J. Mater. Chem.* **2010**, *20* (19), 3814–3826. https://doi.org/10.1039/C000137F.

(16) Uersfeld, D.; Stappert, S.; Li, C.; Müllen, K. Practical Syntheses of Terrylene Chromophores from Naphthalene and Perylene Building Blocks. *Advanced Synthesis & Catalysis* **2017**, *359* (23), 4184–4189. https://doi.org/10.1002/adsc.201701003.

(17) Synthesis and Modification of Terrylenediimides as High-Performance Fluorescent Dyes - Nolde - 2005 - Chemistry – A European Journal - Wiley Online Library https://onlinelibrary.wiley.com/doi/full/10.1002/chem.200401177 (accessed Mar 7, 2019).

(18) Aigner, D.; Borisov, S. M.; Klimant, I. New Fluorescent Perylene Bisimide Indicators—a Platform for Broadband PH Optodes. *Anal Bioanal Chem* **2011**, *400* (8), 2475–2485. https://doi.org/10.1007/s00216-010-4647-y.
(19) Jiang, W.; Li, Y.; Wang, Z. Tailor-Made Rylene Arrays for High Performance n-Channel Semiconductors. *Acc. Chem. Res.* **2014**, *47* (10), 3135–3147. https://doi.org/10.1021/ar500240e.
(20) Kohl, C.; Weil, T.; Qu, J.; Müllen, K. Towards Highly Fluorescent and Water-Soluble Perylene Dyes. *Chemistry – A European Journal* **2004**, *10* (21), 5297–5310. https://doi.org/10.1002/chem.200400291.
(21) Seybold, G. New Perylene and Violanthrone Dyestuffs for Fluorescent Collectors. *Dyes and Pigments* **1989**, *11* (4), 303–317. https://doi.org/10.1016/0143-7208(89)85048-X.
(22) Rademacher, A.; Märkle, S.; Langhals, H. Lösliche Perylen-Fluoreszenzfarbstoffe mit hoher Photostabilität. *Chemische Berichte* **1982**, *115* (8), 2927–2934. https://doi.org/10.1002/cber.19821150823.
(23) Aigner, D.; Borisov, S. M.; Petritsch, P.; Klimant, I. Novel near Infra-Red Fluorescent PH Sensors Based on 1-Aminoperylene Bisimides Covalently Grafted onto Poly(Acryloylmorpholine). *Chem. Commun.* **2013**, *49* (21), 2139–2141. https://doi.org/10.1039/C3CC39151E.
(24) Pfeifer, D.; Klimant, I.; Borisov, S. M. Ultrabright Red-Emitting Photostable Perylene Bisimide Dyes: New Indicators for Ratiometric Sensing of High PH or Carbon Dioxide. *Chemistry – A European Journal* **2018**, *24* (42), 10711–10720. https://doi.org/10.1002/chem.201800867.
(25) Holtrup, F. O.; R. J. Müller, G.; Quante, H.; De Feyter, S.; De Schryver, F. C.; Müllen, K. Terrylenimides: New NIR Fluorescent Dyes. *Chemistry - A European Journal* **1997**, *3* (2), 219–225. https://doi.org/10.1002/chem.19970030209.
(26) Preparation and Characterization of Regioisomerically Pure 1,7-Disubstituted Perylene Bisimide Dyes | The Journal of Organic Chemistry https://pubs.acs.org/doi/abs/10.1021/jo048880d (accessed Jan 10, 2020).
(27) Lee, A. F.; Ellis, P. J.; Fairlamb, I. J. S.; Wilson, K. Surface Catalysed Suzuki–Miyaura Cross-Coupling by Pd Nanoparticles: An Operando XAS Study. *Dalton Trans.* **2010**, *39* (43), 10473–10482. https://doi.org/10.1039/C0DT00412J.
(28) Willemse, T.; Schepens, W.; Vlijmen, H.; Maes, B.; Ballet, S. The Suzuki–Miyaura Cross-Coupling as a Versatile Tool for Peptide Diversification and Cyclization. *Catalysts* **2017**, *7*, 74. https://doi.org/10.3390/catal7030074.
(29) Miyaura, Norio.; Suzuki, Akira. Palladium-Catalyzed Cross-Coupling Reactions of Organoboron Compounds. *Chem. Rev.* **1995**, *95* (7), 2457–2483. https://doi.org/10.1021/cr00039a007.
(30) J. Lennox, A. J.; C. Lloyd-Jones, G. Selection of Boron Reagents for Suzuki–Miyaura Coupling. *Chemical Society Reviews* **2014**, *43* (1), 412–443. https://doi.org/10.1039/C3CS60197H.
(31) Ishiyama, T.; Miyaura, N. Metal-Catalyzed Reactions of Diborons for Synthesis of Organoboron Compounds. *The Chemical Record* **2004**, *3* (5), 271–280. https://doi.org/10.1002/tcr.10068.
(32) Trice, S. L. J. Palladium-Catalyzed Borylation and Cross-Coupling of Aryl and Heteroaryl Halides Utilizing Dibora Derivatives, University of Pennsylvania, 2012.
(33) Zach, P. W.; Freunberger, S. A.; Klimant, I.; Borisov, S. M. Electron-Deficient Near-Infrared Pt(II) and Pd(II) Benzoporphyrins with Dual Phosphorescence and Unusually Efficient Thermally Activated Delayed Fluorescence: First Demonstration of Simultaneous Oxygen and Temperature Sensing with a Single Emitter. *ACS Appl. Mater. Interfaces* **2017**, *9* (43), 38008–38023. https://doi.org/10.1021/acsami.7b10669.

(34) Dempster, D. N.; Morrow, T.; Rankin, R.; Thompson, G. F. Photochemical Characteristics of Cyanine Dyes. Part 1.—3,3′-Diethyloxadicarbocyanine Iodide and 3,3′-Diethylthiadicarbocyanine Iodide. *J. Chem. Soc., Faraday Trans. 2* **1972**, *68* (0), 1479–1496. https://doi.org/10.1039/F29726801479.

(35) Margulies, E. A.; Logsdon, J. L.; Miller, C. E.; Ma, L.; Simonoff, E.; Young, R. M.; Schatz, G. C.; Wasielewski, M. R. Direct Observation of a Charge-Transfer State Preceding High-Yield Singlet Fission in Terrylenediimide Thin Films. *J. Am. Chem. Soc.* **2017**, *139* (2), 663–671. https://doi.org/10.1021/jacs.6b07721.

(36) Dyar, S. M.; Margulies, E. A.; Horwitz, N. E.; Brown, K. E.; Krzyaniak, M. D.; Wasielewski, M. R. Photogenerated Quartet State Formation in a Compact Ring-Fused Perylene-Nitroxide. *J. Phys. Chem. B* **2015**, *119* (43), 13560–13569. https://doi.org/10.1021/acs.jpcb.5b02378.

(37) Weil, T.; Reuther, E.; Beer, C.; Müllen, K. Synthesis and Characterization of Dendritic Multichromophores Based on Rylene Dyes for Vectorial Transduction of Excitation Energy. *Chemistry – A European Journal* **2004**, *10* (6), 1398–1414. https://doi.org/10.1002/chem.200305359.

(38) Liang, N.; Sun, K.; Feng, J.; Chen, Y.; Meng, D.; Jiang, W.; Li, Y.; Hou, J.; Wang, Z. Near-Infrared Electron Acceptors Based on Terrylene Diimides for Organic Solar Cells. *Journal of Materials Chemistry A* **2018**, *6* (39), 18808–18812. https://doi.org/10.1039/C8TA08186G.

(39) Ishihara, K.; Kurihara, H.; Yamamoto, H. An Extremely Simple, Convenient, and Selective Method for Acetylating Primary Alcohols in the Presence of Secondary Alcohols. *J. Org. Chem.* **1993**, *58* (15), 3791–3793. https://doi.org/10.1021/jo00067a005.

(40) Wuts, P. G. M.; Greene, T. W.; Greene, T. W. *Greene's Protective Groups in Organic Synthesis*; Wiley-Interscience: Hoboken, N.J., 2007.

(41) Berberich, M.; Würthner, F. Terrylene Bisimide-Diarylethene Photochromic Switch. *Chemical Science* **2012**, *3* (9), 2771–2777. https://doi.org/10.1039/C2SC20554H.

(42) Wonneberger, H.; Reichelt, H.; Zagranyarski, Y.; Li, C.; Muellen, K.; Chen, L. Double Donor Functionalisation of the Peri-Positions of Perylene and Naphthalene Monoimide via Versatile Building Blocks. US9630973B2, April 25, 2017.

(43) Kaloyanova, S.; Zagranyarski, Y.; Ritz, S.; Hanulová, M.; Koynov, K.; Vonderheit, A.; Müllen, K.; Peneva, K. Water-Soluble NIR-Absorbing Rylene Chromophores for Selective Staining of Cellular Organelles. *J. Am. Chem. Soc.* **2016**, *138* (9), 2881–2884. https://doi.org/10.1021/jacs.5b10425.

(44) Liu, Y.; Zhuang, J.; Liu, H.; Li, Y.; Lu, F.; Gan, H.; Jiu, T.; Wang, N.; He, X.; Zhu, D. Self-Assembly and Characterization of Hydrogen-Bond-Induced Nanostructure Aggregation. *ChemPhysChem* **2004**, *5* (8), 1210–1215. https://doi.org/10.1002/cphc.200400165.

(45) Costa, A.; Saá, J. M. On the Metalation of Phenolic Compounds: Ready Access to Highly Substituted Phenols. *Tetrahedron Letters* **1987**, *28* (45), 5551–5554. https://doi.org/10.1016/S0040-4039(00)96778-9.

(46) Kobayashi, S.; Hachiya, I.; Araki, M.; Ishitani, H. Scandium Trifluoromethanesulfonate (Sc(OTf)3). A Novel Reusable Catalyst in the Diels-Alder Reaction. *Tetrahedron Letters* **1993**, *34* (23), 3755–3758. https://doi.org/10.1016/S0040-4039(00)79220-3.

(47) Kawada, A.; Yasuda, K.; Abe, H.; Harayama, T. Rare Earth Metal Trifluoromethanesulfonates Catalyzed Benzyl-Etherification. *Chem. Pharm. Bull.* **2002**, *50* (3), 380–383. https://doi.org/10.1248/cpb.50.380.

(48) *Organikum: organisch-chemisches Grundpraktikum*, 21., neu bearb. und erw. Aufl.; Becker, H. G. O., Ed.; Wiley-VCH: Weinheim, 2001.
(49) Feiler, L.; Langhals, H.; Polborn, K. Synthesis of Perylene-3,4-Dicarboximides — Novel Highly Photostable Fluorescent Dyes. *Liebigs Annalen* **1995**, *1995* (7), 1229–1244. https://doi.org/10.1002/jlac.1995199507164.
(50) Sakamoto, T.; Pac, C. A "Green" Route to Perylene Dyes: Direct Coupling Reactions of 1,8-Naphthalimide and Related Compounds under Mild Conditions Using a "New" Base Complex Reagent, t-BuOK/DBN. *J. Org. Chem.* **2001**, *66* (1), 94–98. https://doi.org/10.1021/jo0010835.
(51) Holtrup, F. O.; Müller, G. R. J.; Quante, H.; Feyter, S. D.; Schryver, F. C. D.; Müllen, K. Terrylenimides: New NIR Fluorescent Dyes. *Chemistry – A European Journal* **1997**, *3* (2), 219–225. https://doi.org/10.1002/chem.19970030209.
(52) Takagi, J.; Takahashi, K.; Ishiyama, T.; Miyaura, N. Palladium-Catalyzed Cross-Coupling Reaction of Bis(Pinacolato)Diboron with 1-Alkenyl Halides or Triflates: Convenient Synthesis of Unsymmetrical 1,3-Dienes via the Borylation-Coupling Sequence. *J. Am. Chem. Soc.* **2002**, *124* (27), 8001–8006. https://doi.org/10.1021/ja0202255.
(53) Ishiyama, T.; Murata, M.; Miyaura, N. Palladium(0)-Catalyzed Cross-Coupling Reaction of Alkoxydiboron with Haloarenes: A Direct Procedure for Arylboronic Esters. *J. Org. Chem.* **1995**, *60* (23), 7508–7510. https://doi.org/10.1021/jo00128a024.
(54) Miyaura, N.; Yamada, K.; Suzuki, A. A New Stereospecific Cross-Coupling by the Palladium-Catalyzed Reaction of 1-Alkenylboranes with 1-Alkenyl or 1-Alkynyl Halides. *Tetrahedron Letters* **1979**, *20* (36), 3437–3440. https://doi.org/10.1016/S0040-4039(01)95429-2.
(55) Nagao, Y.; Abe, Y.; Misono, T. Synthesis and Properties of N-Alkylbromoperylene-3,4-Dicarboximides. *Dyes and Pigments* **1991**, *16* (1), 19–25. https://doi.org/10.1016/0143-7208(91)87017-H.
(56) Kim, H. N.; Puhl, L.; Nolde, F.; Li, C.; Chen, L.; Basché, T.; Müllen, K. Energy Transfer at the Single-Molecule Level: Synthesis of a Donor–Acceptor Dyad from Perylene and Terrylene Diimides. *Chemistry – A European Journal* **2013**, *19* (28), 9160–9166. https://doi.org/10.1002/chem.201300439.
(57) Aigner, D.; Ungerböck, B.; Mayr, T.; Saf, R.; Klimant, I.; M. Borisov, S. Fluorescent Materials for PH Sensing and Imaging Based on Novel 1,4-Diketopyrrolo-[3,4- c]Pyrrole Dyes. *Journal of Materials Chemistry C* **2013**, *1* (36), 5685–5693. https://doi.org/10.1039/C3TC31130A.
(58) Kaiser, H.; Lindner, J.; Langhals, H. Synthese von Nichtsymmetrisch Substituierten Perylen-Fluoreszenzfarbstoffen. *Chemische Berichte* **1991**, *124* (3), 529–535. https://doi.org/10.1002/cber.19911240319.
(59) Roy, C. D.; Brown, H. C. Stability of Boronic Esters – Structural Effects on the Relative Rates of Transesterification of 2-(Phenyl)-1,3,2-Dioxaborolane. *Journal of Organometallic Chemistry* **2007**, *692* (4), 784–790. https://doi.org/10.1016/j.jorganchem.2006.10.013.
(60) Bernardini, R.; Oliva, A.; Paganelli, A.; Menta, E.; Grugni, M.; Munari, S. D.; Goldoni, L. Stability of Boronic Esters to Hydrolysis: A Comparative Study. *Chem. Lett.* **2009**, *38* (7), 750–751. https://doi.org/10.1246/cl.2009.750.
(61) Zhang, H.; Ruiz-Castillo, P.; Buchwald, S. L. Palladium-Catalyzed C-O Cross-Coupling of Primary Alcohols. *Org. Lett.* **2018**, *20* (6), 1580–1583. https://doi.org/10.1021/acs.orglett.8b00325.
(62) Cunico, R. F.; Bedell, L. The Triisopropylsilyl Group as a Hydroxyl-Protecting Function. *J. Org. Chem.* **1980**, *45* (23), 4797–4798. https://doi.org/10.1021/jo01311a058.

(63) Zhang, W.; Robins, M. J. Removal of Silyl Protecting Groups from Hydroxyl Functions with Ammonium Fluoride in Methanol. *Tetrahedron Letters* **1992**, *33* (9), 1177–1180. https://doi.org/10.1016/S0040-4039(00)91889-6.
(64) Cremlyn, R. J. W. *Chlorosulfonic Acid: A Versatile Reagent*; Royal Society of Chemistry: Cambridge, UK, 2002.
(65) The solvatochromic comparison method. 6. The .pi.* scale of solvent polarities | Journal of the American Chemical Society https://pubs.acs.org/doi/abs/10.1021/ja00460a031 (accessed Feb 18, 2020).
(66) Schutting, S.; Jokic, T.; Strobl, M.; Borisov, S. M.; Beer, D. de; Klimant, I. NIR Optical Carbon Dioxide Sensors Based on Highly Photostable Dihydroxy-Aza-BODIPY Dyes. *J. Mater. Chem. C* **2015**, *3* (21), 5474–5483. https://doi.org/10.1039/C5TC00346F.
(67) Green to red emitting BODIPY dyes for fluorescent sensing and imaging of carbon dioxide | Elsevier Enhanced Reader (accessed Feb 24, 2020). https://doi.org/10.1016/j.snb.2019.127312.

7. List of figures

8. List of tables

9. Appendix

Compound (2):

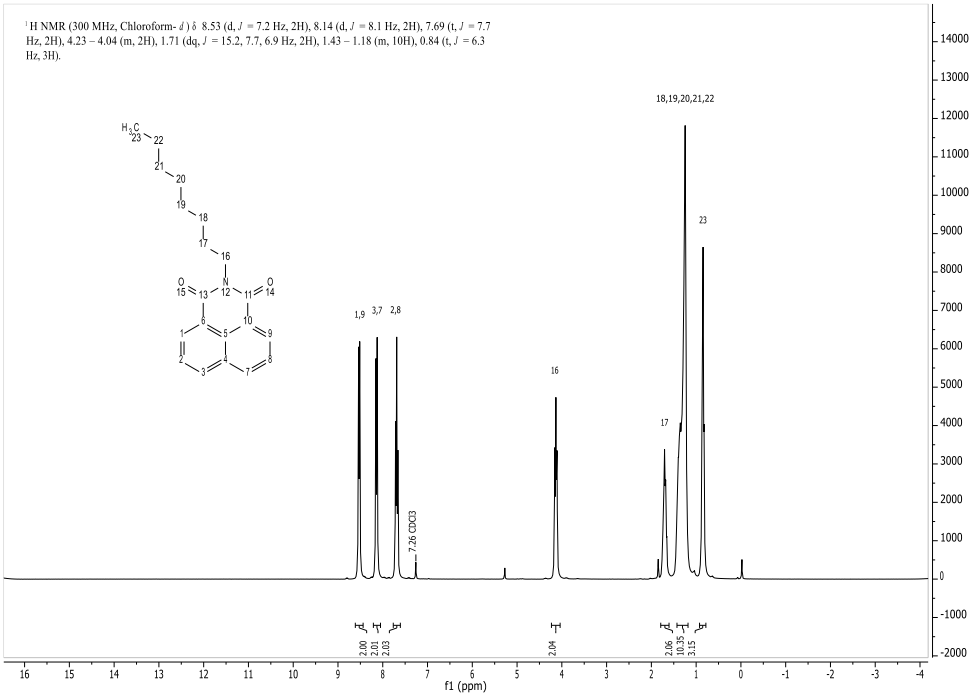

Figure 46: ^{1}H NMR spectrum of compound (2) in chloroform-*d* at room temperature (300 MHz)

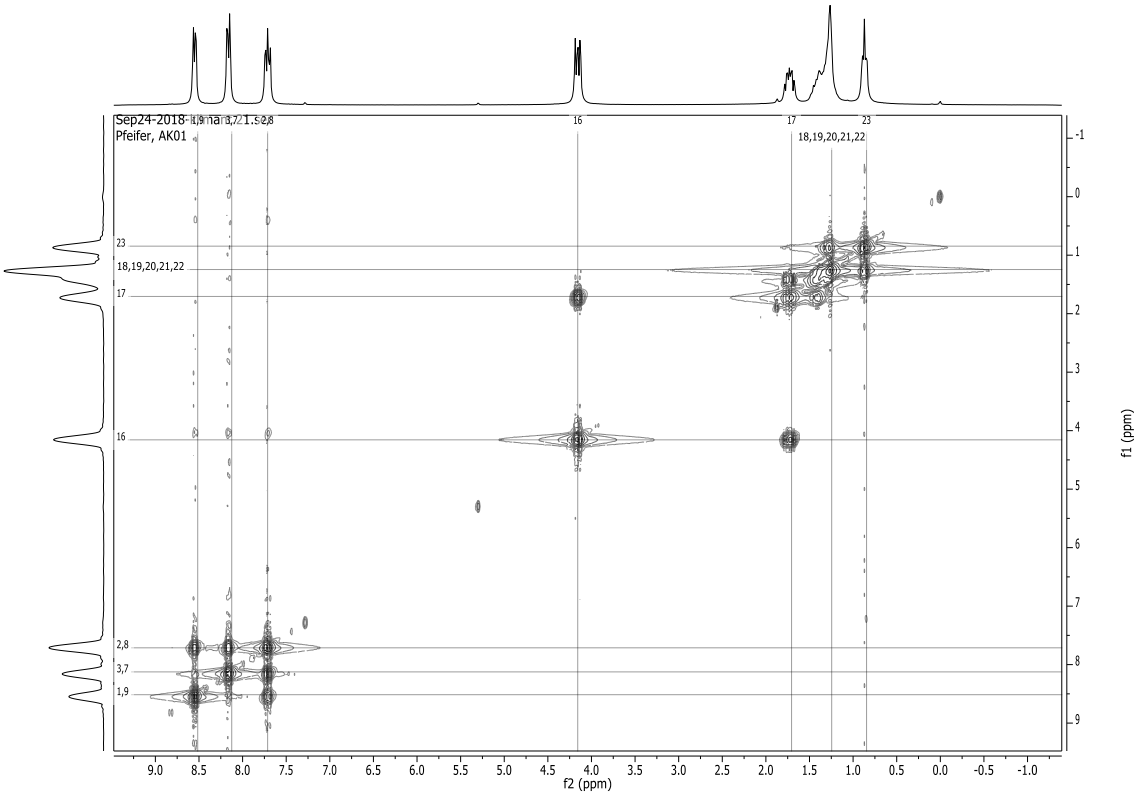

Figure 47: COSY spectrum of compound (2) in chloroform-*d* at room temperature (300 MHz)

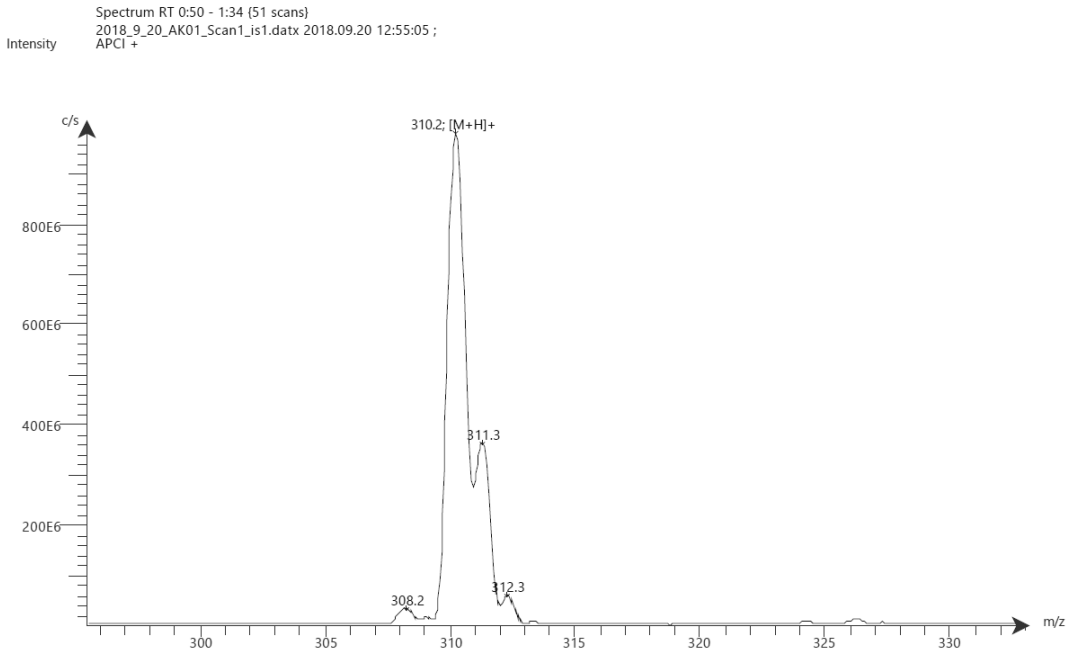

Figure 48: Mass spectrum of compound (2) recorded on Advion expression CMS

Compound (4):

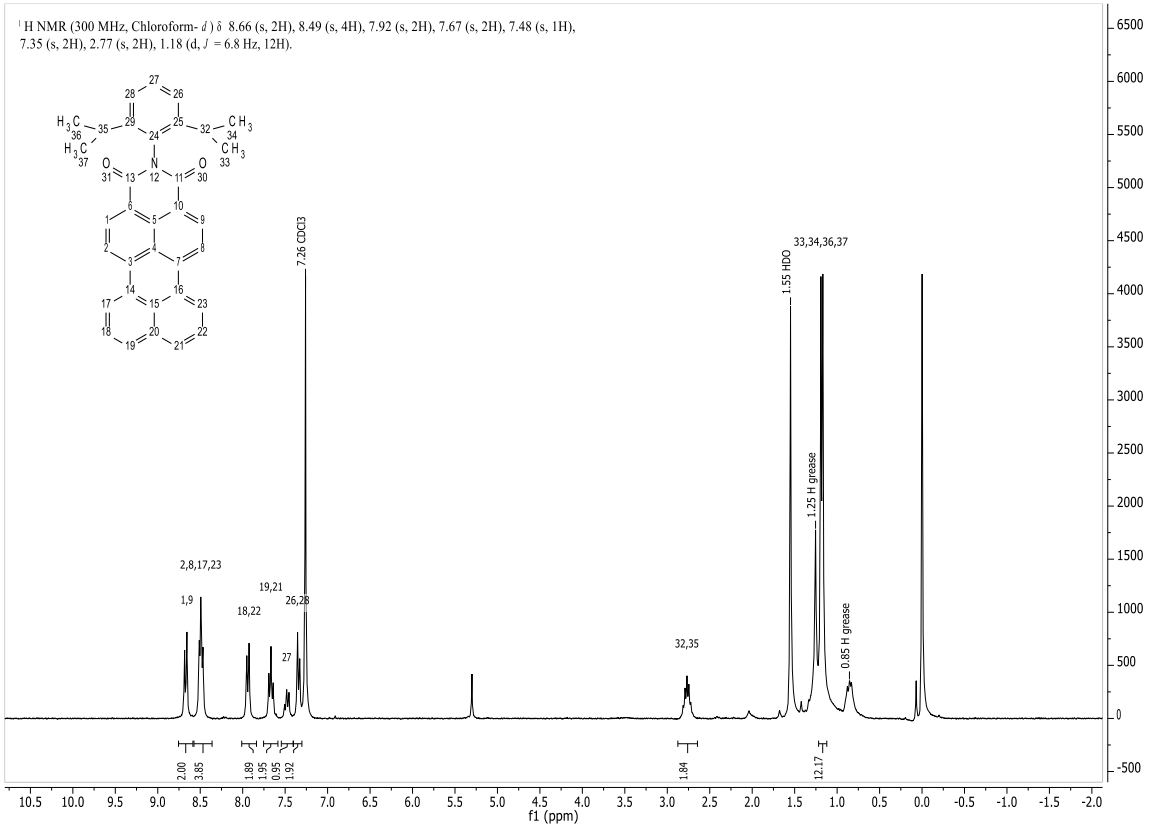

Figure 49: ^{1}H NMR spectrum of compound (4) in chloroform-*d* at room temperature (300 MHz)

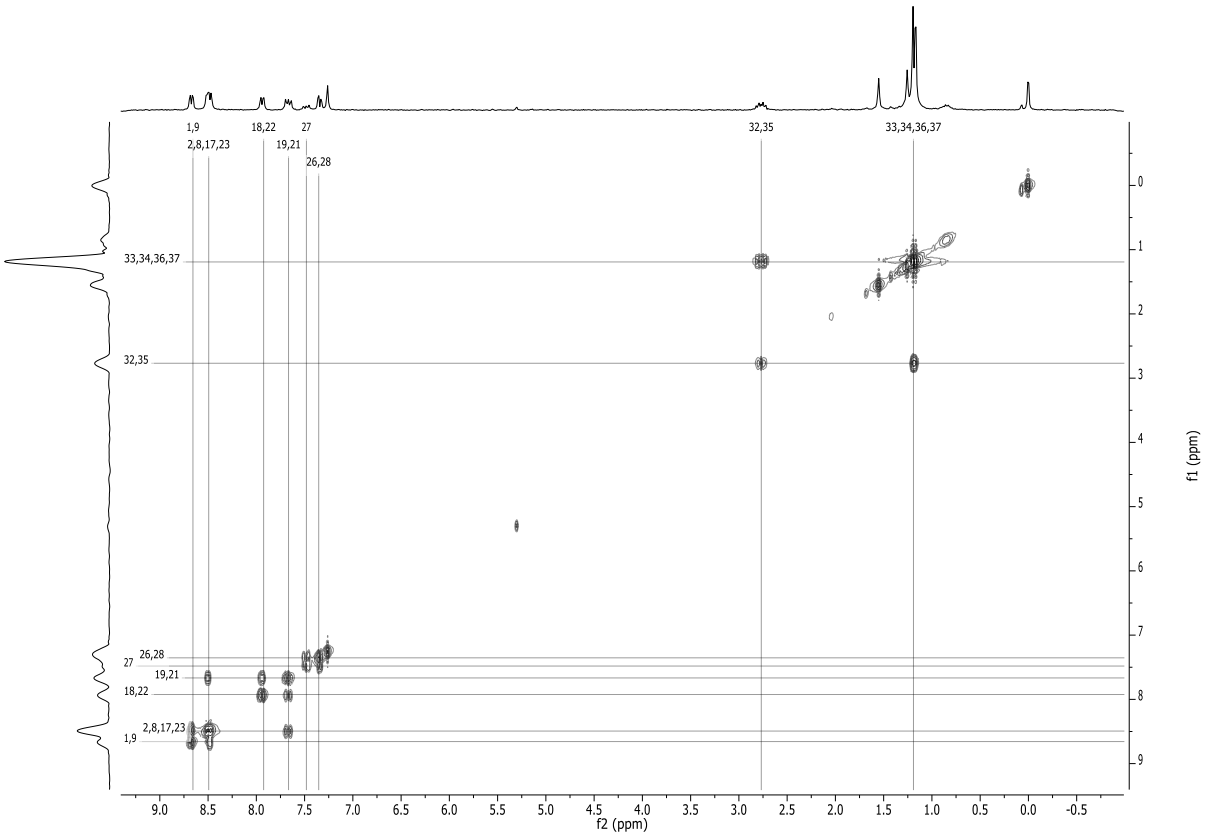

Figure 50: COSY spectrum of compound (4) in chloroform-*d* at room temperature (300 MHz)

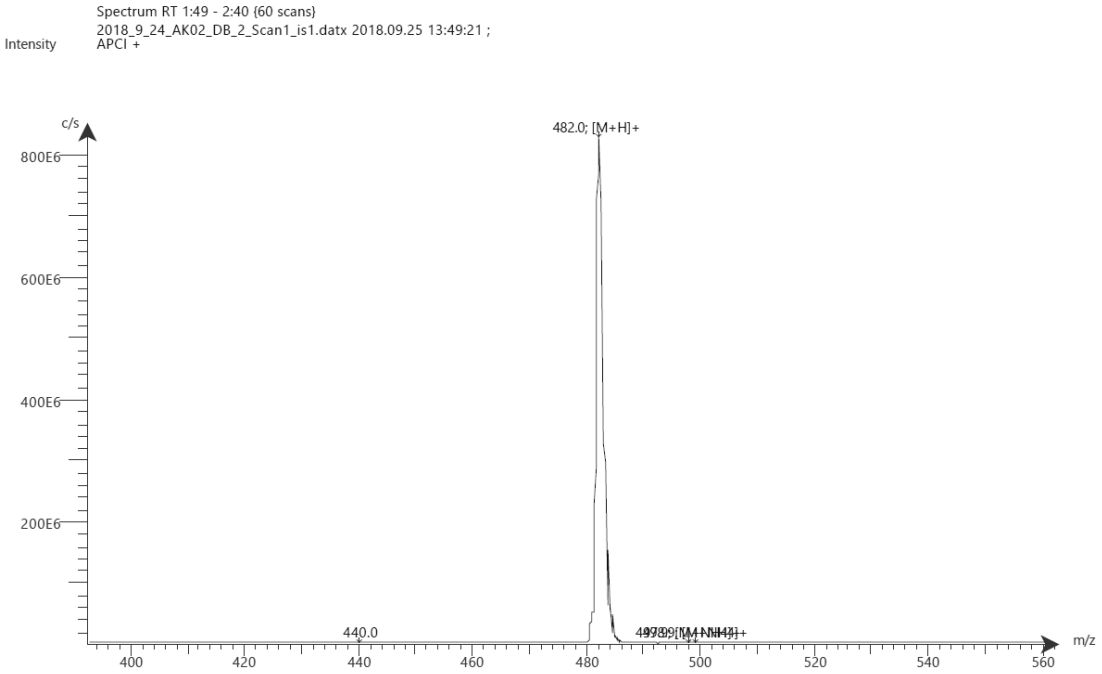

Figure 51: Mass spectrum of compound (4) recorded on Advion expression CMS

Compound (7):

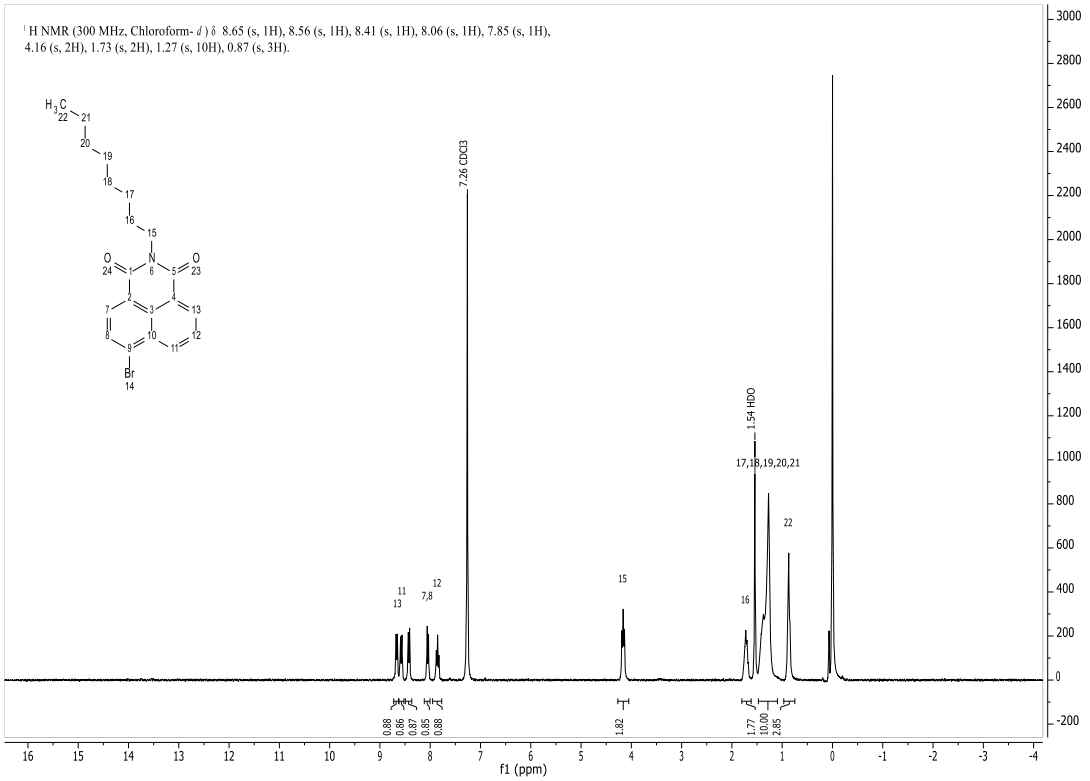

Figure 52: ^{1}H NMR spectrum of compound (7) in chloroform-*d* at room temperature (300 MHz)

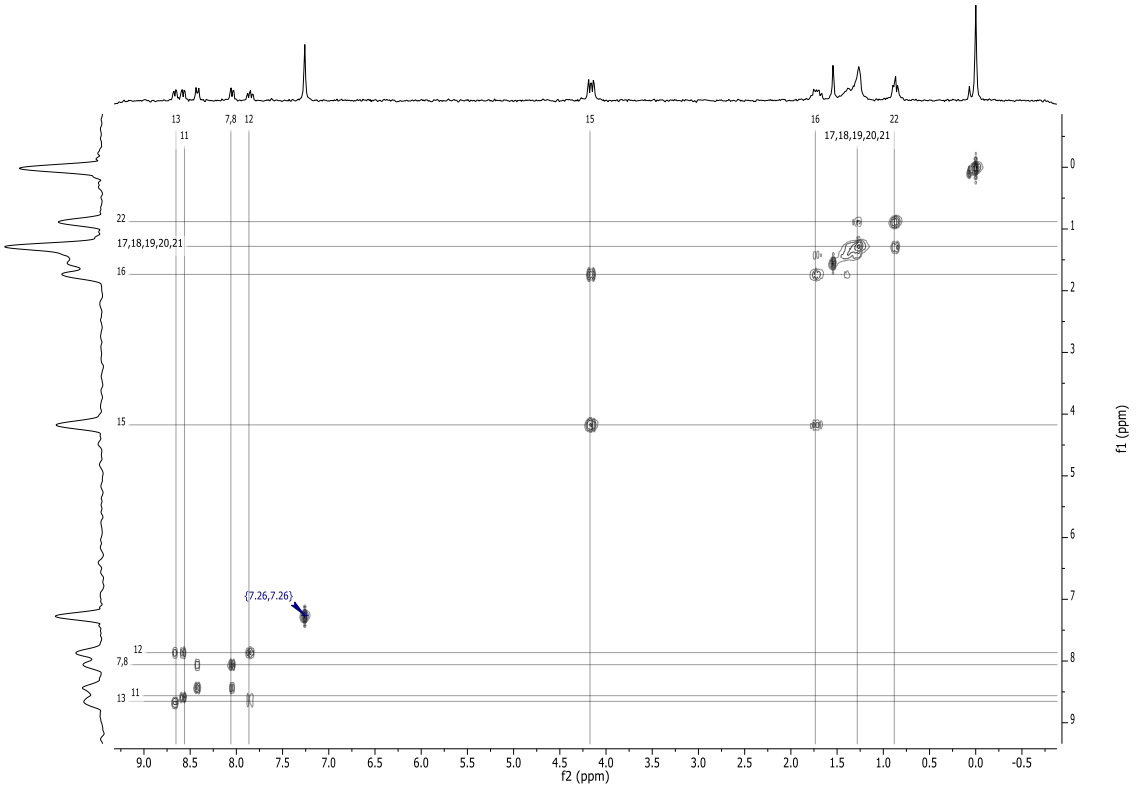

Figure 53: COSY spectrum of compound (7) in chloroform-*d* at room temperature (300 MHz)

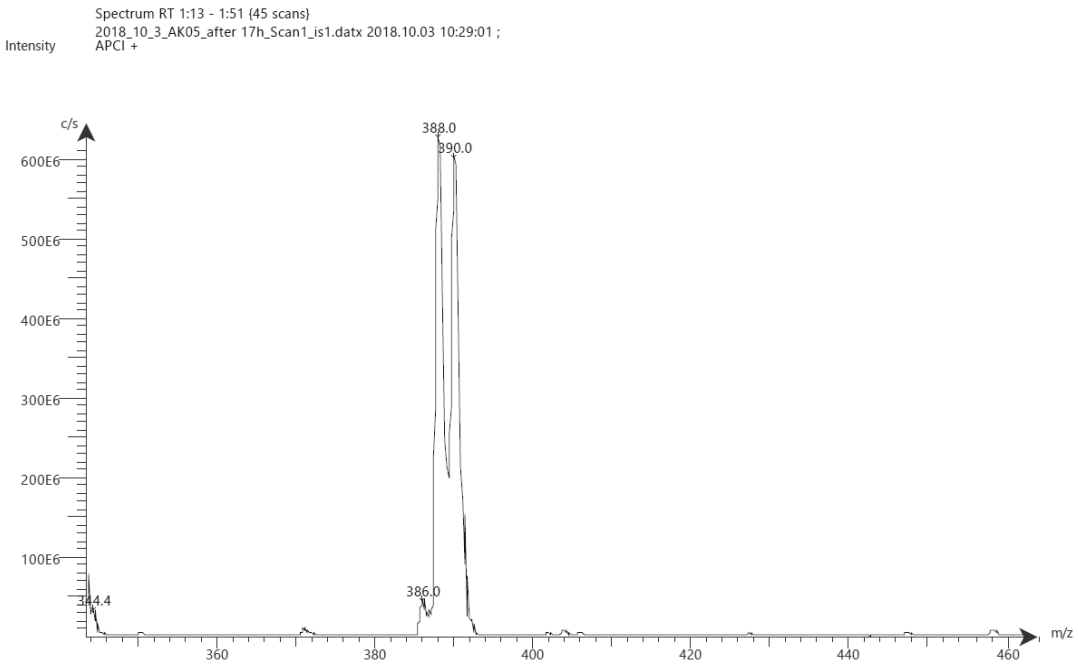

Figure 54: Mass spectrum of compound (7) recorded on Advion expression CMS

Compound (8):

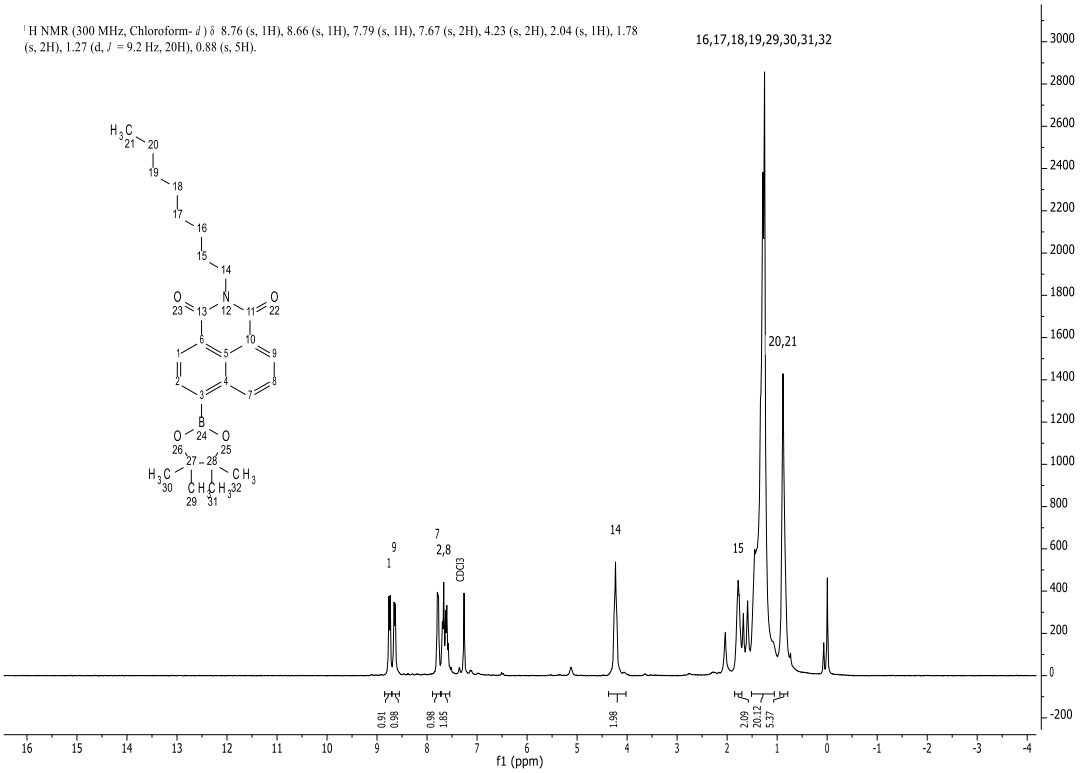

Figure 55: ^{1}H NMR spectrum of compound (8) in chloroform-*d* at room temperature (300 MHz)

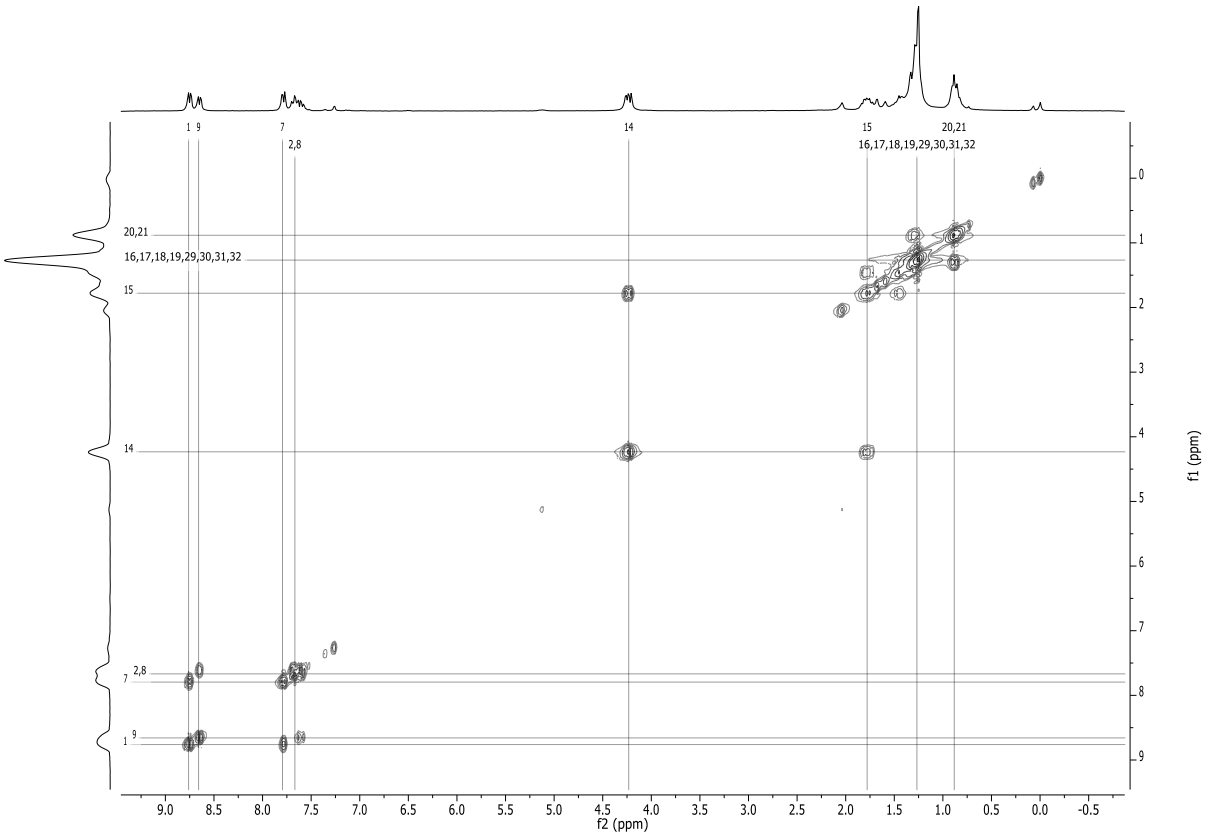

Figure 56: COSY spectrum of compound (8) in chloroform-*d* at room temperature (300 MHz)

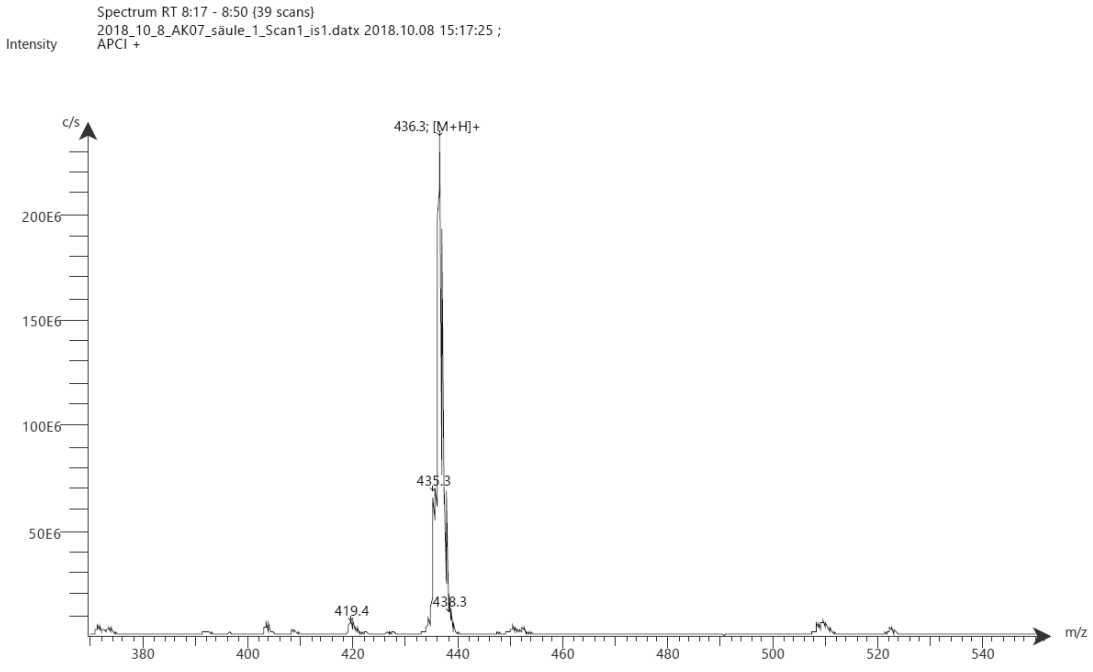

Figure 57: Mass spectrum of compound (4) recorded on Advion expression CMS

Compound (9):

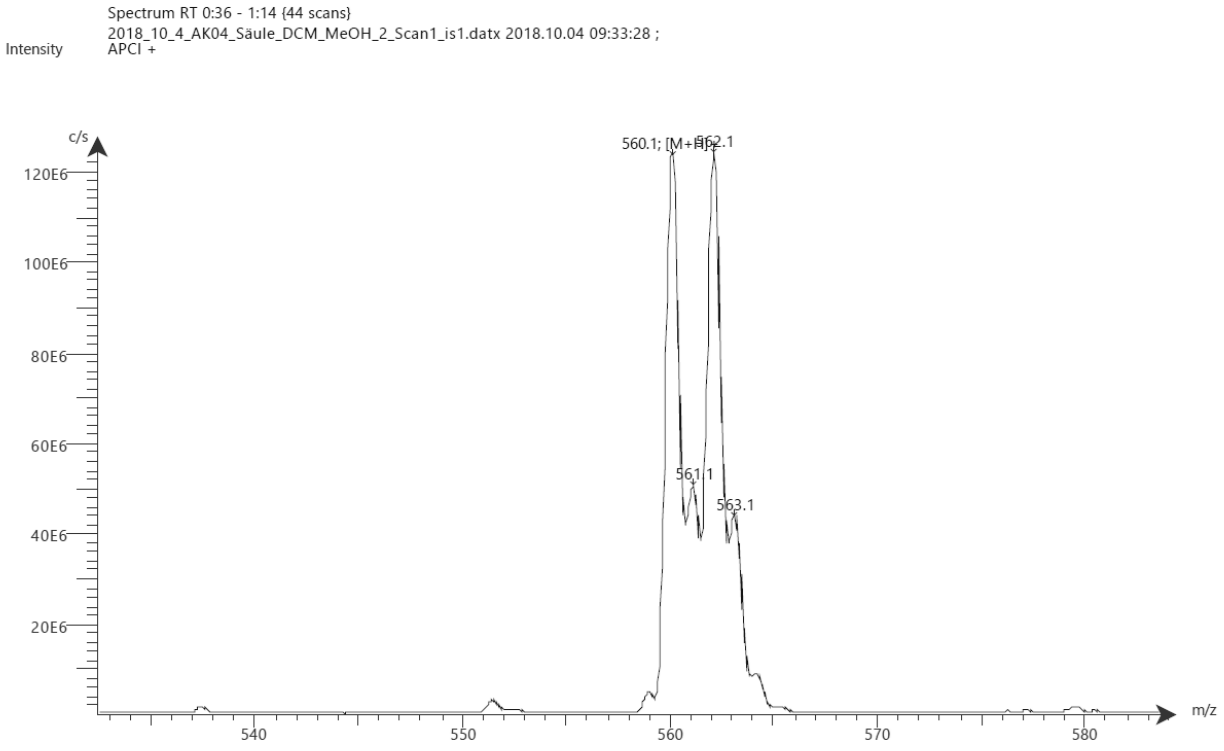

Figure 58: Mass spectrum of compound (9) recorded on Advion expression CMS

Compound (10):

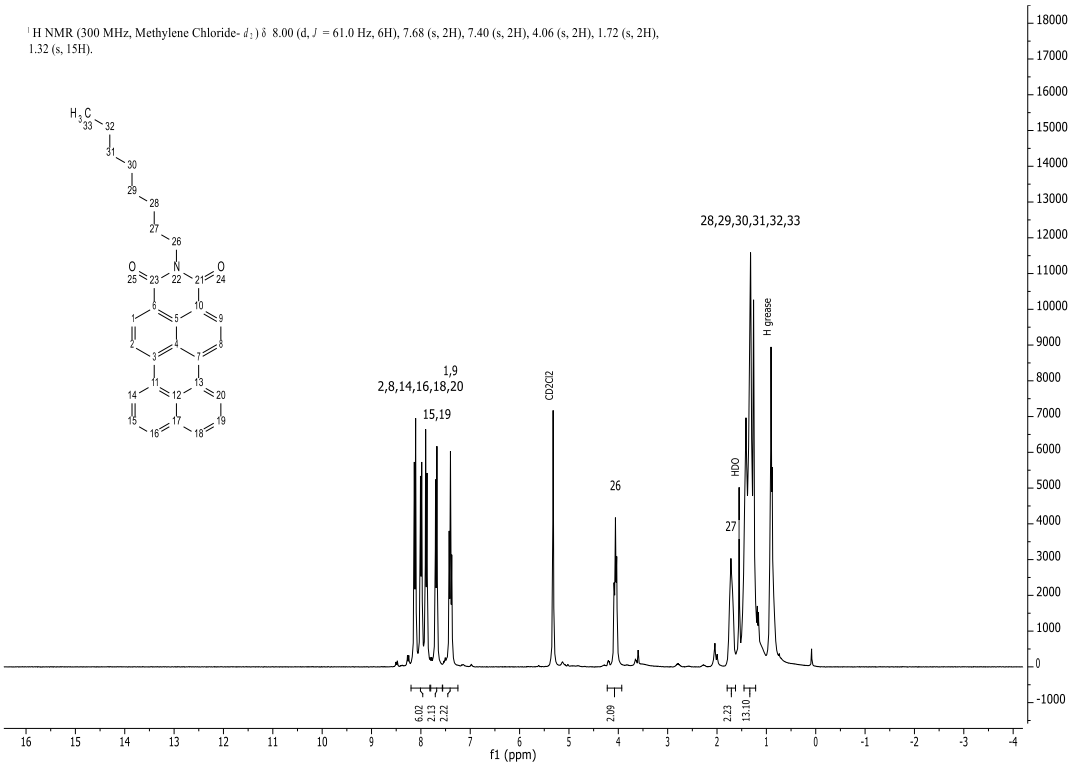

Figure 59: ^{1}H NMR spectrum of compound (10) in methylene chloride-d_2 at room temperature (300 MHz)

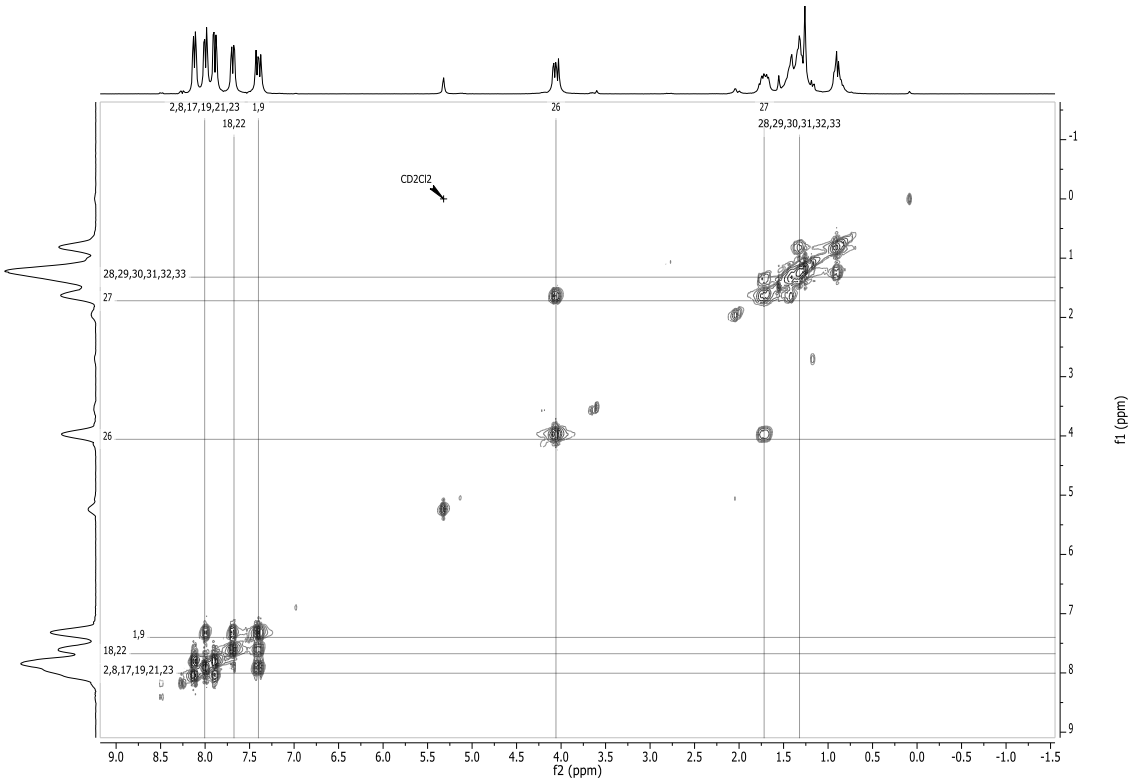

Figure 60: COSY spectrum of compound (10) in methylene chloride-d_2 at room temperature (300 MHz)

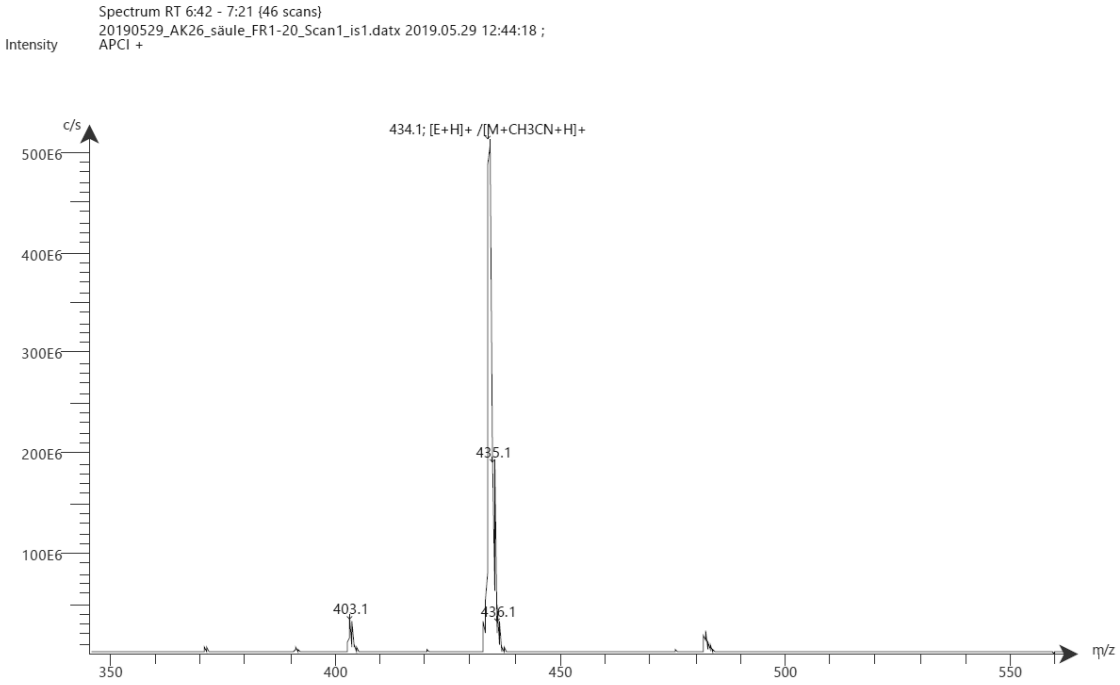

Figure 61: Mass spectrum of compound (10) recorded on Advion expression CMS

Compound (12):

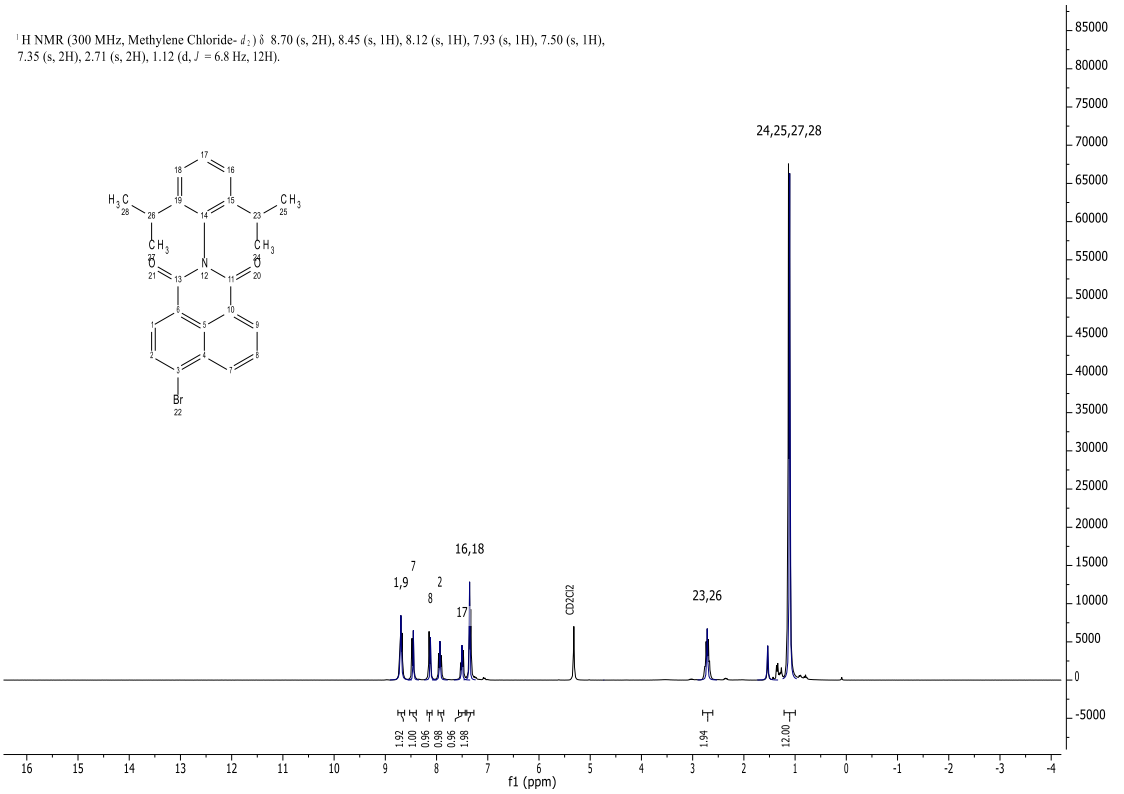

Figure 62: ^{1}H NMR spectrum of compound (12) in methylene chloride-d_2 at room temperature (300 MHz)

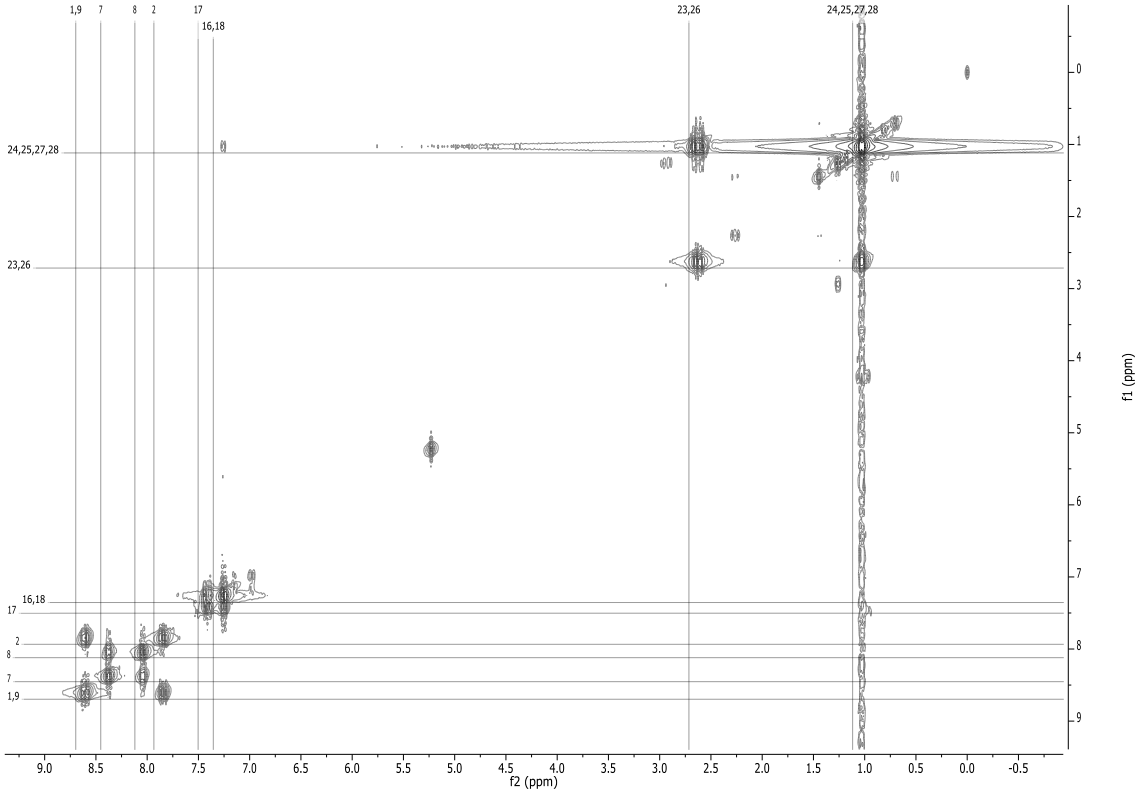

Figure 63: COSY spectrum of compound (12) in methylene chloride-d_2 at room temperature (300 MHz)

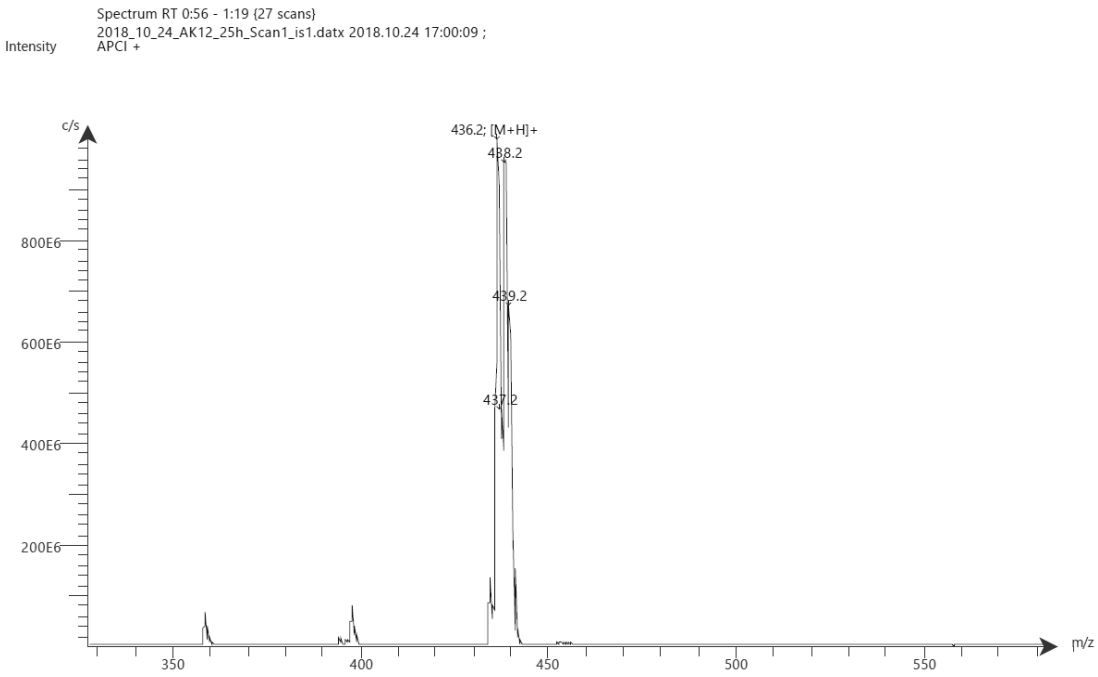

Figure 64: Mass spectrum of compound (12) recorded on Advion expression CMS

Compound (13):

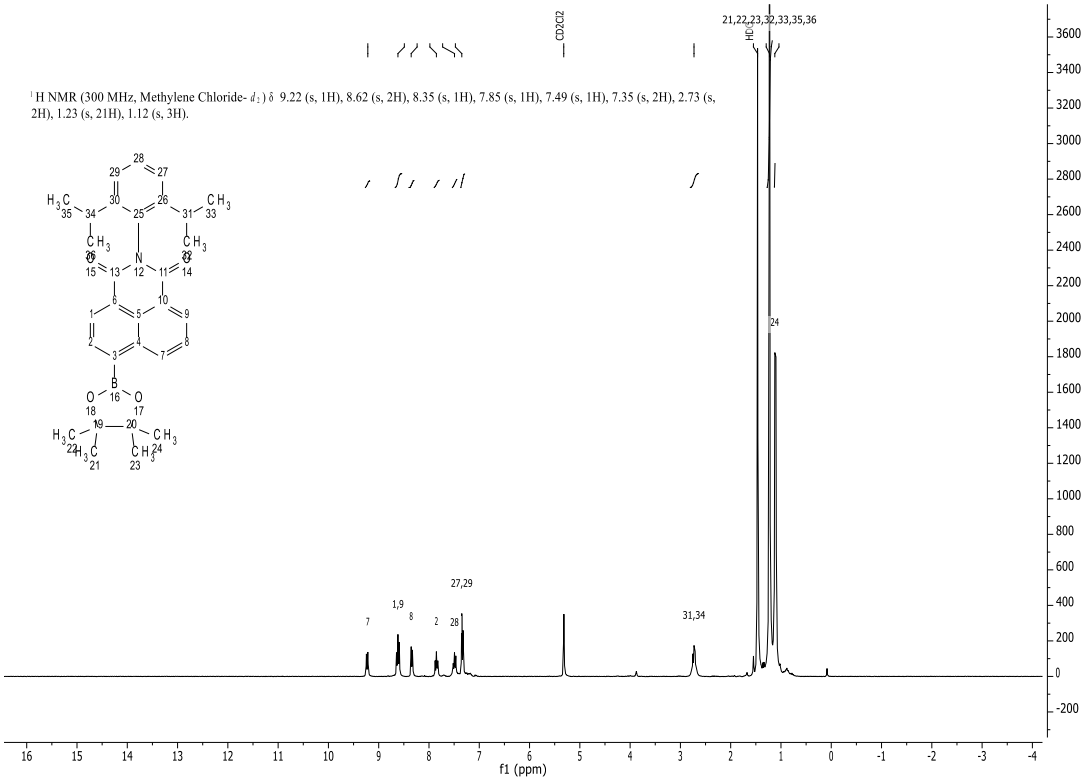

Figure 65: ^{1}H NMR spectrum of compound (13) in methylene chloride-d_2 at room temperature (300 MHz)

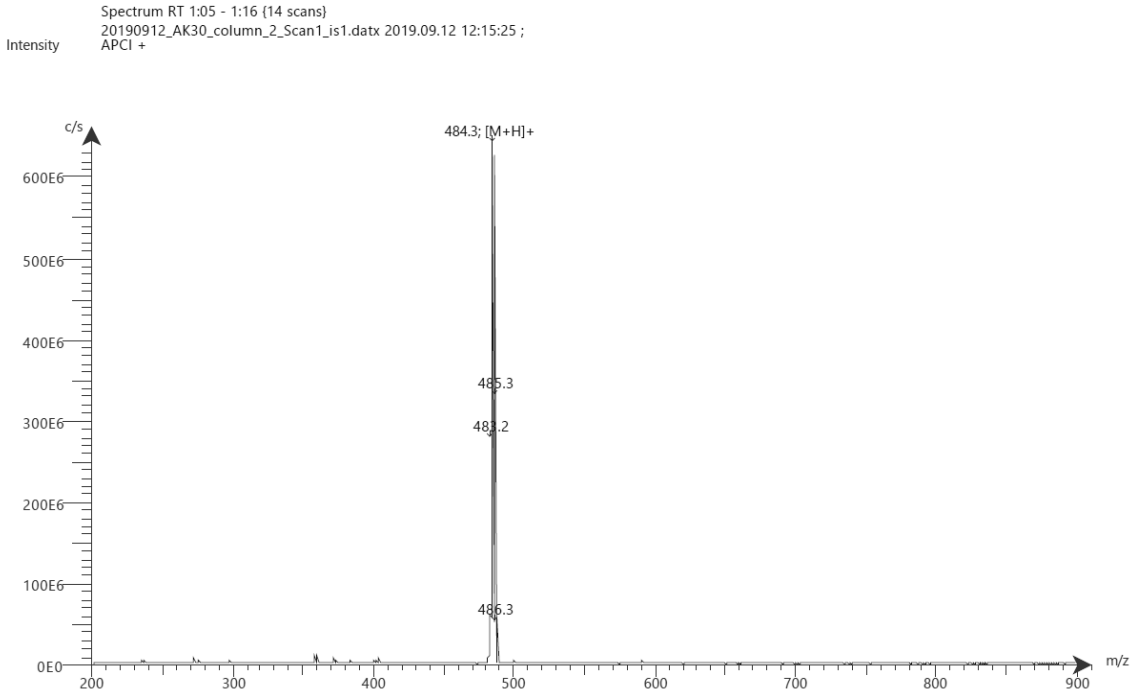

Figure 66: Mass spectrum of compound (13) recorded on Advion expression CMS

TDI-U:

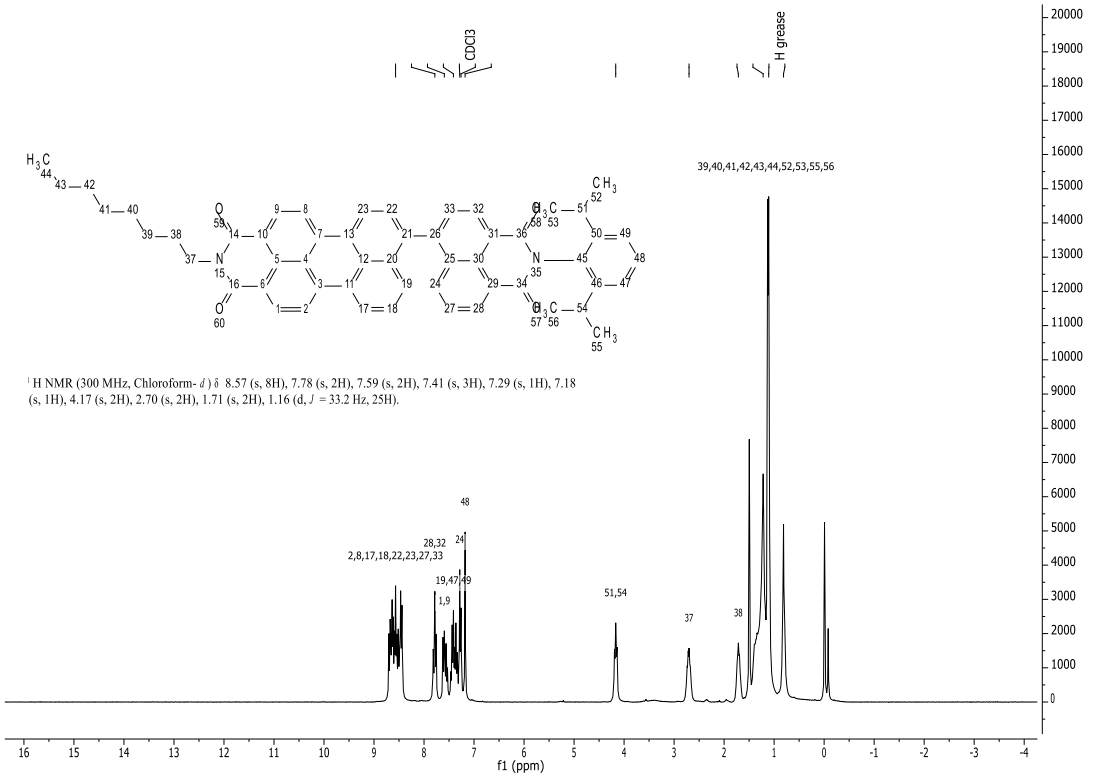

Figure 67: ^{1}H NMR spectrum of TDI-U in chloroform-*d* at room temperature (300 MHz)

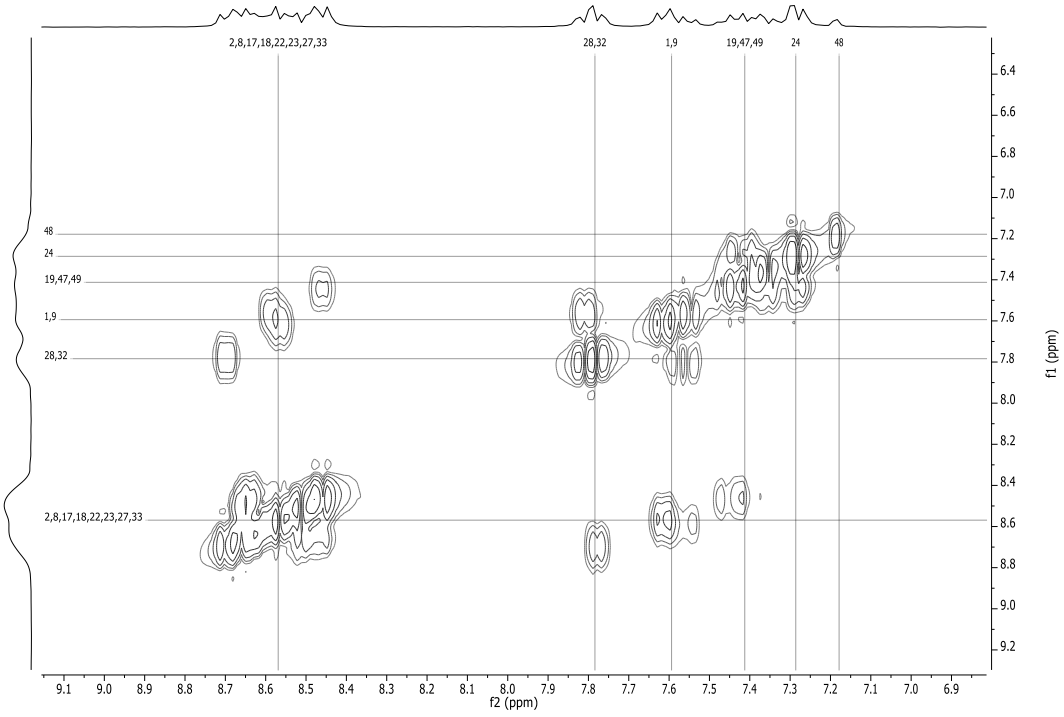

Figure 68: COSY spectrum of TDI-U in chloroform-*d* at room temperature (300 MHz)

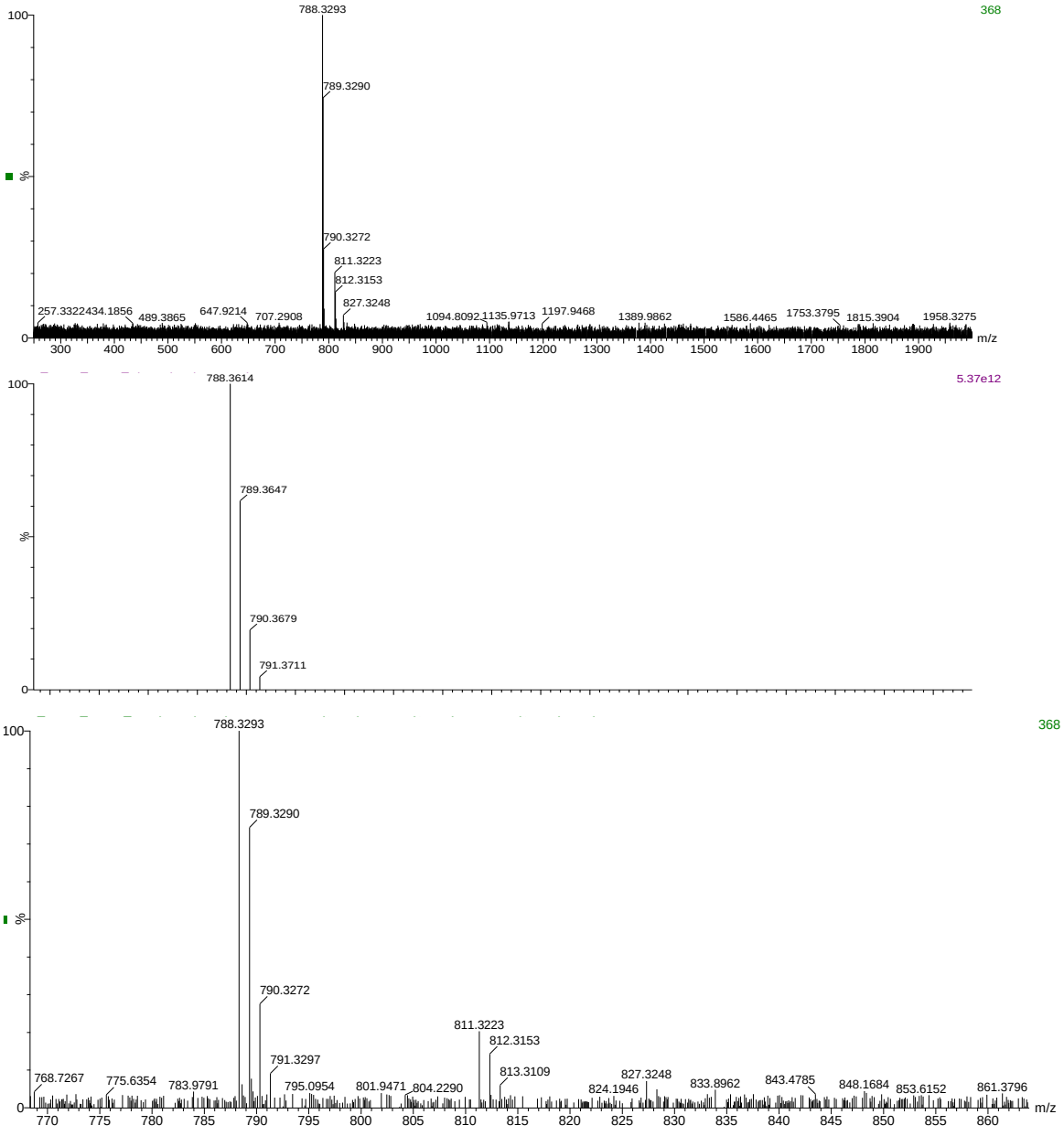

Figure 69: Experimental MALDI-TOF mass spectrum (upper part); mass relevant range for theoretical isotope pattern (middle) and experimental MALDI-TOF-mass spectrum (lower part) of TDI-U

TDI:

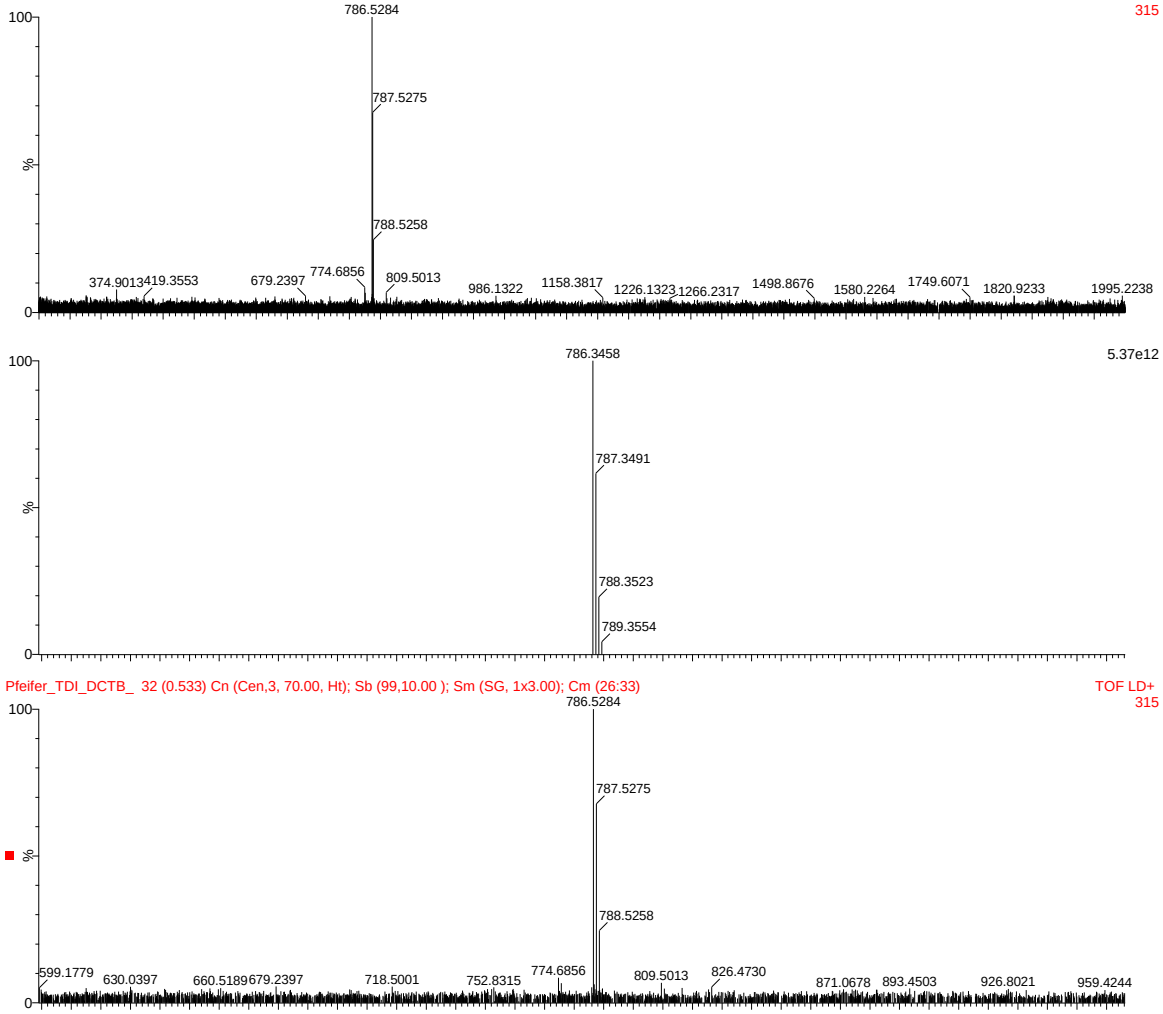

Figure 70: Experimental MALDI-TOF mass spectrum (upper part); mass relevant range for theoretical isotope pattern (middle) and experimental MALDI-TOF-mass spectrum (lower part) of TDI.

TDI-4Br:

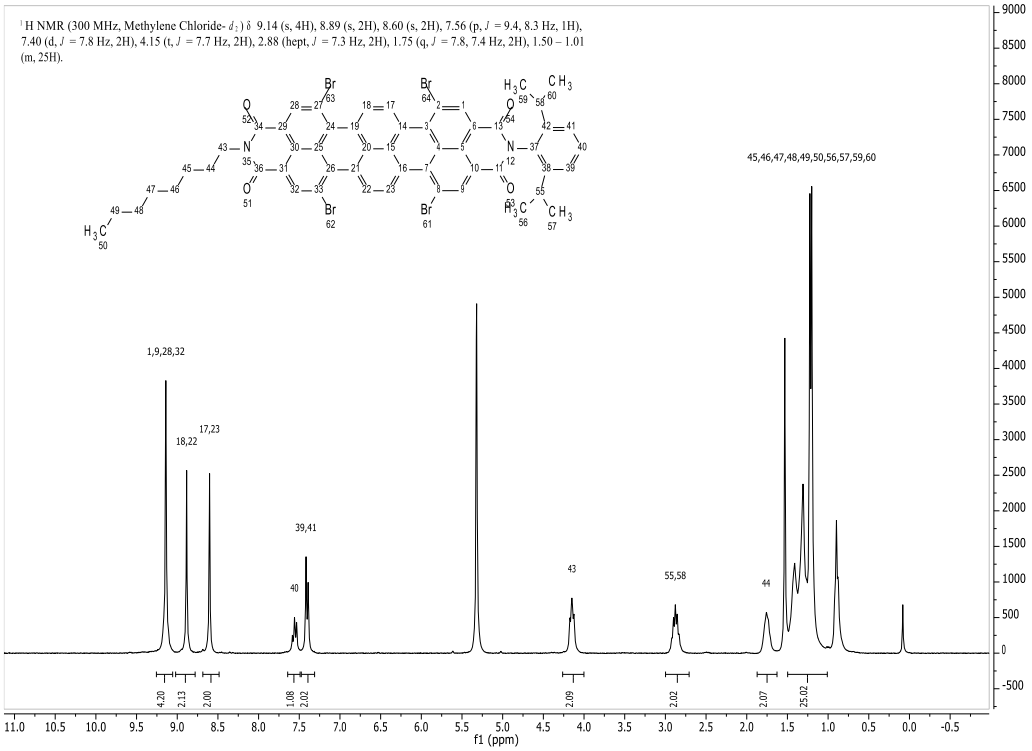

Figure 71: ^{1}H NMR spectrum of TDI-4Br in methylene chloride-d_2 at room temperature (300 MHz)

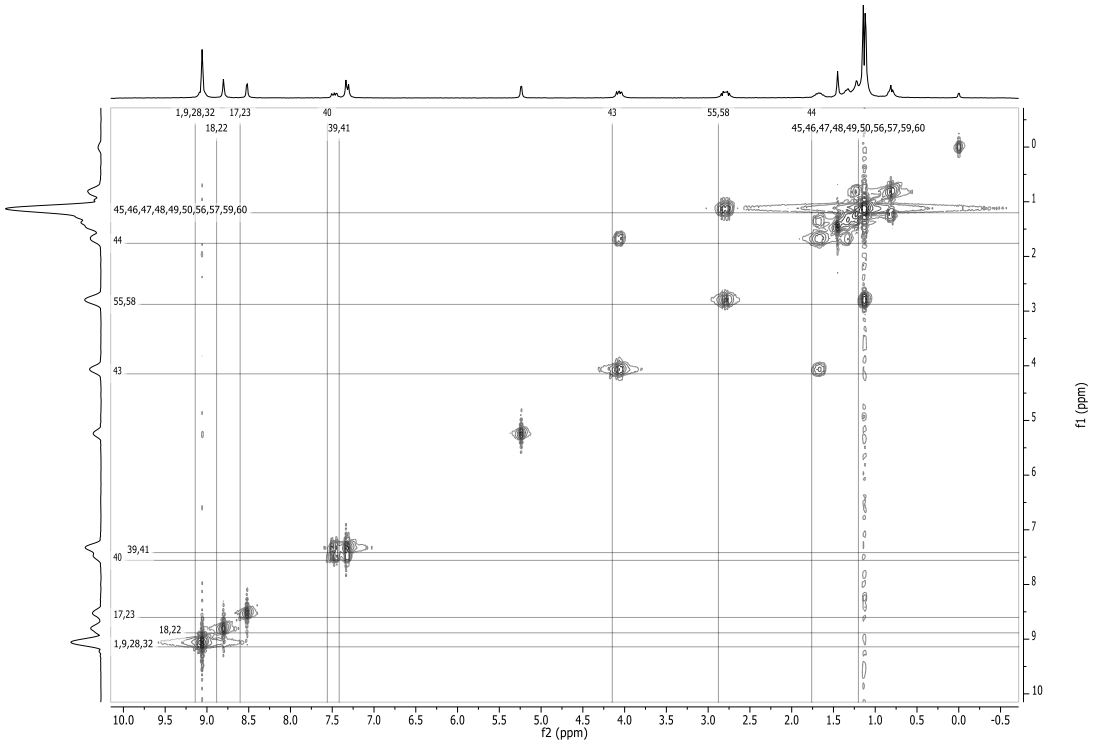

Figure 72: COSY spectrum of TDI-4Br in methylene chloride-d_2 at room temperature (300 MHz)

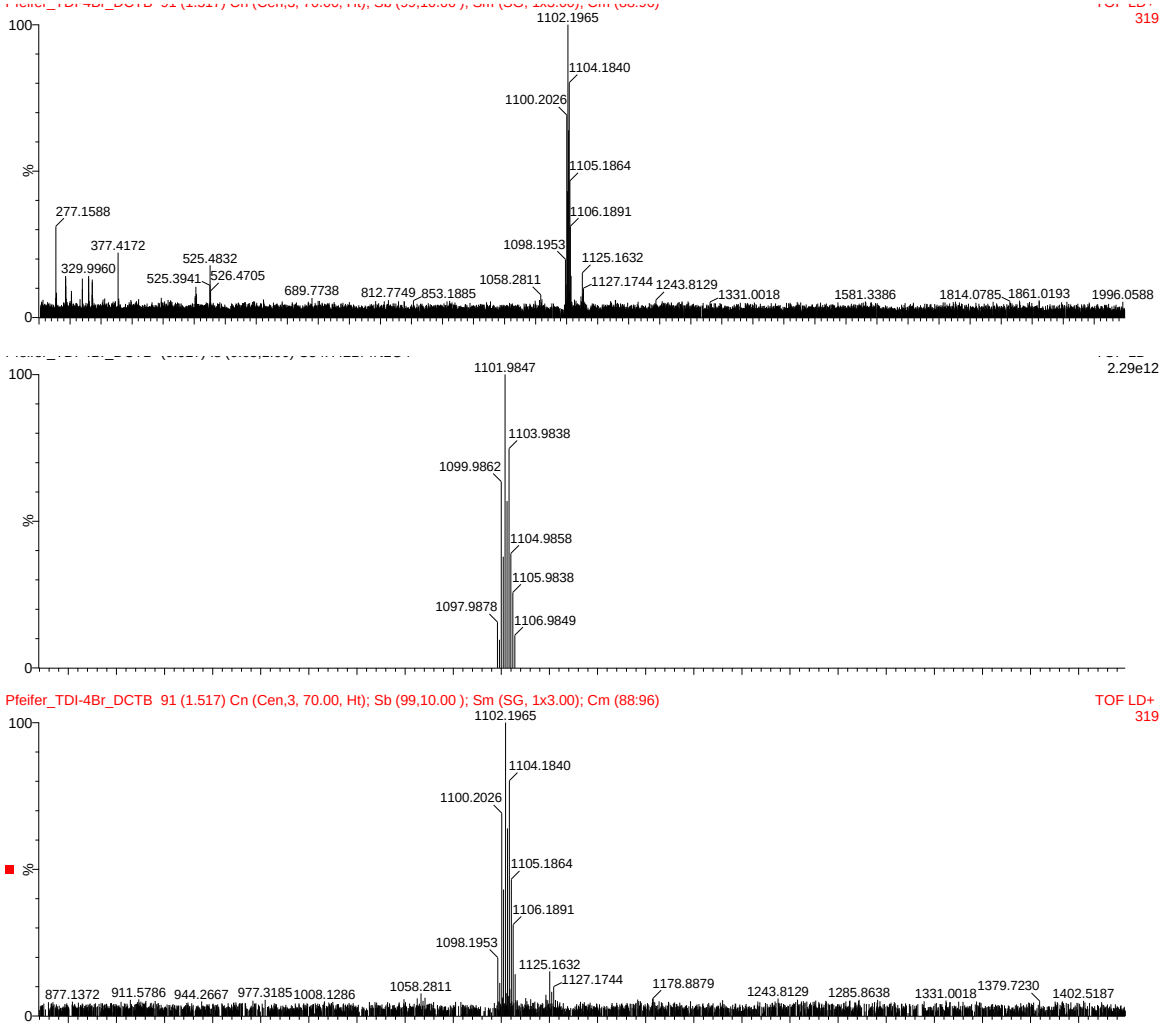

Figure 73: Experimental MALDI-TOF mass spectrum (upper part); mass relevant range for theoretical isotope pattern (middle) and experimental MALDI-TOF-mass spectrum (lower part) of TDI-4Br.

TDI-4Ph:

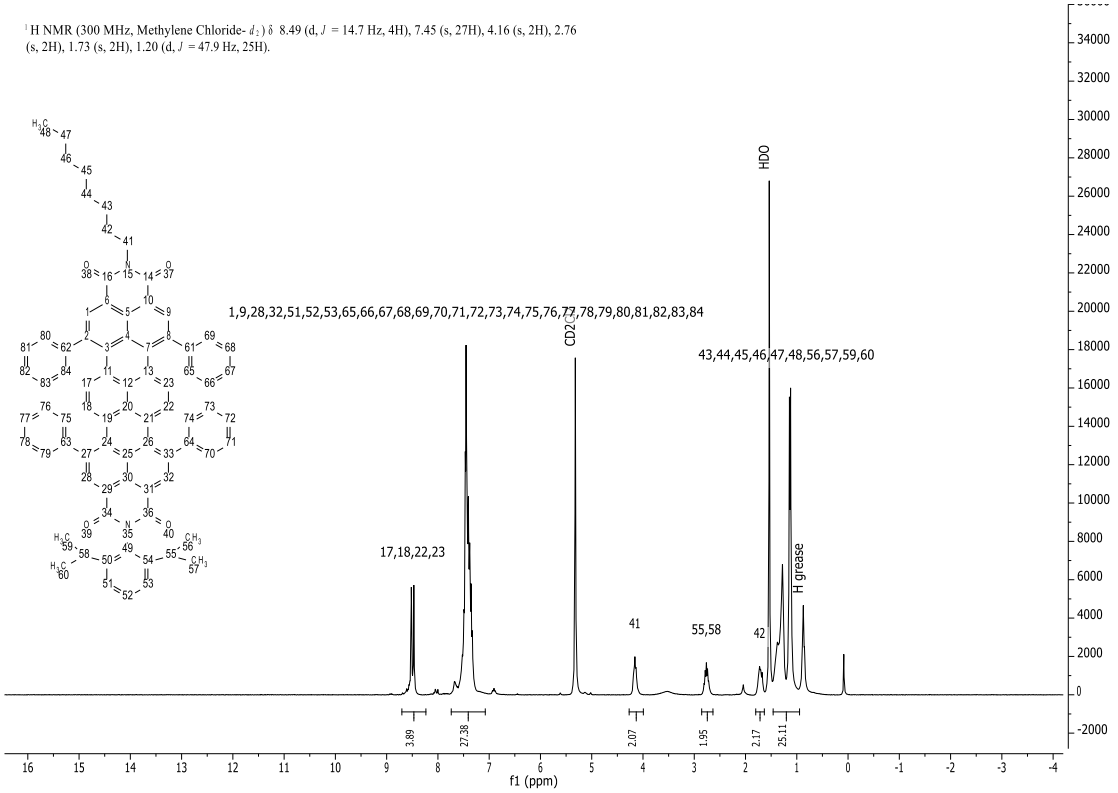

Figure 74: ^{1}H NMR spectrum of TDI-4Ph in methylene chloride-d_2 at room temperature (300 MHz)

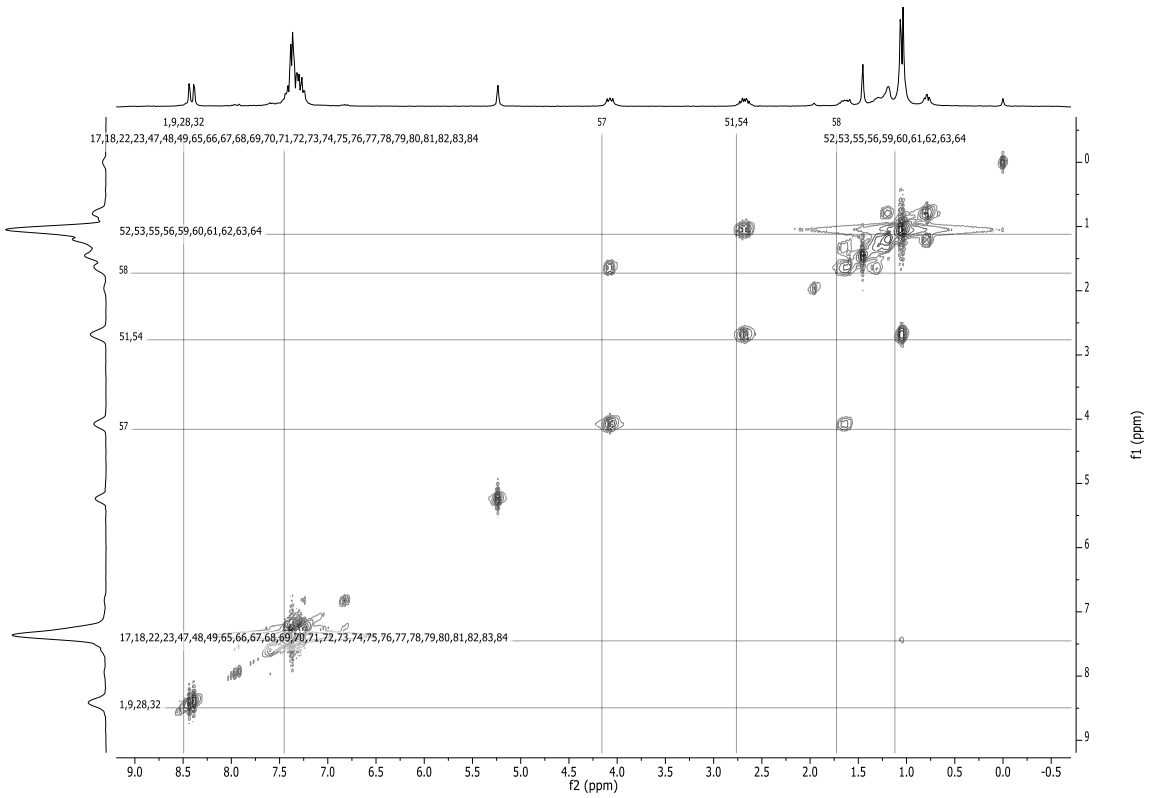

Figure 75: COSY spectrum of TDI-4Ph in methylene chloride-d_2 at room temperature (300 MHz)

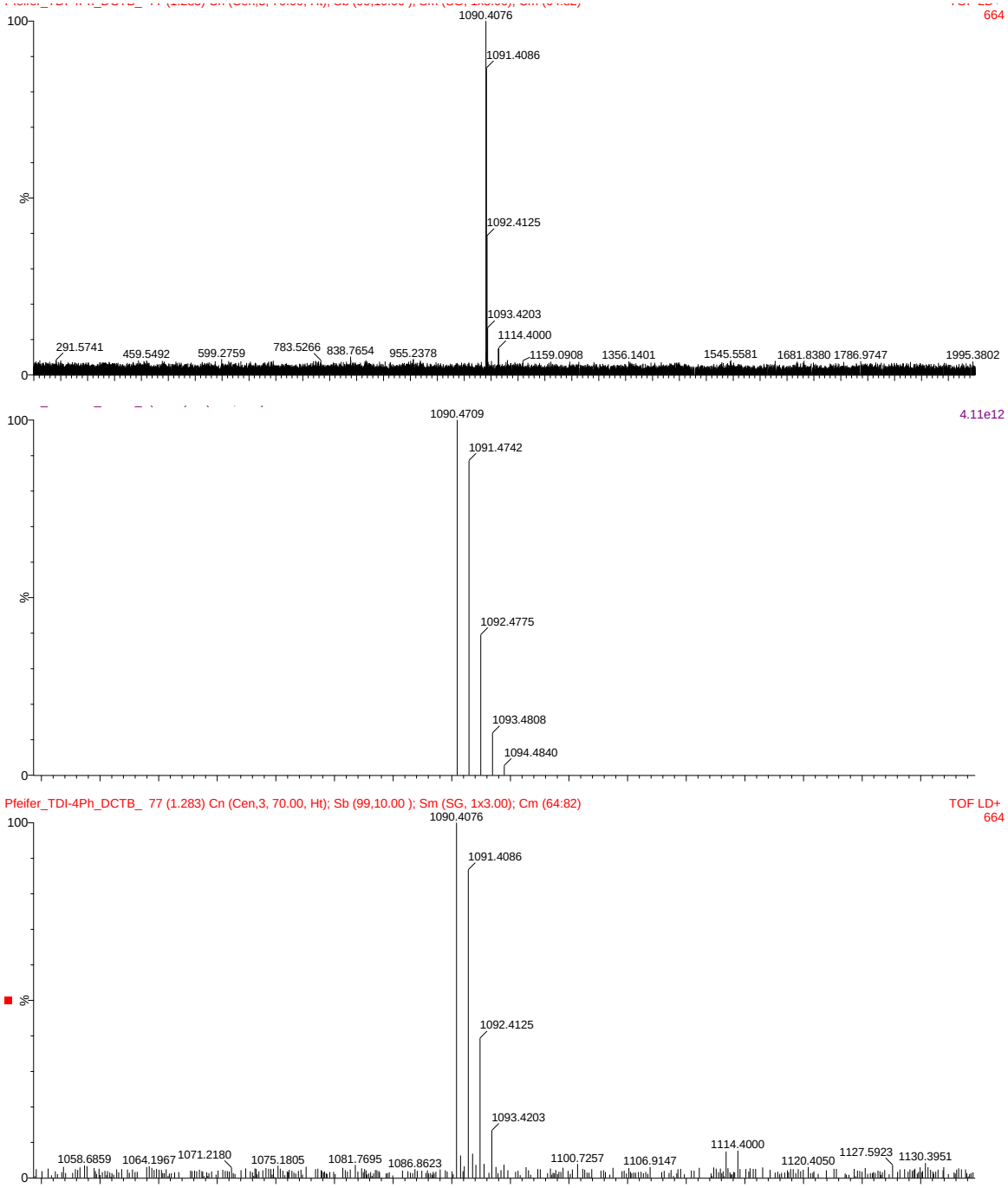

Figure 76: Experimental MALDI-TOF mass spectrum (upper part); mass relevant range for theoretical isotope pattern (middle) and experimental MALDI-TOF-mass spectrum (lower part) of TDI-4Ph

TDI-4Mo

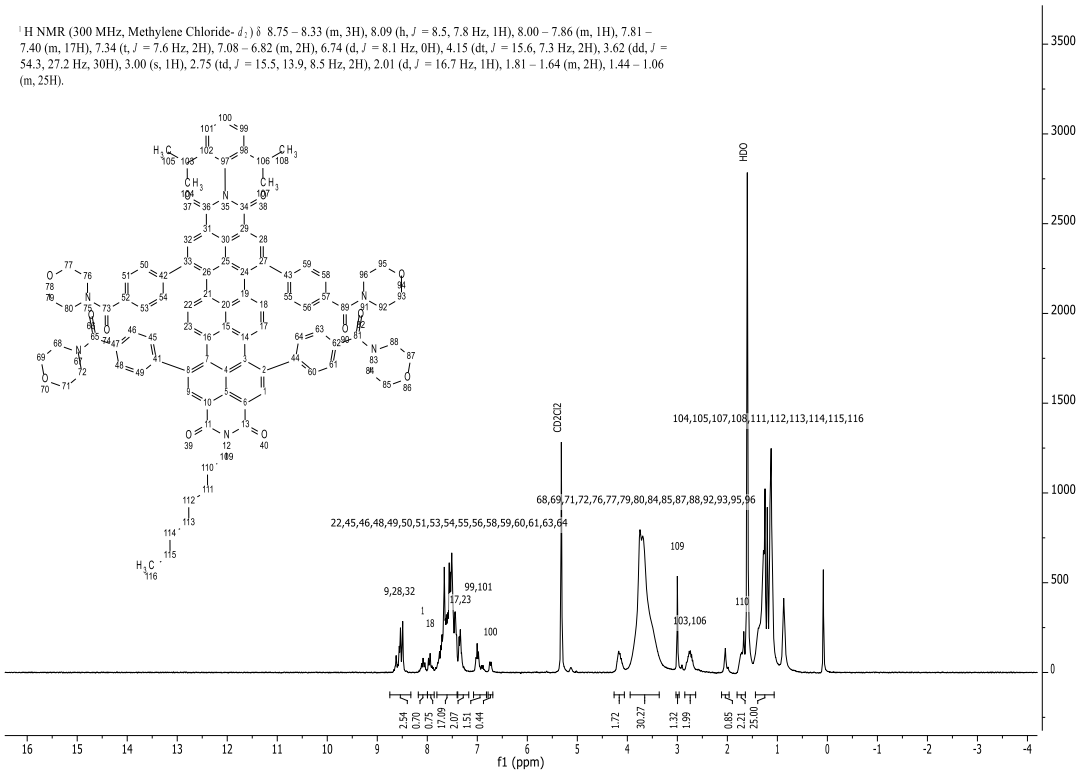

Figure 77: ^{1}H NMR spectrum of TDI-4Mo in methylene chloride-d_2 at room temperature (300 MHz)

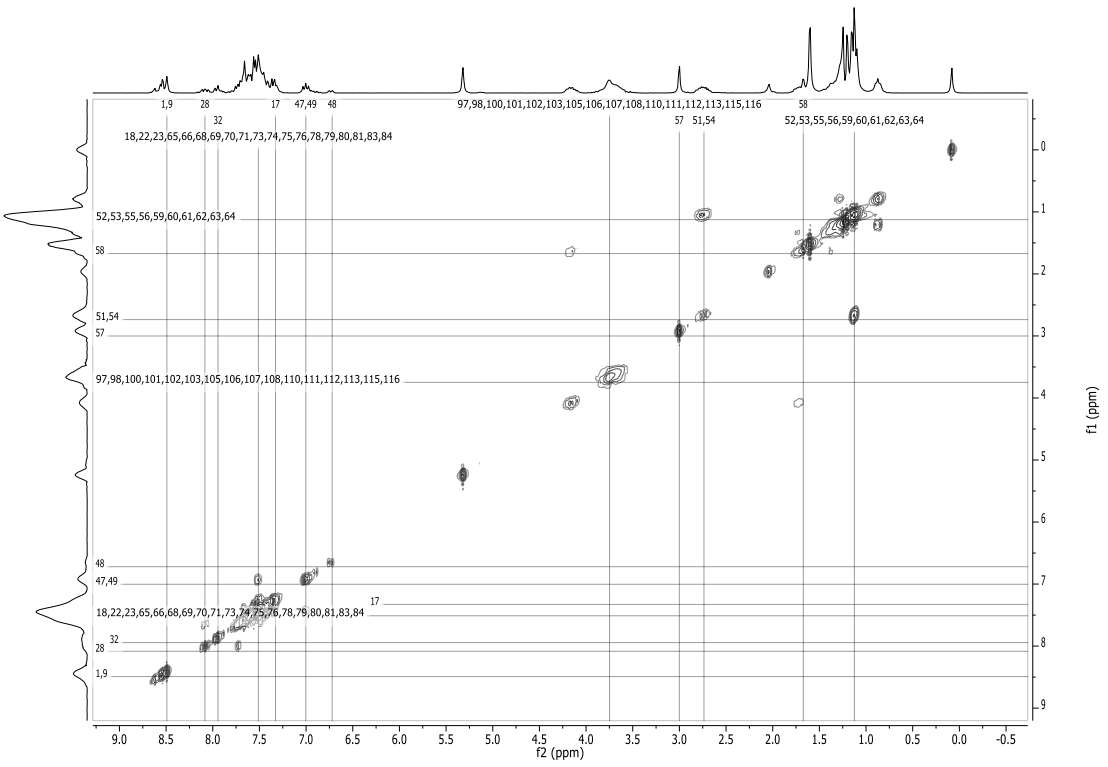

Figure 78: COSY spectrum of TDI-4Ph in methylene chloride-d_2 at room temperature (300 MHz)

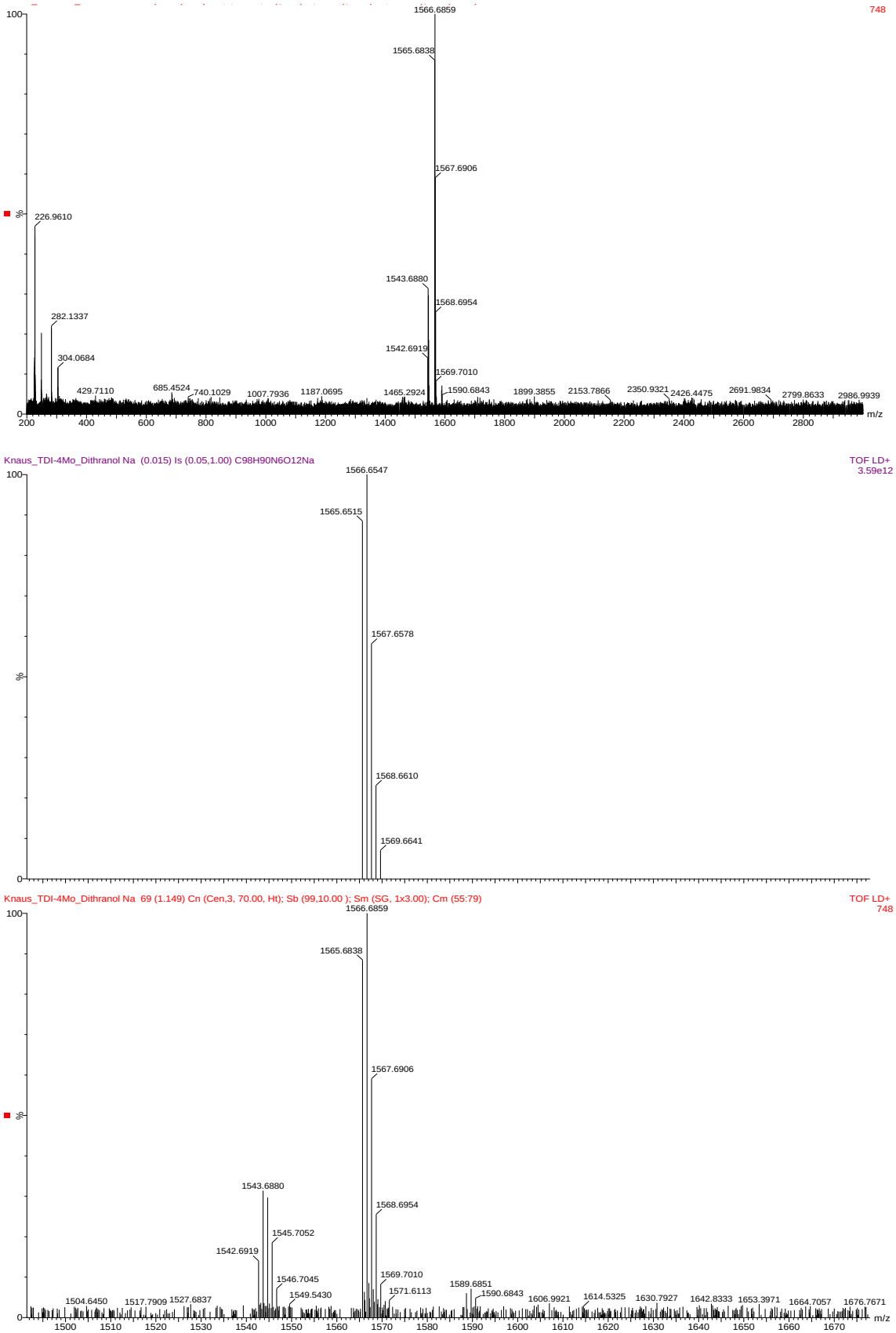

Figure 79: Experimental MALDI-TOF mass spectrum (upper part); mass relevant range for theoretical isotope pattern (middle) and experimental MALDI-TOF-mass spectrum (lower part) of TDI-4Mo.

Compound (28)-Tips:

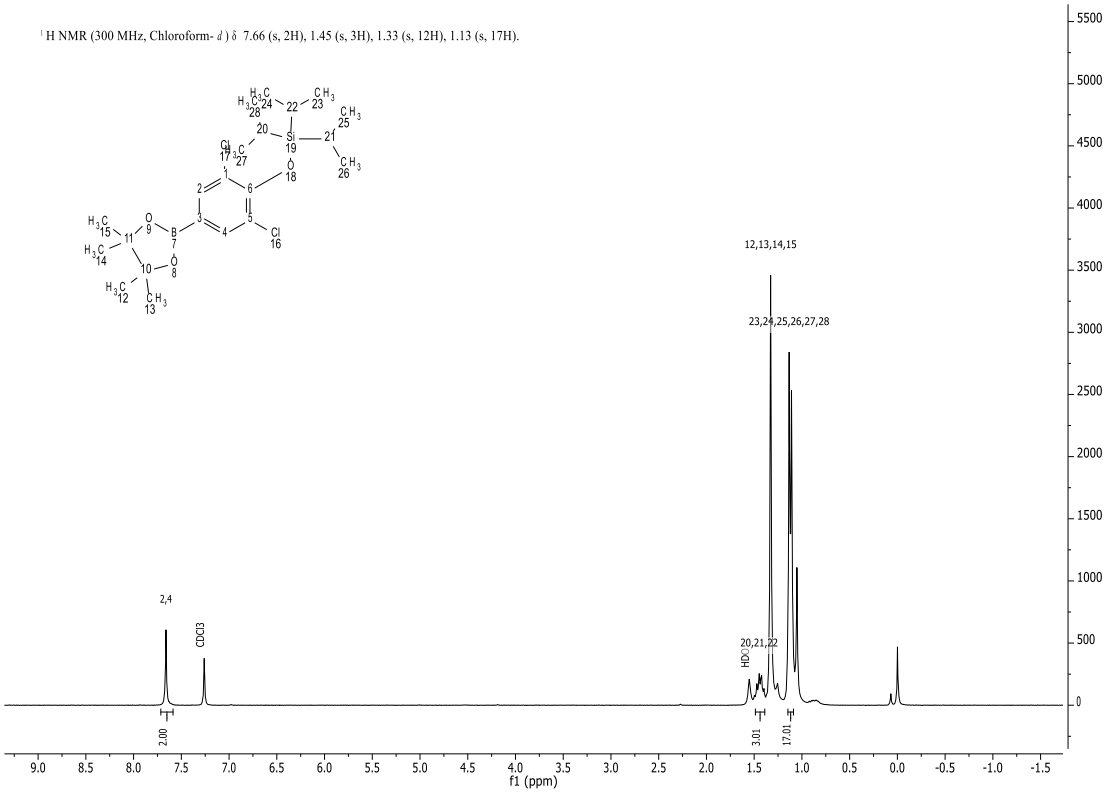

Figure 80: ^{1}H NMR spectrum of (28)-TIPS in chloroform-*d* at room temperature (300 MHz)

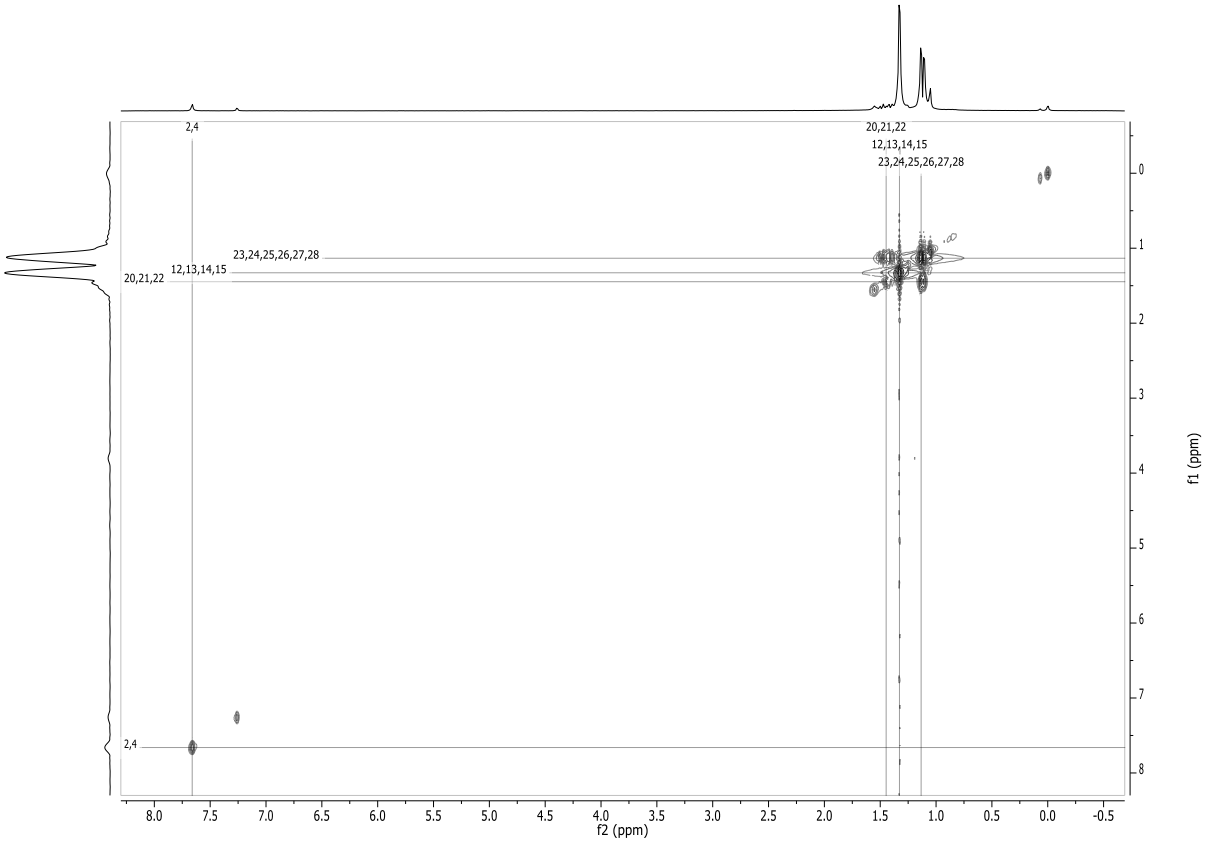

Figure 81: COSY spectrum of (28)-TIPS in chloroform-*d* at room temperature (300 MHz)

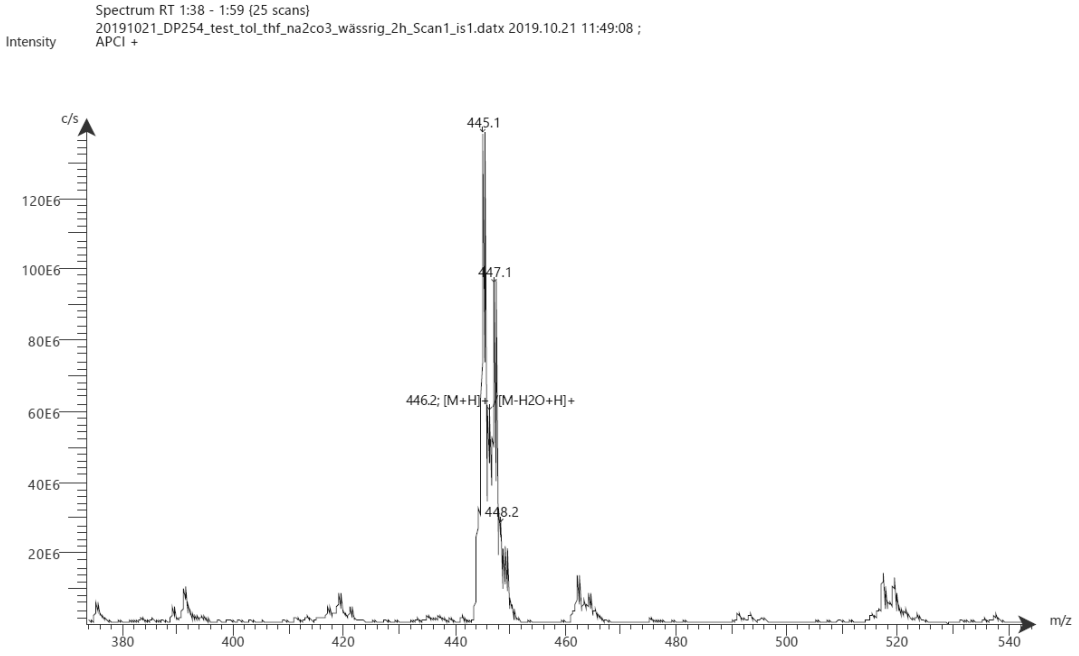

Figure 82: Mass spectrum of (28)-TIPS recorded on Advion expression CMS

Compound (28)-OAc:

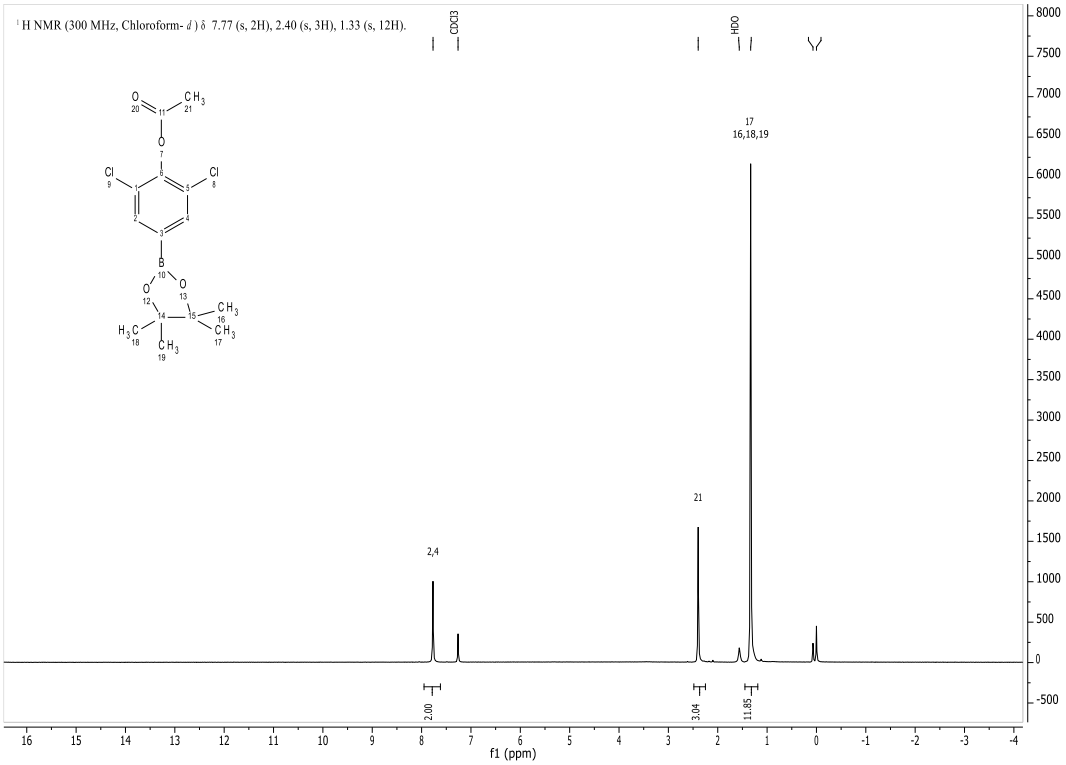

Figure 83: ^{1}H NMR spectrum of (28)-OAc in chloroform-*d* at room temperature (300 MHz)

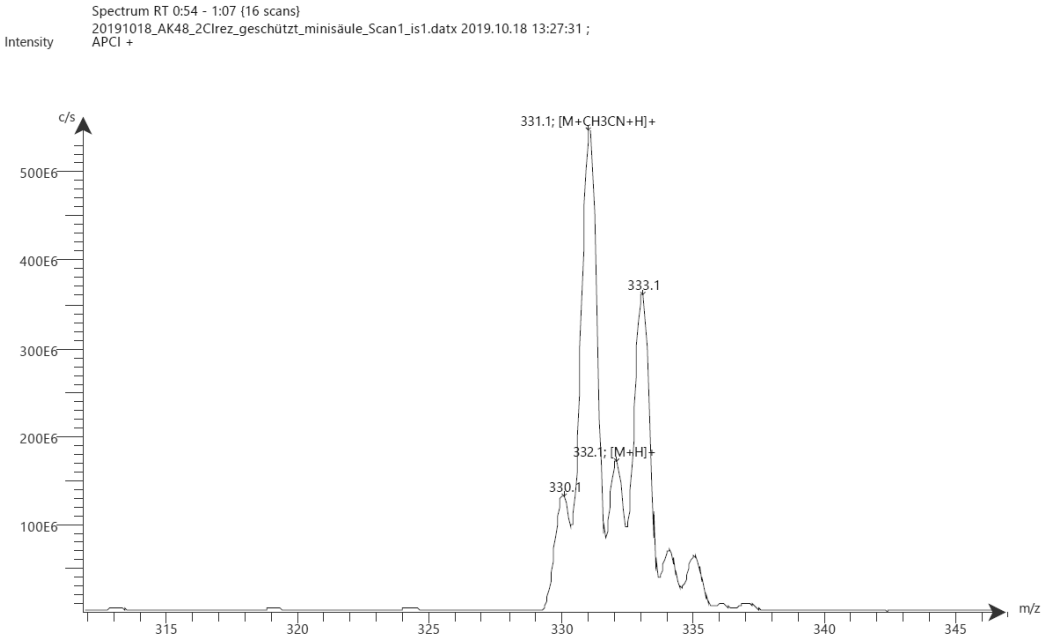

Figure 84: Mass spectrum of (28)-OAc recorded on Advion expression CMS

Compound (15):

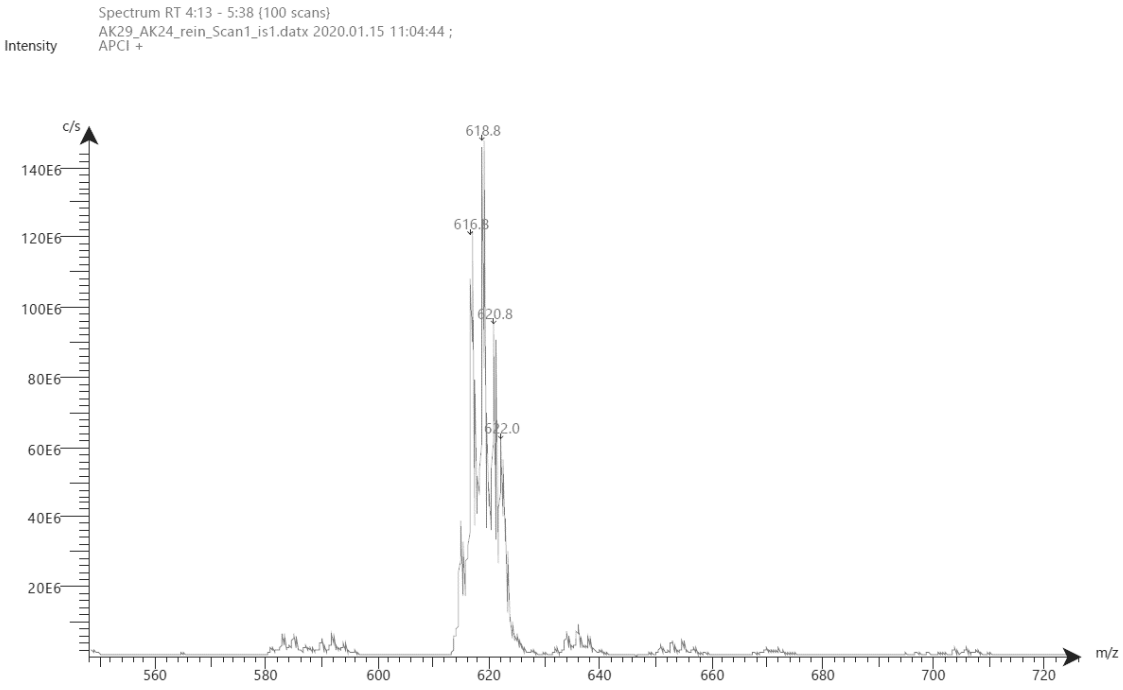

Figure 85: Mass spectrum of compound (15) recorded on Advion expression CMS

Compound (16):

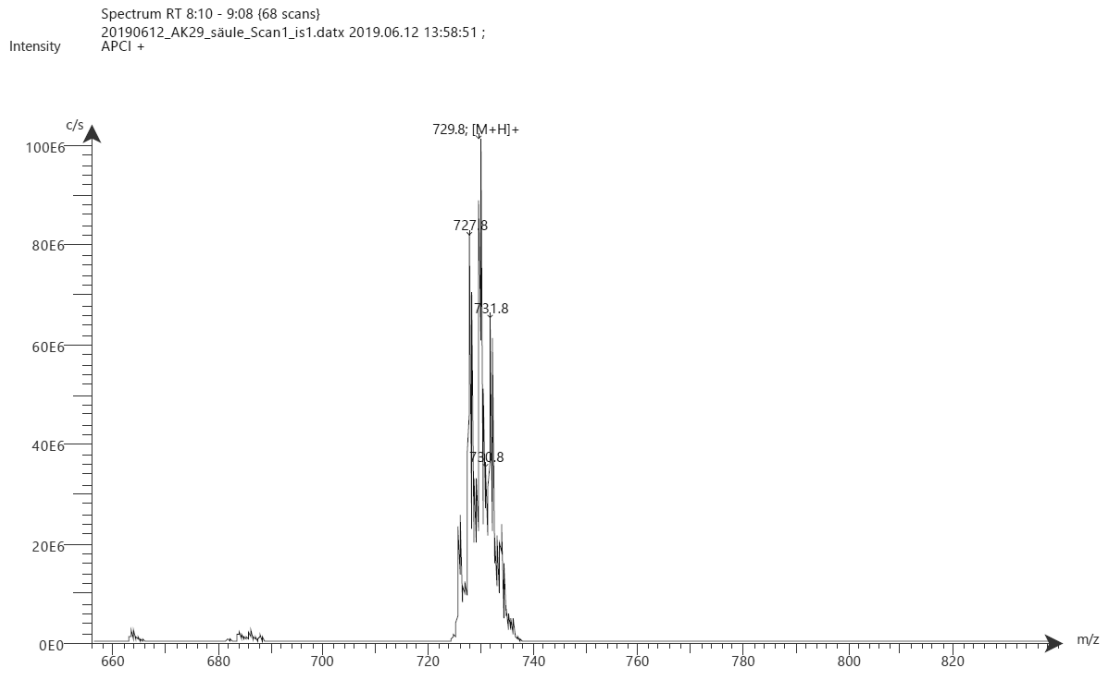

Figure 86: Mass spectrum of compound (16) recorded on Advion expression CMS

Compound (19):

1)

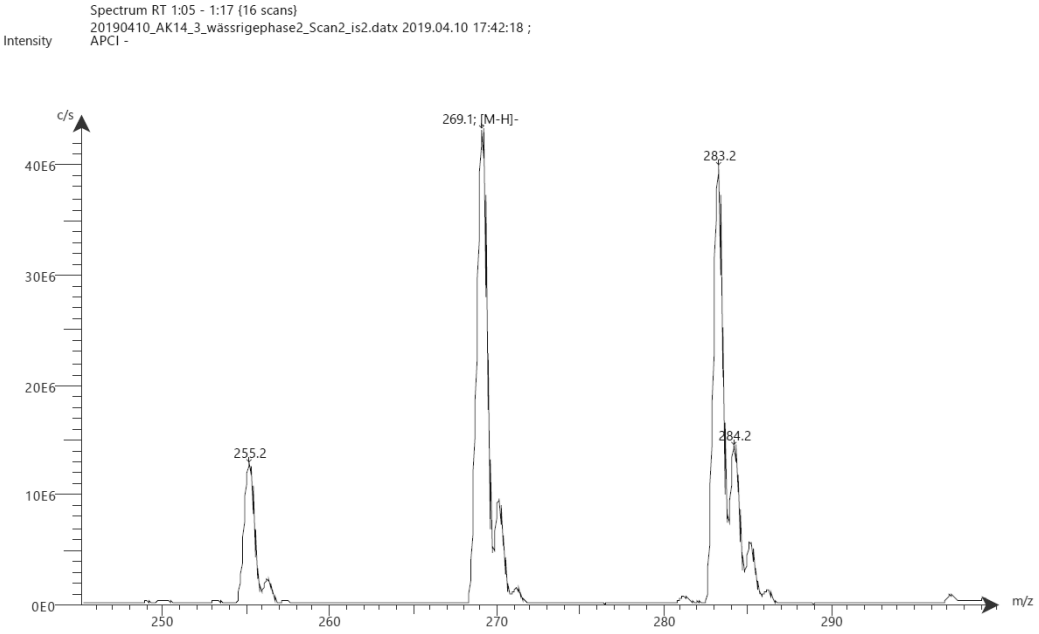

Figure 87: Mass spectrum of compound (19) recorded on Advion expression CMS

2)

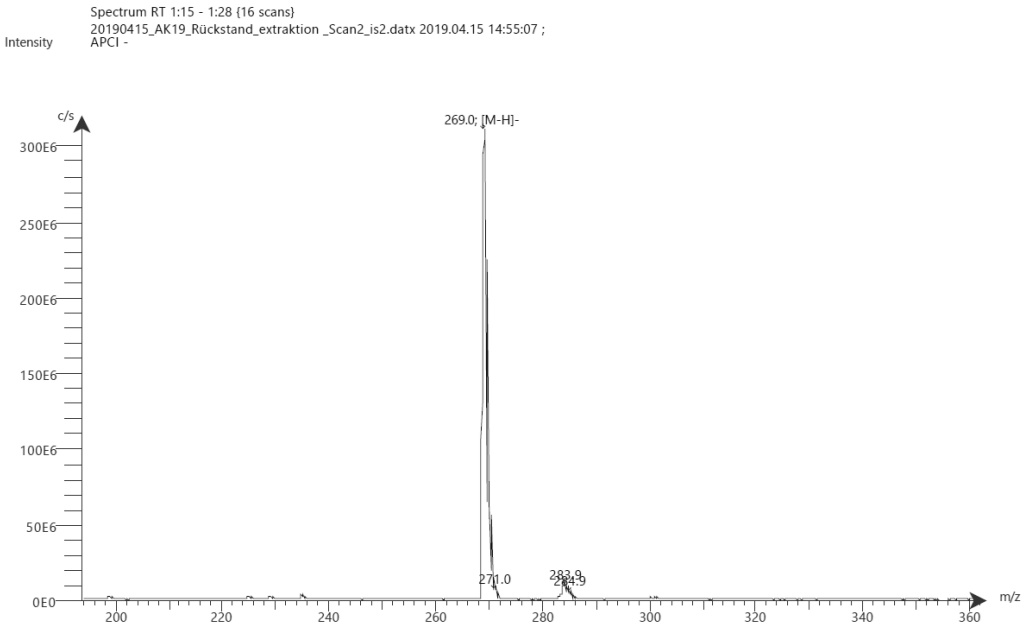

Figure 88: Mass spectrum of compound (19) recorded on Advion expression CMS

Compound (20):

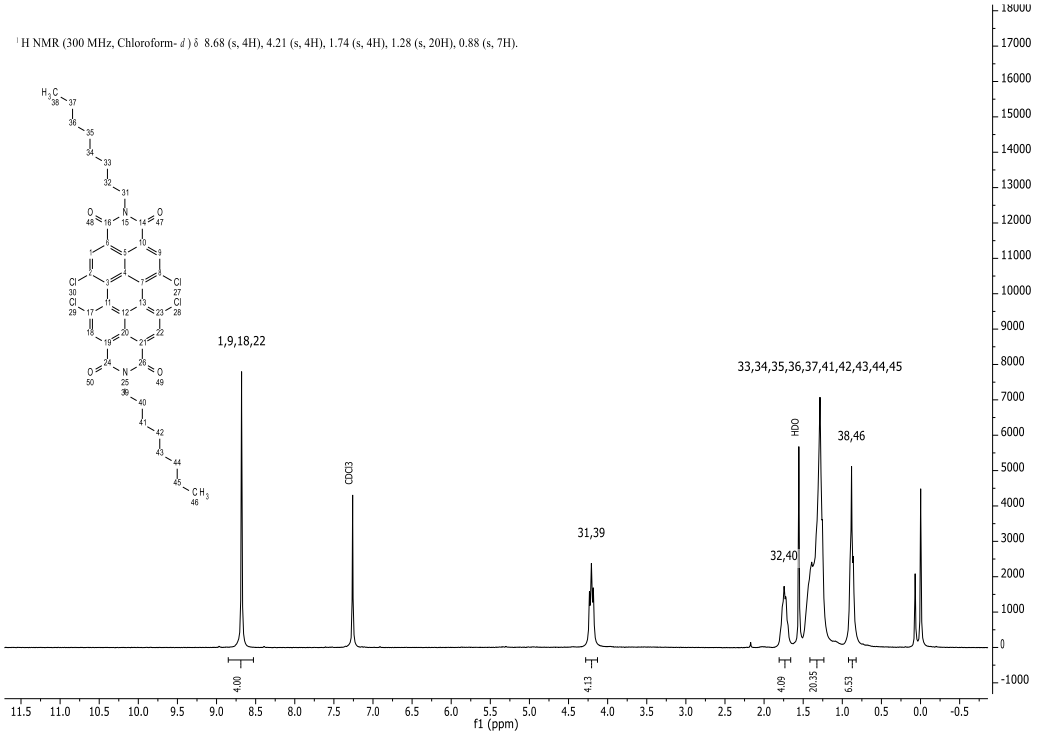

Figure 89: ^{1}H NMR spectrum of compound (20) in chloroform-*d* at room temperature (300 MHz)

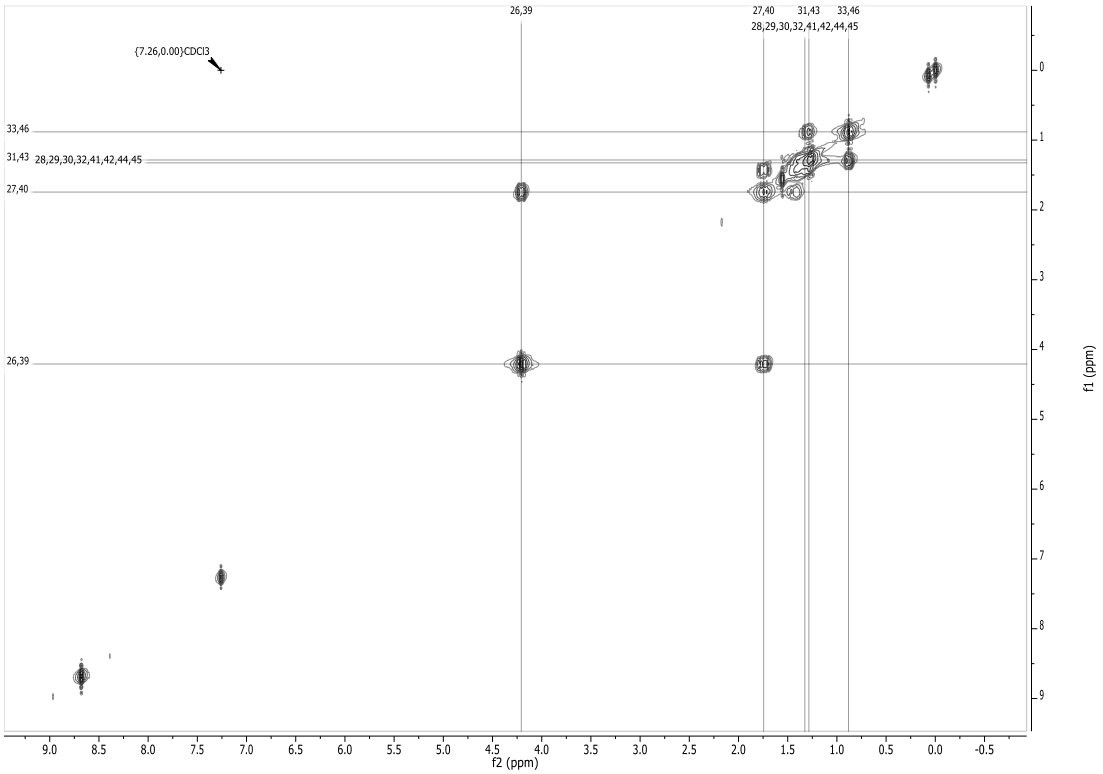

Figure 90: COSY spectrum of compound (20) in chloroform-*d* at room temperature (300 MHz)

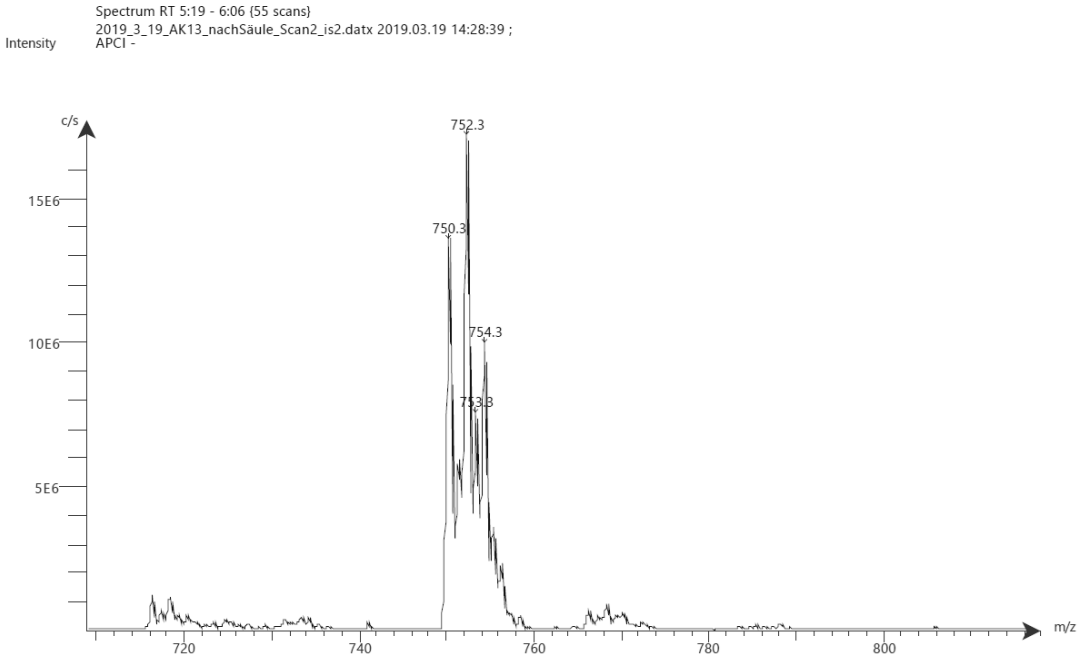

Figure 91: Mass spectrum of compound (20) recorded on Advion expression CMS